Recent and Emerging Trends in Low Phase-Noise Signal Soucres: High Frequency DROs

[1-3]Ulrich L. Rohde, [1]Ajay K. Poddar
[1]Synergy Microwave Corp. NJ,USA
[2]Universitat der Bundeswehr, Munich, Germany
[3]IIT (Indian Institute of Technology) Delhi,

Outline

M B I U S

- Signal Sources: Problem Statement, Motivations, and Challenges !
- Innovation-Semiconductor Devices, Artificial Material (Metamaterial)
- Artificial Material (Metamaterial) Fabrication Technology
- Noise in Circuits and Systems
- Design Challenges and New Approaches
- Resonator Q and Effect of Q on Oscillator Phase Noise
- High Frequency Los Noise Signal Sources
- Examples: Low Phase Noise Oscillator
- Emerging Technologies: Low Phase Noise DROs
- Conclusion

M B I U S

Why Care about Signal Sources (Oscillator/VCO)?

- Our World has become wireless
- Data links use different frequency bands for transmission (5G, Satellite links, Radar,…)
- Oscillators generate the frequencies to transport the data

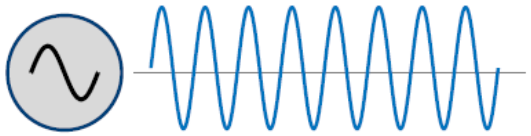

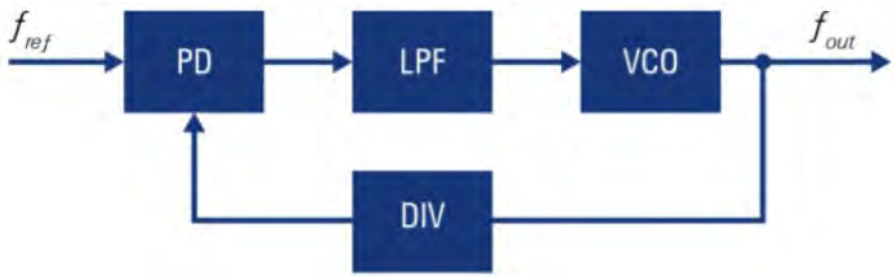

- VCO: Voltage Controlled Oscillator
  - Tunable for different frequency bands
  - Create Radar chips through tuning
  - Fine frequency adjustments within a locked loop (PLL) Synthesizer

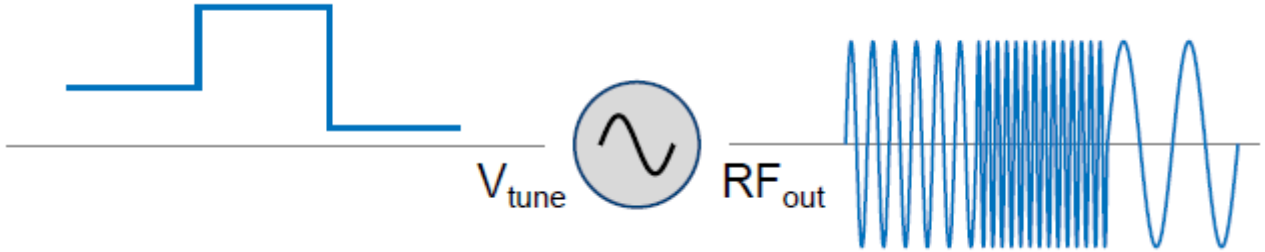

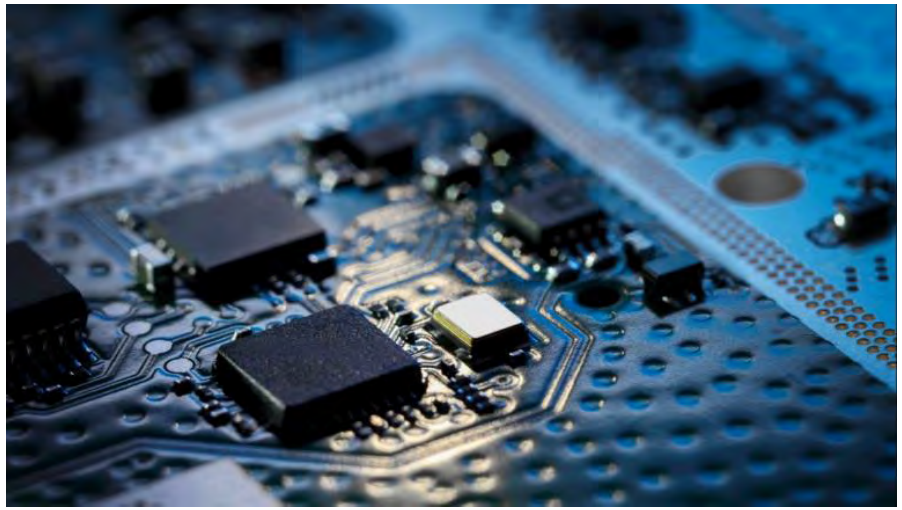

Courtesy: Rohde & Schwarz)

Problem Statements, Motivation and Challenges

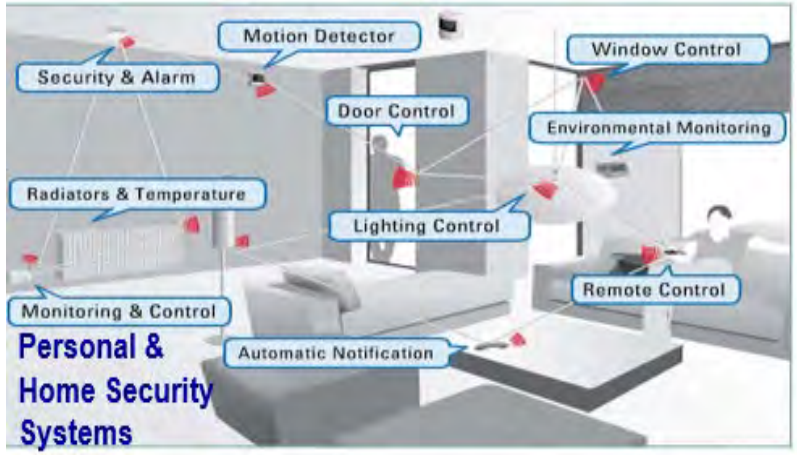

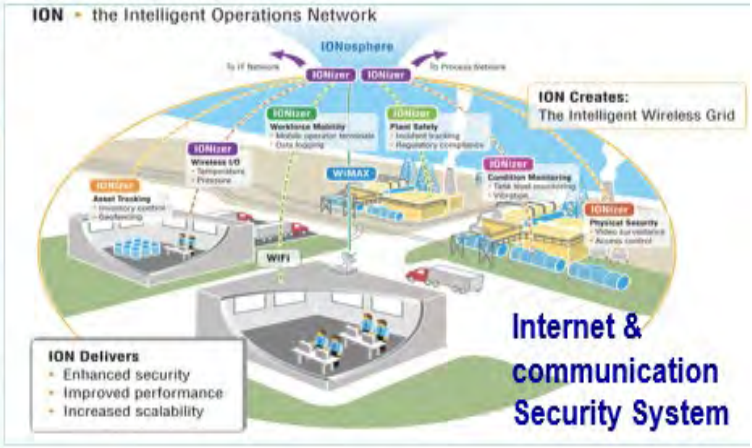

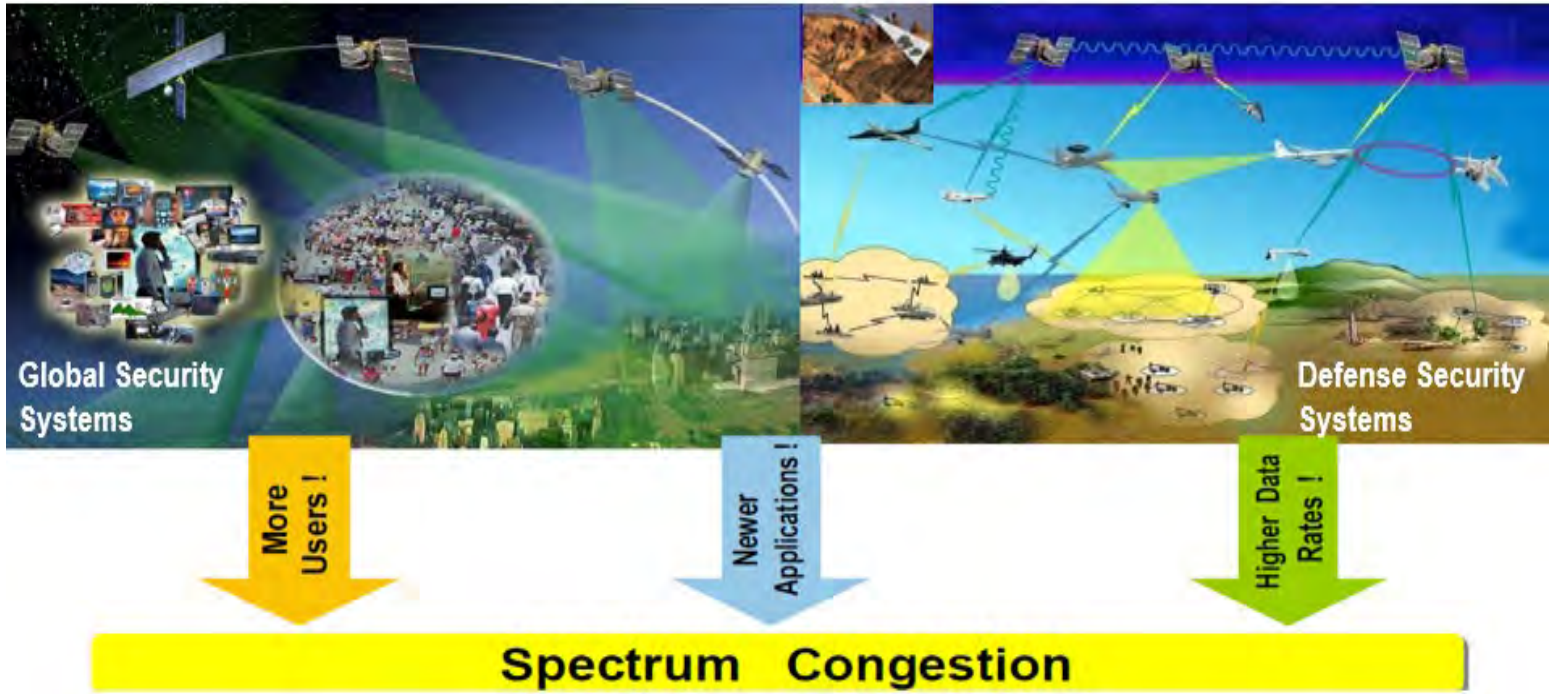

Problem Statements

- Spectrum Congestion is a concern to both Civilian and Military Users
- Security is Concerned for Everyone !

Motivations

- Signal generations and Signal Processing Circuits Play Important Role in Sensors, RADAR and Time Keeping Devices !!

Challenges

- Low Cost, Compact , Power-Efficient, Reliable Solutions for current and later generation communication systems !!!

Courtesy: Online images and view graphs from Internet

Signal Sources are Everywhere !

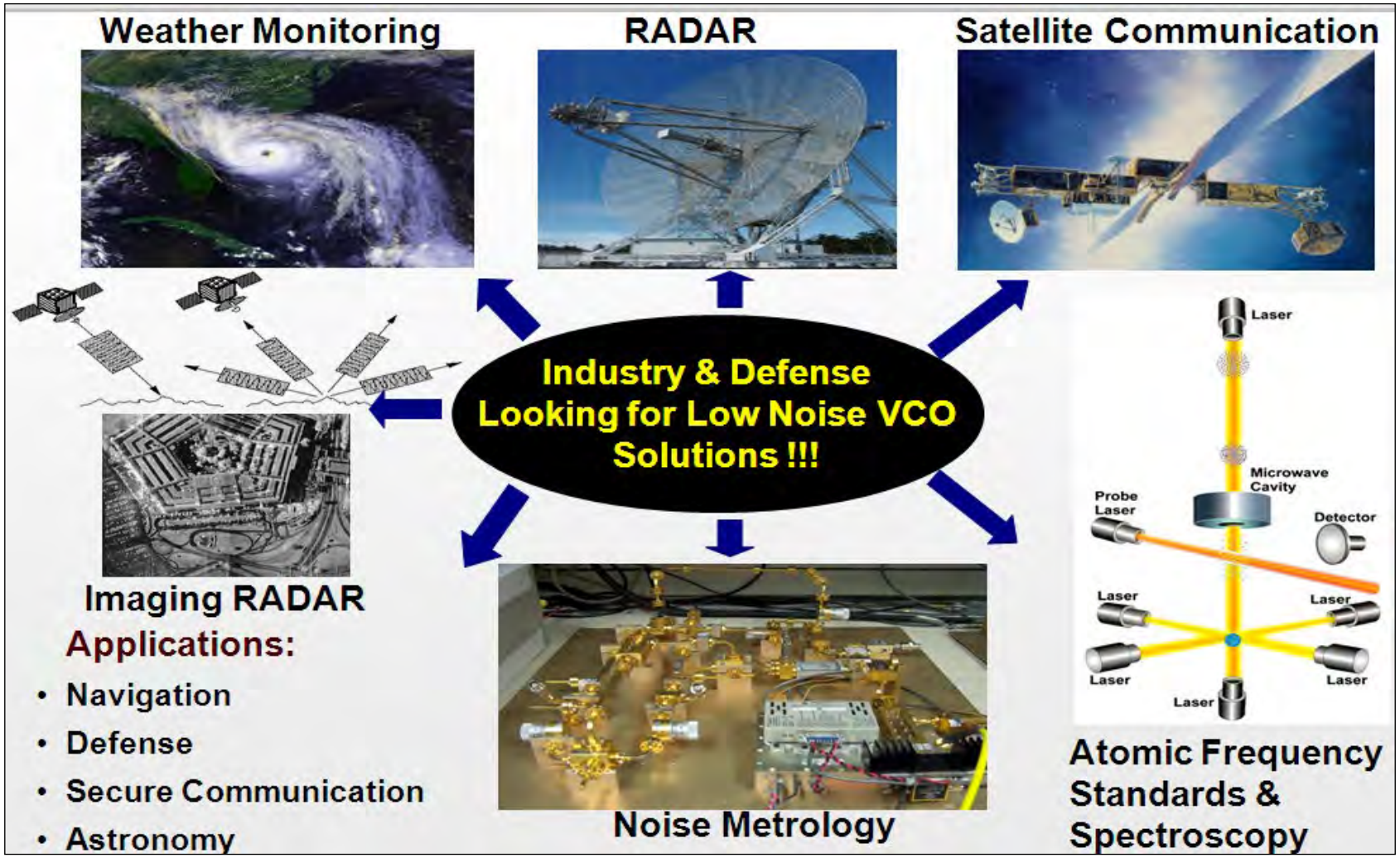

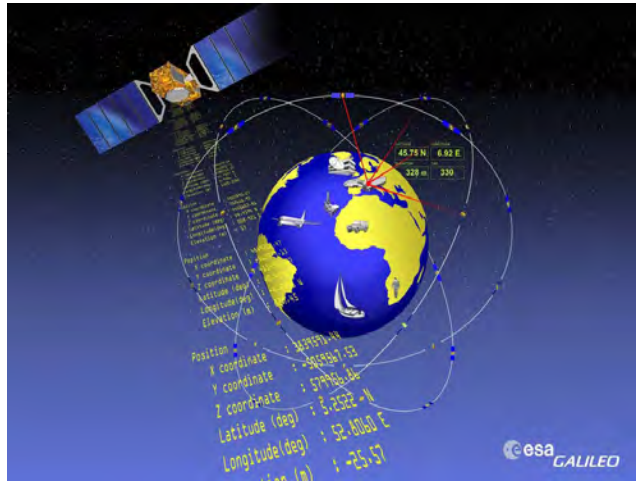

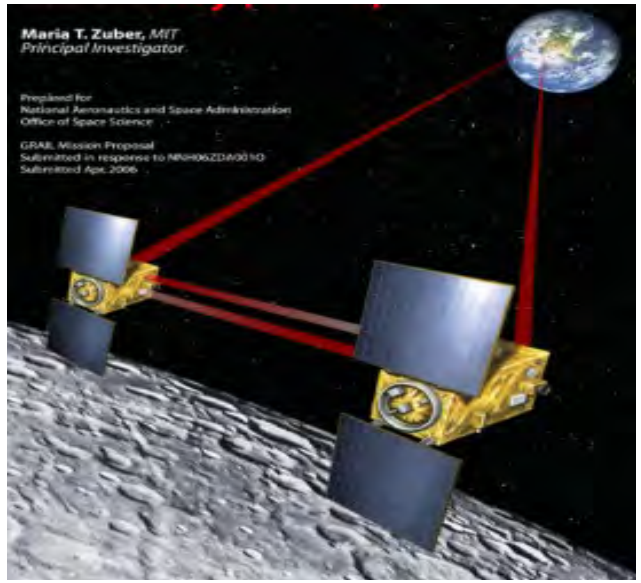

Courtesy: Online images and view graphs from Internet

Motivation-Signal Source is Everywhere !

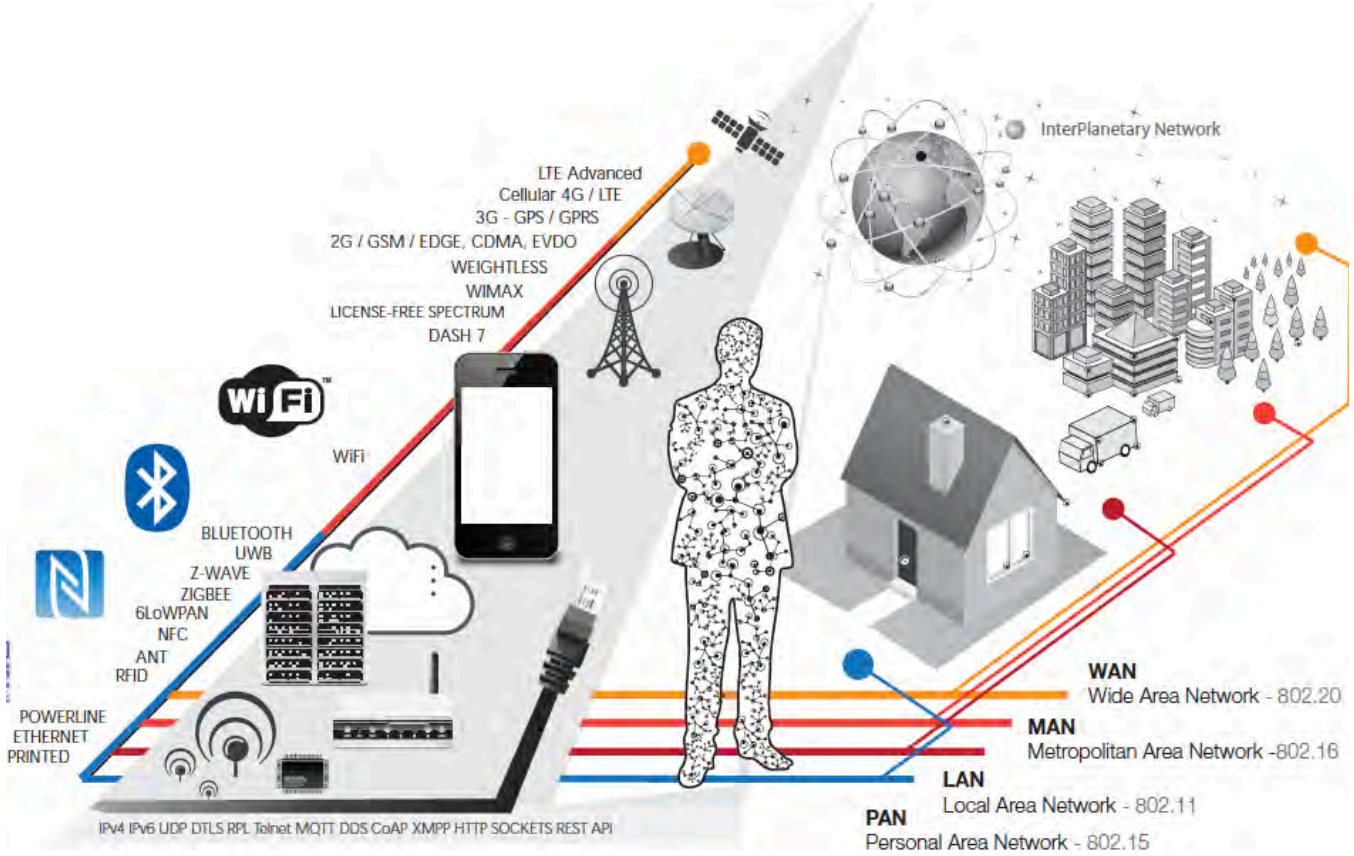

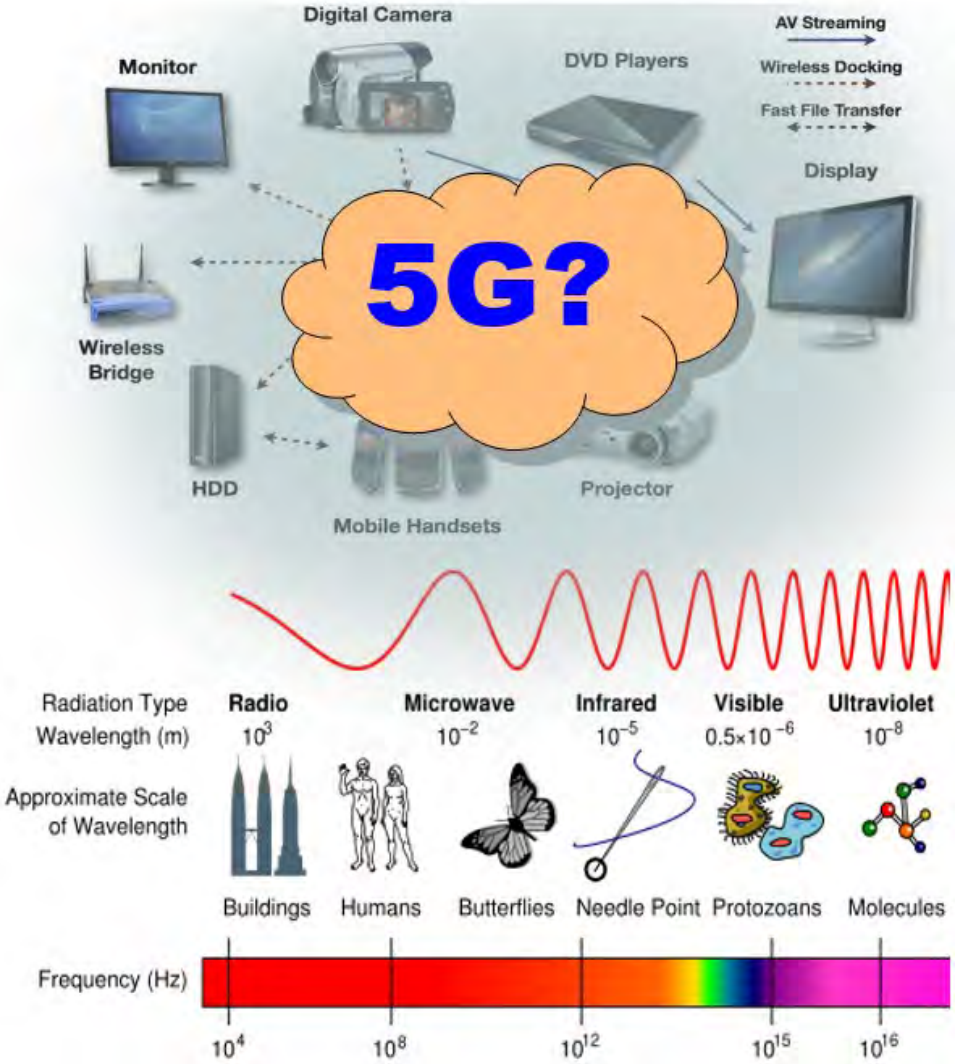

Signal generation and signal processing electronic modules supports Physical (PHY) layer technology for 5G and IoT applications. **Challenge: Low Cost, compact and Energy Efficient Electronics Solutions !**

Courtesy: Online images and view graphs from Internet

Courtesy: Online images and view graphs from Internet

Innovation

Size-Atomic Structure Perspective

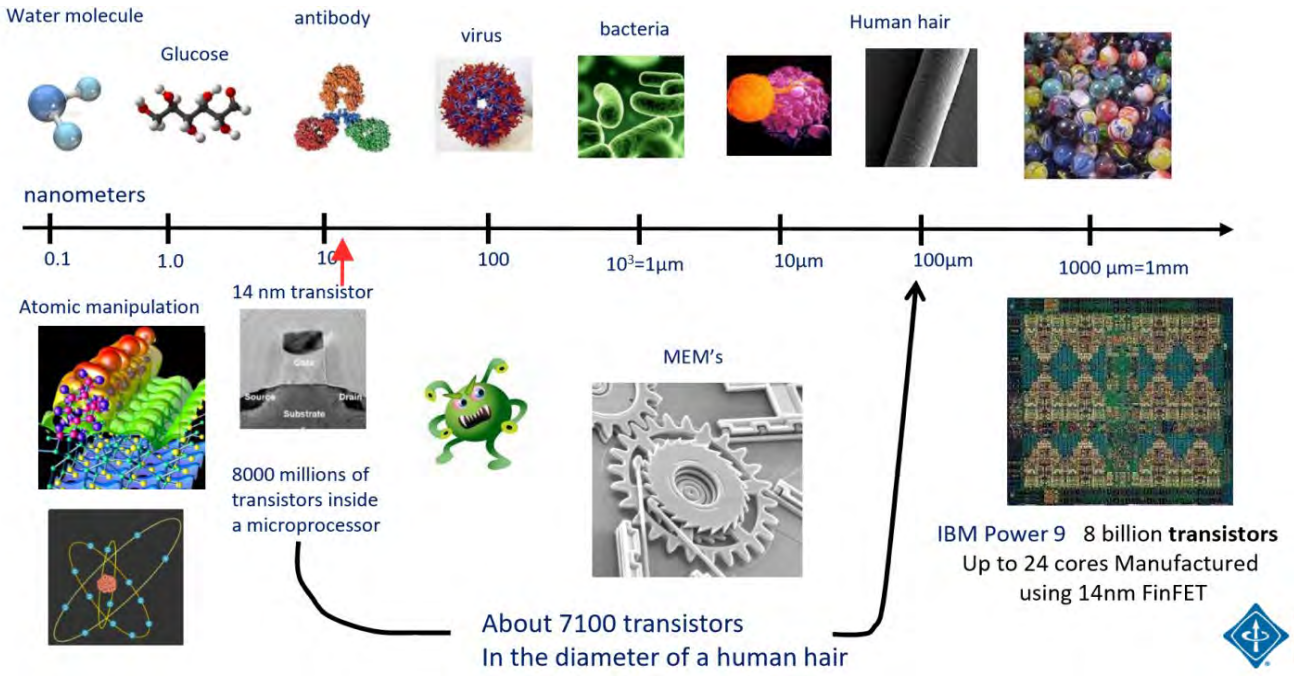

The photo above shows the innovation in semiconductor devices.

It can be seen in the size perspective, from marble 1mm to water molecule 0.1 nanometer. The lower half shows the scaling of the semiconductor devices. It is amazing to understand that in the diameter of a human hair 100micromeer, abot 7100 transistors and in the size of antibody, about 10 nm, 8000 million transistor inside a microprocessors.

Ref. F. Guarín, "Semiconductor technology and devices for the benefit of humanity", Talk at NJIT, Dec 04, 2019

Size- Array of Resonant Composite Structure

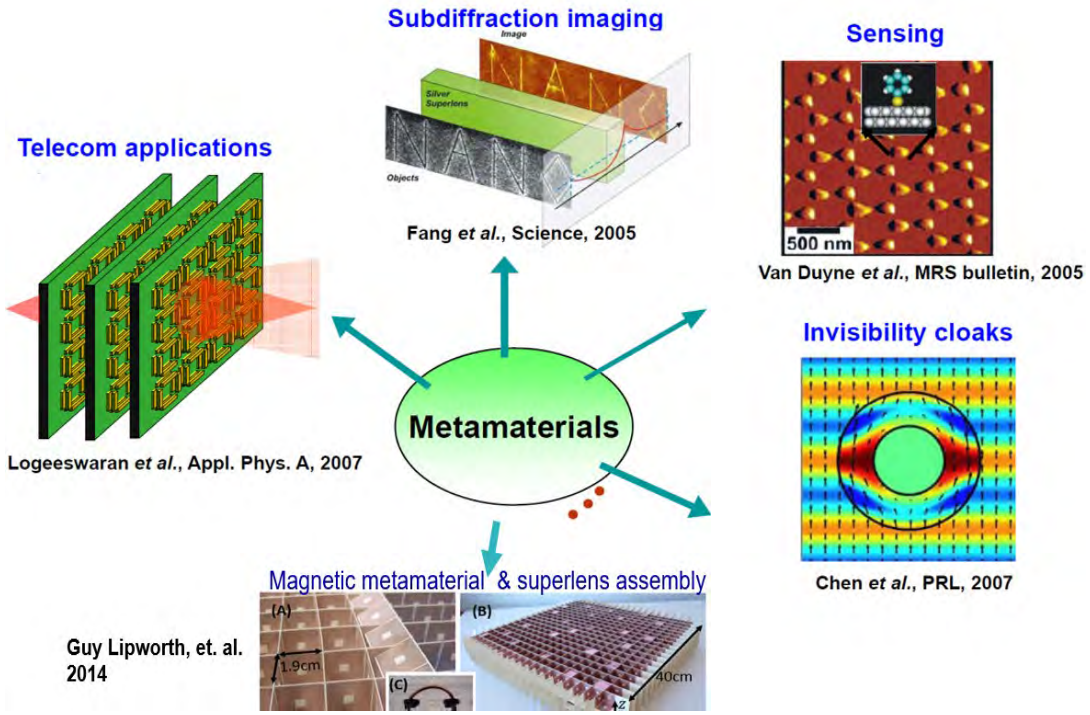

The photo above shows the innovation in artifial composite materials (Metamaterial)

- Metamaterial Resonator Structure -Today's top 10 advances in material science over the past 50 years
- Metamaterial Resonator (Artificial Composite Structure) offers attractive solutions in DRO performance and power consumptions

Courtesy: Online images and view graphs from Internet

Metamaterial-Fabrication Technologies

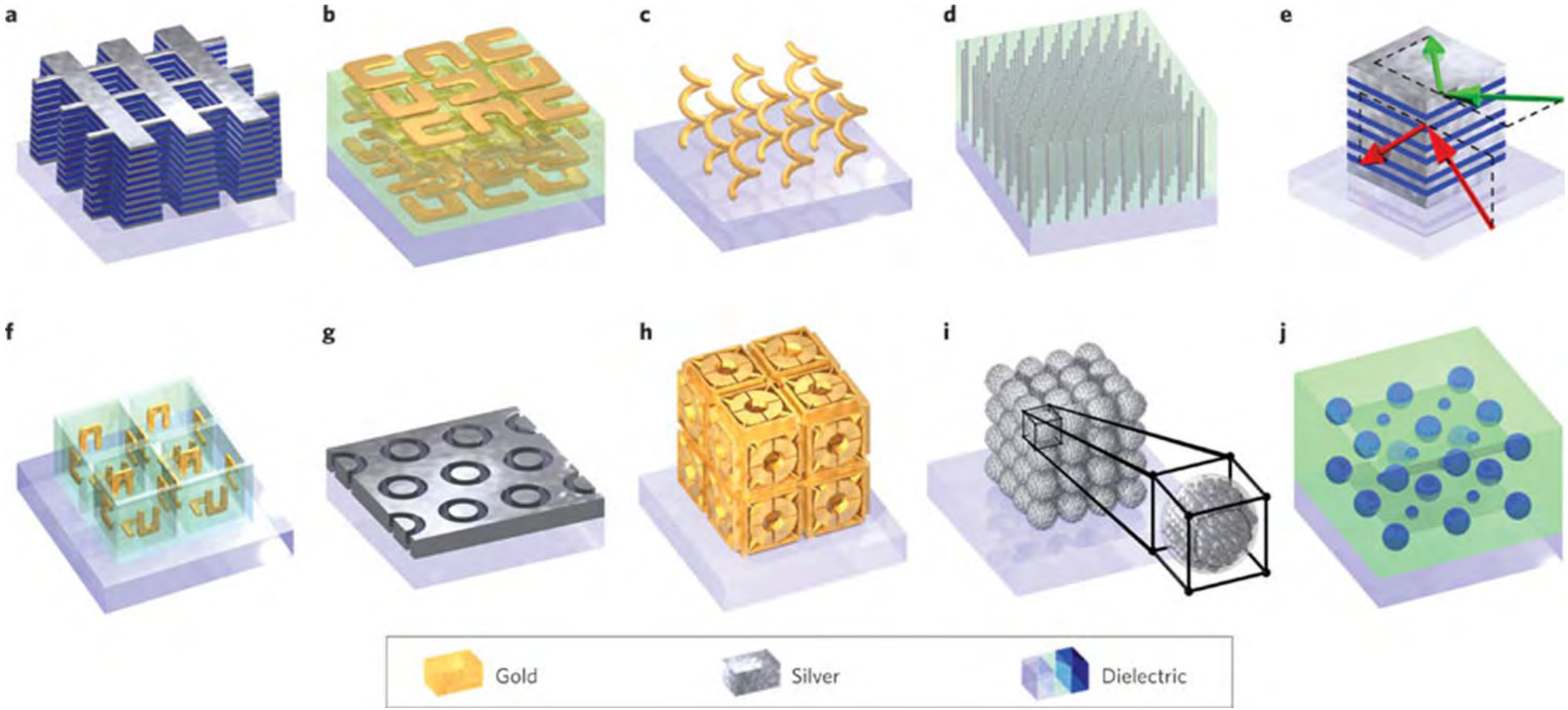

Courtesy: Online images and view graphs from Internet

Noise: Major Culprit in Radar System

- The quantum dynamics of high Q-factor **Quartz crystal, Ceramic, Dielectric, WGM, resonator** is **nonlinear** and **drive-level dependent.**
- Therefore, nonlinearities associated with these resonators can lead to unwanted aliasing of low-frequency noise to carrier side-bands.

Noise aliasing in oscillator comprises of nonlinear resonator

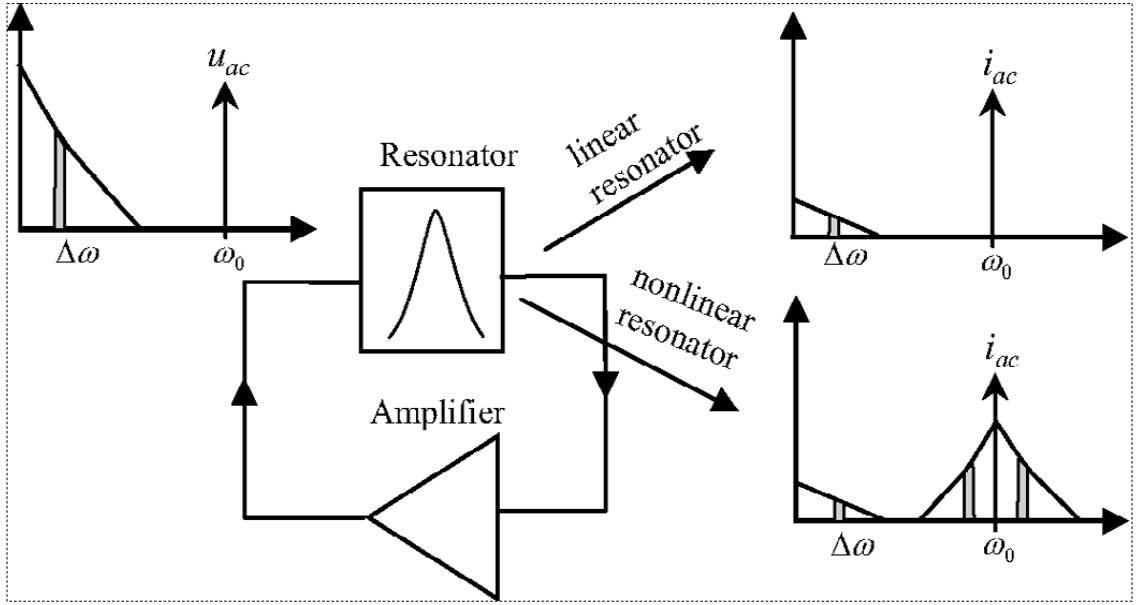

Problem: 1/f noise

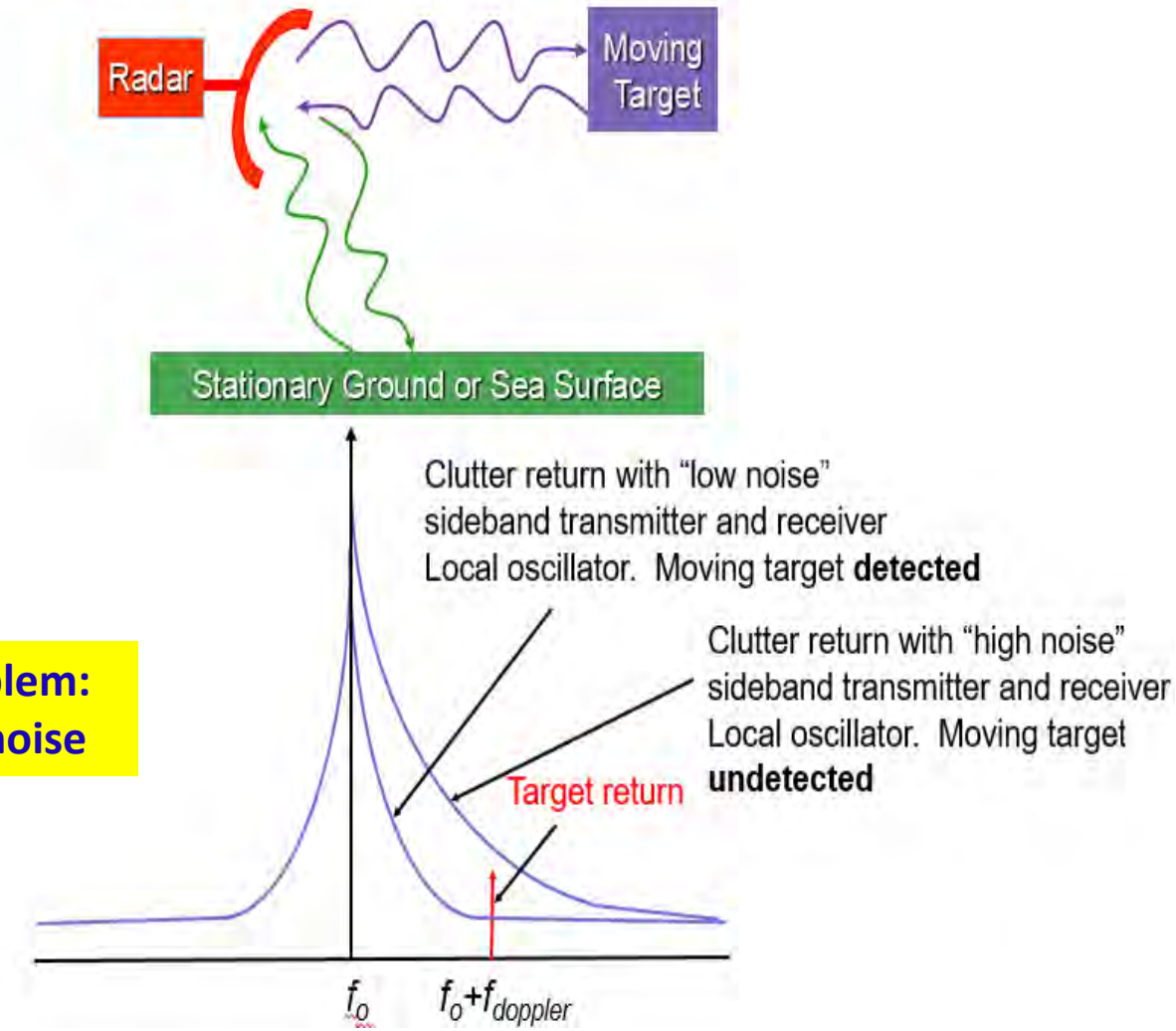

Courtesy: Online images and view graphs from Internet

Noise Types

Typical Noise Types

- **Passive Devices**
  - Thermal f^{0}
  - Some have flicker (magnetic, carbon resistors) f^{-1}
  - Higher order noise may come from temperature effects f^{-4}
- **Active Devices**
  - Almost all have thermal and flicker f^{0} and f^{-1}
  - Possible temperature effects f^{-4}
- **Sources (May some or all of the higher order types)**
  - White PM or Thermal f^{0}
  - Flicker PM f^{-1}
  - White FM f^{-2}
  - Flicker FM f^{-3}
  - Random Walk f^{-4}

Noise Type's contd.

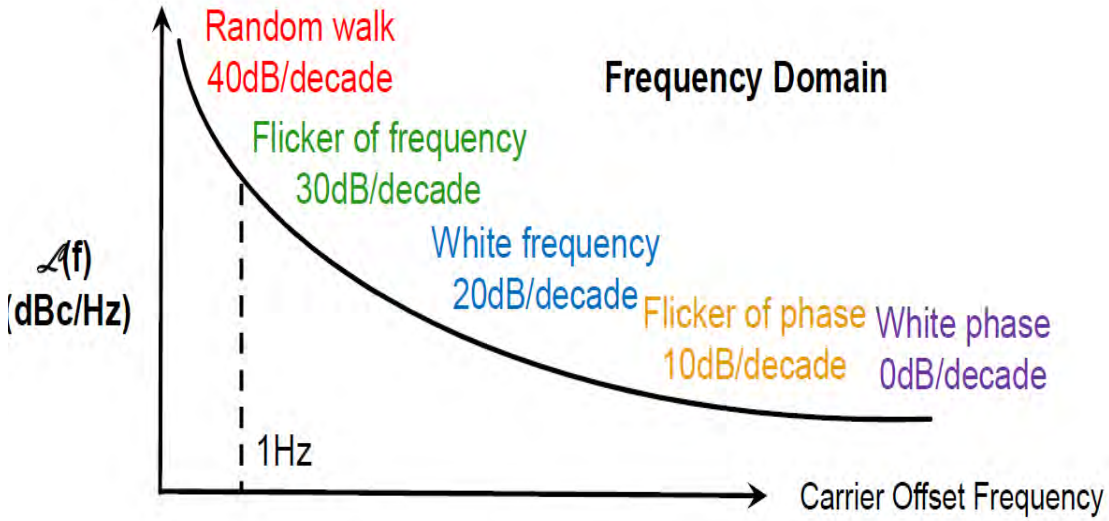

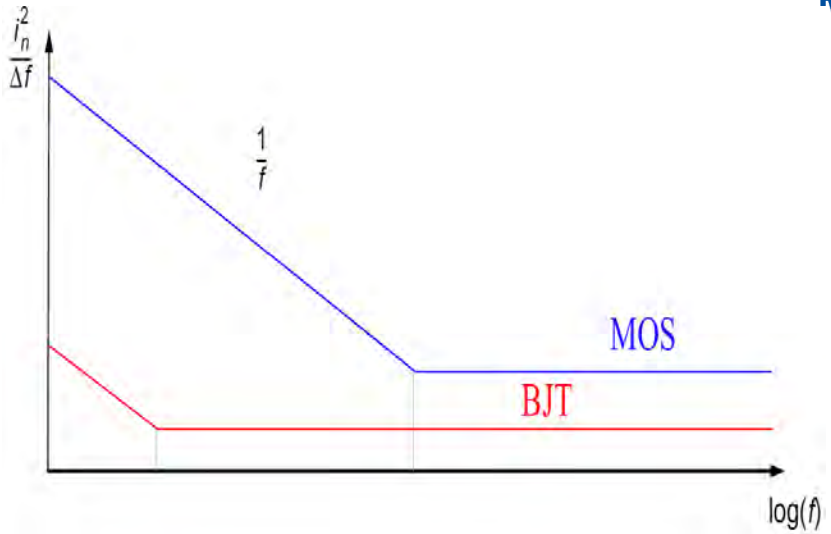

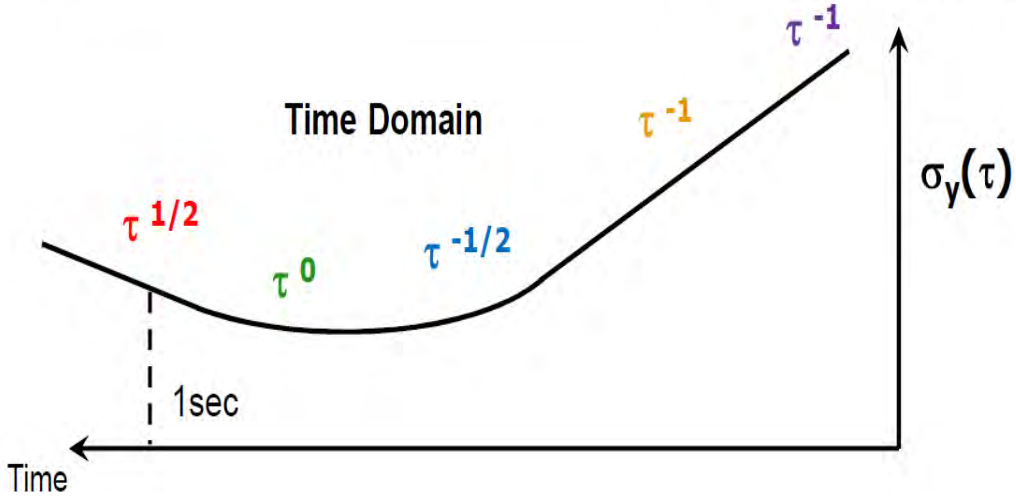

Substrate and Supply Noise

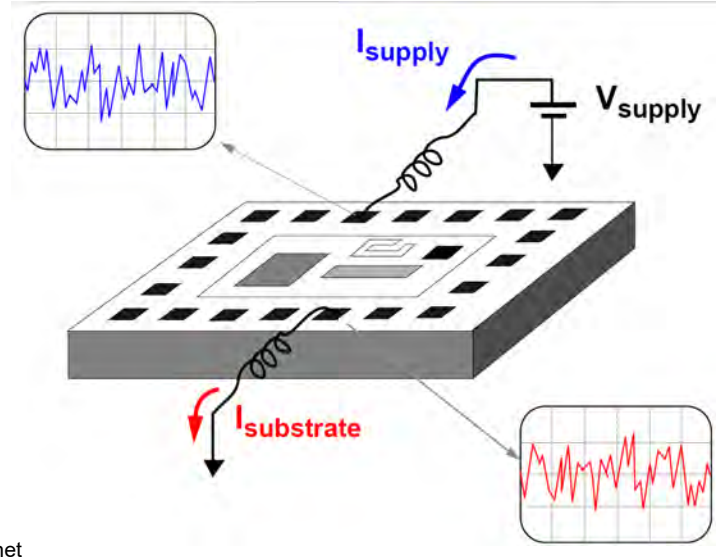

Courtesy: Online images and view graphs from Internet

Noiseless and Noisy Oscillator

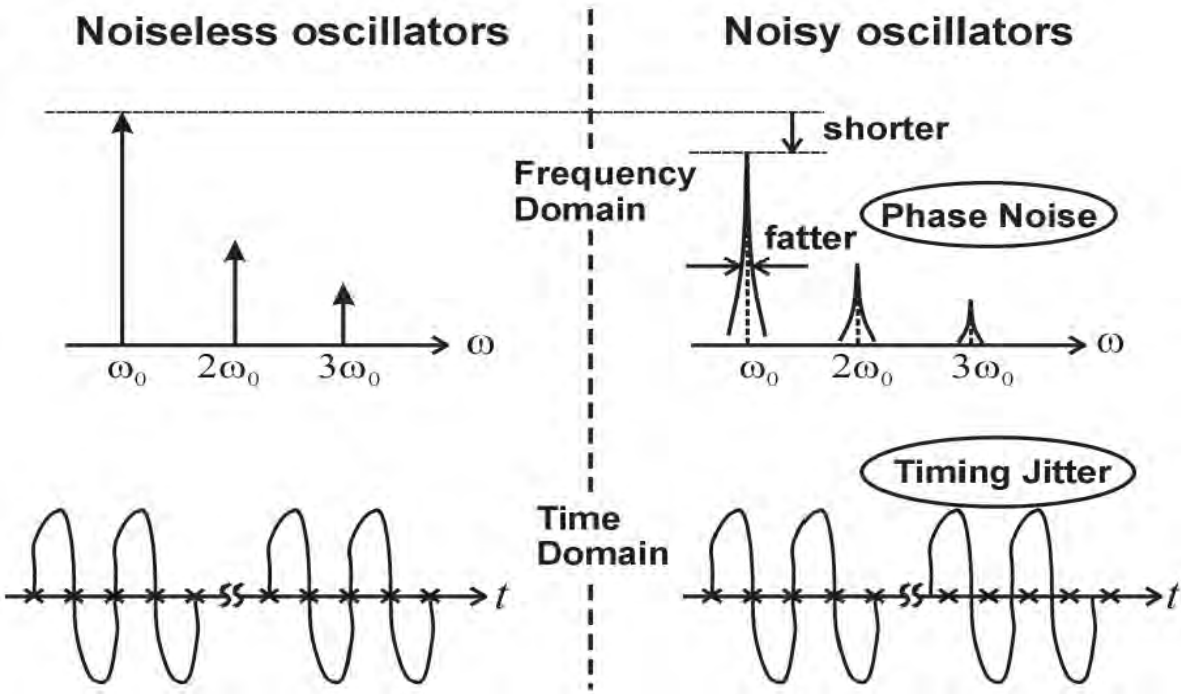

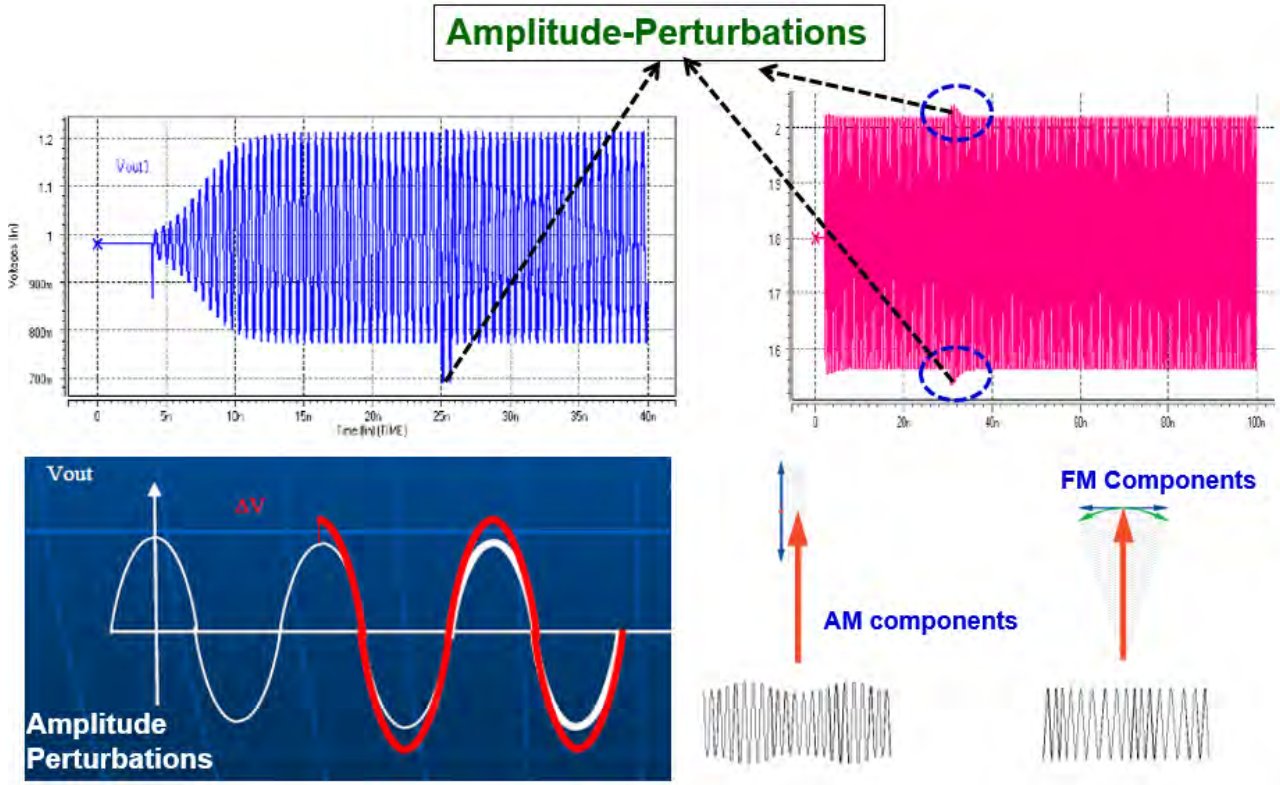

Courtesy: Online images and view graphs from Internet

Design Challenges & New Approaches

Typical Simplified model for Microwave Oscillator Circuit

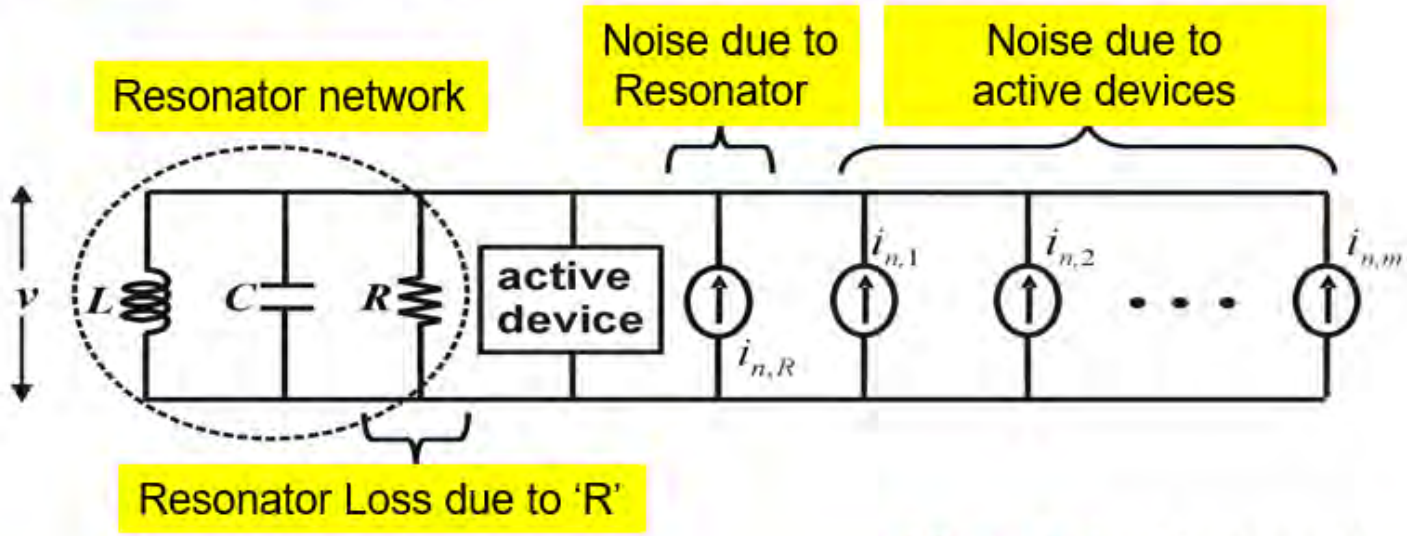

Wish List : Resonator Loss → 0 !

Design Challenges:

- Low loss resonator (high quality factor)
- Planar & compatible to IC (integrate circuit)
- Compact size and cost effective
- Multi-band & multi-mode operation
- Insensitive to microphonics, shock, vibration

Attempting New Possibilities:

Realization of high Q-factor resonator

- Möbius Strips Resonator
- Metamaterial Möbius Strips (MMS) Resonator

Development of Low Noise Oscillators

- Multi-Band, Multi-Mode Oscillators

Wish List-Resonator Loss → 0 !

LCR Circuit: Electrical Analogy

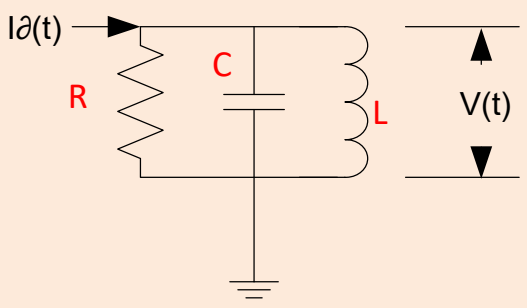

$$Z = \frac{j\omega L}{1-\omega^2 LC + j\omega L/R}$$

- **L,C,R forms an impedance "tank"**
- **Voltage across tank oscillates**

$$V(t) = \sqrt{2}\frac{I}{C}e^{-t/2RC}\cos\left(\sqrt{\frac{1}{LC}-\frac{1}{4R^2C^2}}\cdot t\right)$$

R>0

Wish List

R → 0

High Q Resonator

Loaded Spring: Mechanical Analogy

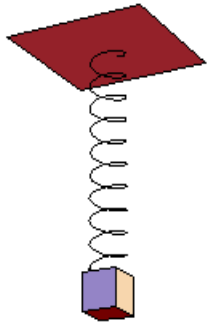

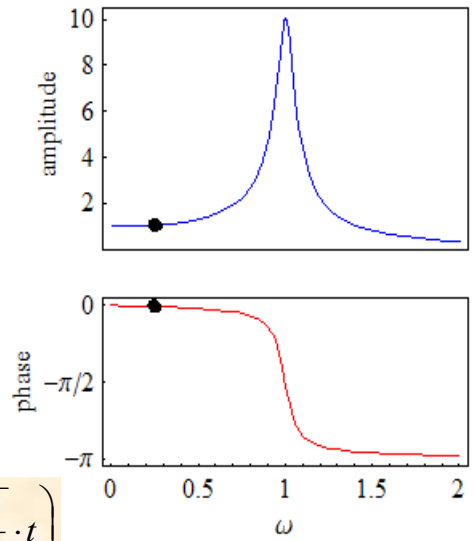

$$V(t) = \sqrt{2}\frac{I}{C}\cos\left(\sqrt{\frac{1}{LC}}\cdot t\right)$$

R=0

Courtesy: Online images and view graphs from Internet

Definition of Resonator Q-Factor ?

- The definition of Q-factor is ambiguous for the positive feedback device, in particular when resonator loss is 100% compensated by gain block, resulting Q→∞
- The energy based definition cannot explain the oscillation when a resonator has no energy storage elements (such as L or C), as in the case of ring or distributed oscillators
- **The definition of Q-factor become questionable for negative index resonator (negative permittivity and negative permeability).**
- Keep in view of above, there is need of revisiting the definition of Q factor !

  - **Definition of Q Factor for Passive Resonant Circuit**
    - Fractional 3-dB bandwidth
    - Phase-to-frequency slope
    - Stored-to-dissipated energy ratio
  - **Definition of Q Factor for Active Resonant Circuit**
    - Noise spectrum Basis: commonly used
    - Source-Pull/Push Basis: takes into account of pushing and Load pulling effect
    - Injection locking Basis: takes into account of injection–locking range

Oscillator: Topologies

Conventional Oscillator Topologies:

- ✓ **Colpitts Oscillator Topology**
  - **Advantages:**
    - Low Phase Noise, Power-Efficient
  - **Disadvantages:**
    - Narrow Tuning, Not Configurable
- ✓ **Band Switched Mode VCOs**
  - **Advantages:**
    - Multi-Band Signal Sources
  - **Disadvantages:**
    - Switching Noise, Not Concurrent
- ✓ **Wideband VCOs (YIG Tuned VCO)**
  - **Advantages:**
    - Multi-Octave Band, Low Phase Noise
  - **Disadvantages:**
    - Expensive, Current Hungry

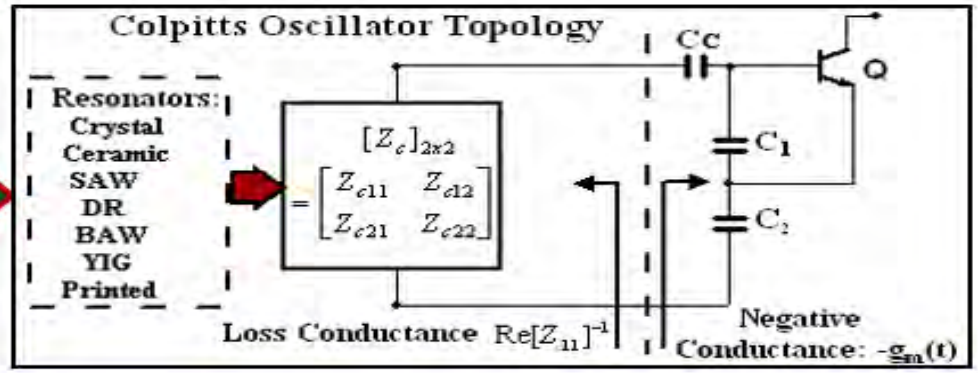

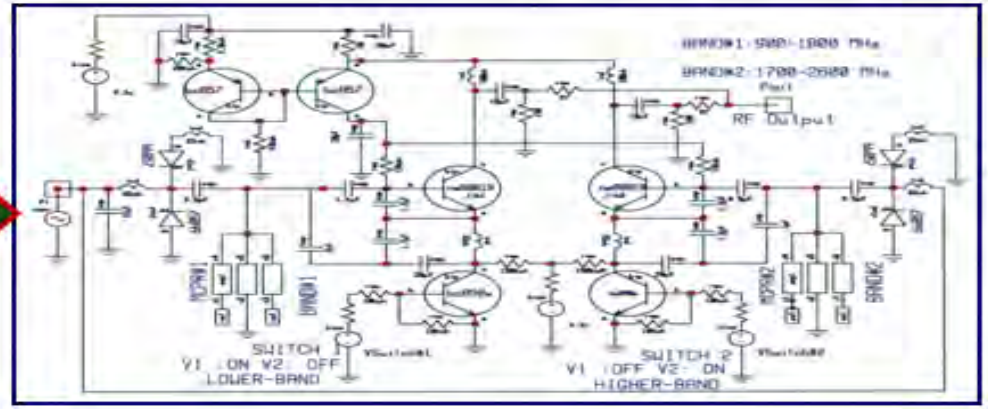

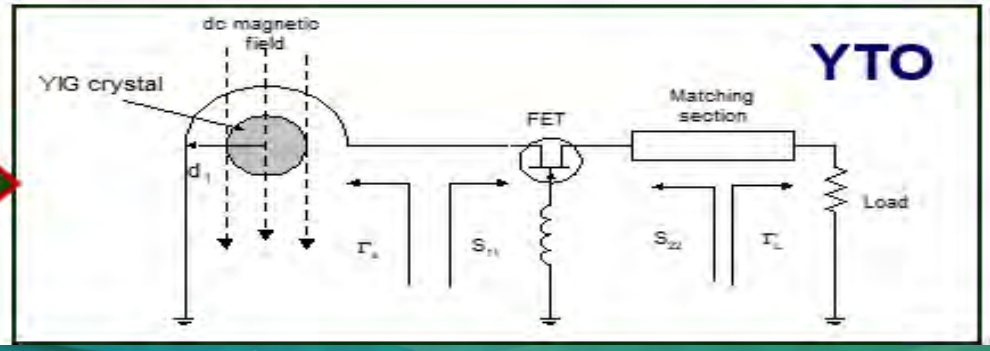

Q-Factor: Passive Resonant Circuit

1. Fractional 3-dB bandwidth

$$Q = \frac{\omega_0}{\omega_2 - \omega_1} = \frac{f_0}{f_2 - f_1}$$

Needs only scalar analysis, but sometimes inaccurate.

1-port resonator

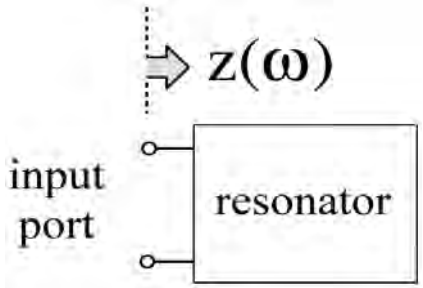

Impedance vs Freq. response

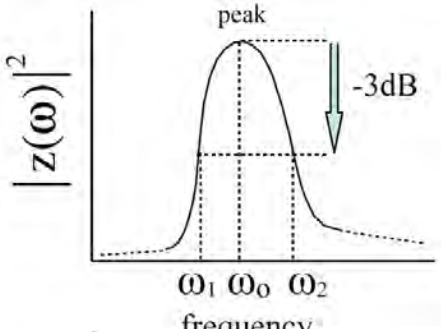

2. Phase-to-frequency slope

$$Q = \frac{\omega_0}{2}\left|\frac{\partial\varphi(\omega)}{\partial\omega}\right|_{\omega=\omega_0} = \frac{\omega_0}{2}|\varphi'(\omega_0)|$$

Fairly accurate, but still neglects amplitude slope

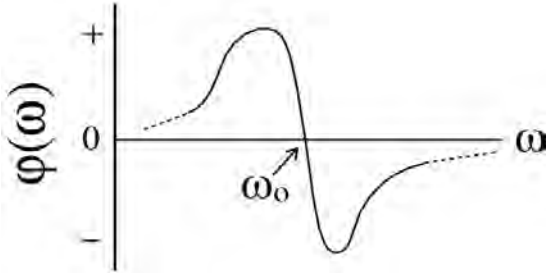

phase vs freq. response

3. Stored-to-dissipated energy ratio

$$Q = \omega_0 \frac{W_e(\omega_0)+W_m(\omega_0)}{P(\omega_0)}$$

$$P(\omega) = \frac{1}{2}Re\{v_{ex}i_{ex}^*\}, \qquad W_e(\omega) = \frac{1}{4}\sum_k^{cap} C_k|v_k|^2 \; W_m(\omega) = \frac{1}{4}\sum_k^{ind} L_k|i_k|^2$$

Invalid if oscillates due to external excitation

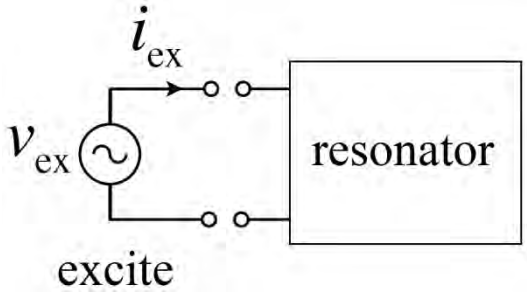

Ref. T. Ohira, "Dedicated Q factor formulas stemming from oscillation frequency stability against source and load deviations", Tutorial Lecture 2012

Q-Factor for Active Resonant Circuit

Active NISO Circuit Q-Factor [Reflection coefficient $\Gamma(\omega)$ Basis]

$$Q = \omega_o \left| \frac{\Gamma'(\omega)}{1-\Gamma^2(\omega_O)} \right|$$

NISO: No Input Single Output

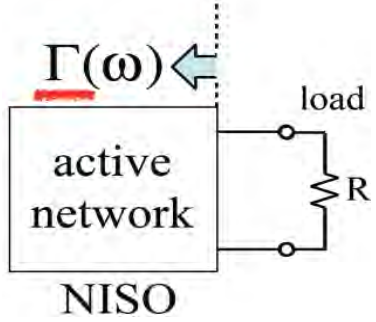

Typical 1-port oscillator

The expression for reflection coefficient $\Gamma(\omega)$ for 1-port network

$$\Gamma(\omega) = \left| \frac{z(\omega) - z_o}{z(\omega) + z_o} \right| \Rightarrow \quad \Gamma'(\omega) = \left| \left\{ \frac{[z(\omega) - z_o]\, z'(\omega) - [z(\omega) + z_o] z'(\omega)}{[z(\omega) + z_o]^2} \right\} \right|$$

$$\Gamma'(\omega) = \left[\frac{d\Gamma(\omega)}{d\omega} \right]$$

Active NISO Circuit Q-Factor (Energy Basis)

$$Q = \frac{\omega_0}{P_r} \sqrt{\frac{1}{4}\left(\frac{\partial P_r}{\partial \omega}\right)^2 + \left(\frac{\omega_0 \partial \Delta W}{\partial \omega}\right)^2} \qquad Q \cong \frac{\omega_0^2}{P_r} \left| \frac{\partial W_e}{\partial \omega} - \frac{\partial W_m}{\partial \omega} \right|$$

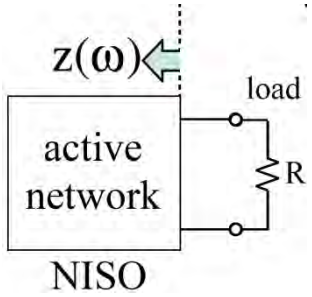

$$\underbrace{\Psi(\alpha, \omega)}_{\text{complex power}} = \frac{1}{2}[v_1(\omega) i_1^*(\omega) + v_2(\omega) i_2^*(\omega) + v_3(\omega) i_3^*(\omega) + \ldots + v_K(\omega) i_K^*(\omega)]$$

$$= P_a - P_r + 2j\omega W_e - 2j\omega W_m = \Delta P + 2j\omega \Delta W$$

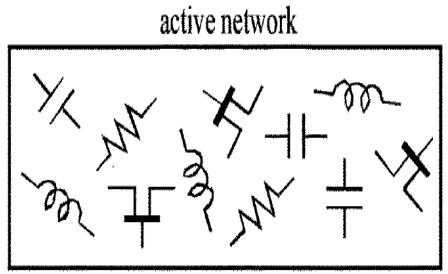

Ref. T. Ohira, "Dedicated Q factor formulas stemming from oscillation frequency stability against source and load deviations", Tutorial Lecture 2012

Q-Factor for Active Resonant Circuit

Active NISO Circuit Q-Factor (Noise Spectrum Basis)

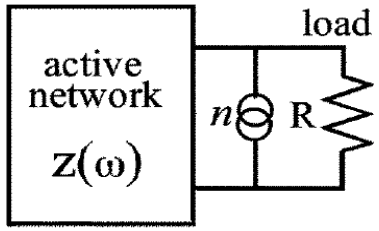

1-port Active NISO model of Oscillator circuit

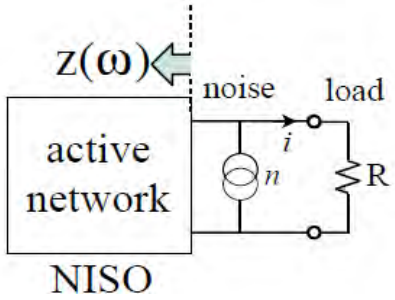

Equivalent noise model of NISO

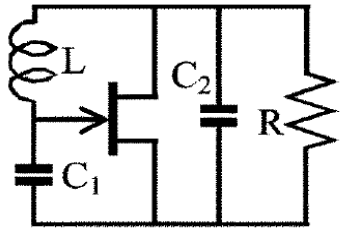

Colpitts example representing NISO model

$$Q = \frac{\omega_o}{2}\left|\frac{z'(\omega_o)}{z(\omega_o)}\right| \qquad z'(\omega) = \left[\frac{dz(\omega)}{d\omega}\right] \qquad z(\omega) = z(\omega_o) + \frac{dz(\omega_o)}{d\omega_o}\delta\omega + \cdots$$ Taylor expansion

$$Q(pz) = \frac{\omega_o}{2}\left|\frac{pz'(\omega_o)}{pz(\omega_o)}\right| = \frac{\omega_o}{2}\left|\frac{z'(\omega_o)}{z(\omega_o)}\right| = \quad Q(z) \rightarrow Scaling\ operation$$

$$Q(z^{-1}) = Q(y) = \frac{\omega_o}{2}\left|\frac{y'(\omega_o)}{y(\omega_o)}\right| = \frac{\omega_o}{2}\left|\frac{z'(\omega_o)}{z(\omega_o)}\right| = \quad Q(z) \rightarrow Inverse\ operation$$

$$Q(z^*) = \frac{\omega_o}{2}\left|\frac{z'(\omega_o)^*}{z(\omega_o)^*}\right| = \frac{\omega_o}{2}\left|\frac{z'(\omega_o)}{z(\omega_o)}\right| = \quad Q(z) \rightarrow Conjugate\ operation$$

The above definition of Q is valid for any active network, regardless of oscillator topology that is comprised of types of active devices for providing closed loop gain ≥ 1 and compensating the loss of resonator; Q is invariant against the three operations (p-scaling, inverse, and conjugate)

Ref. T. Ohira, "Dedicated Q factor formulas stemming from oscillation frequency stability against source and load deviations", Tutorial Lecture 2012

Q-Factor for Resonant Tank

Resonator Quality Factor

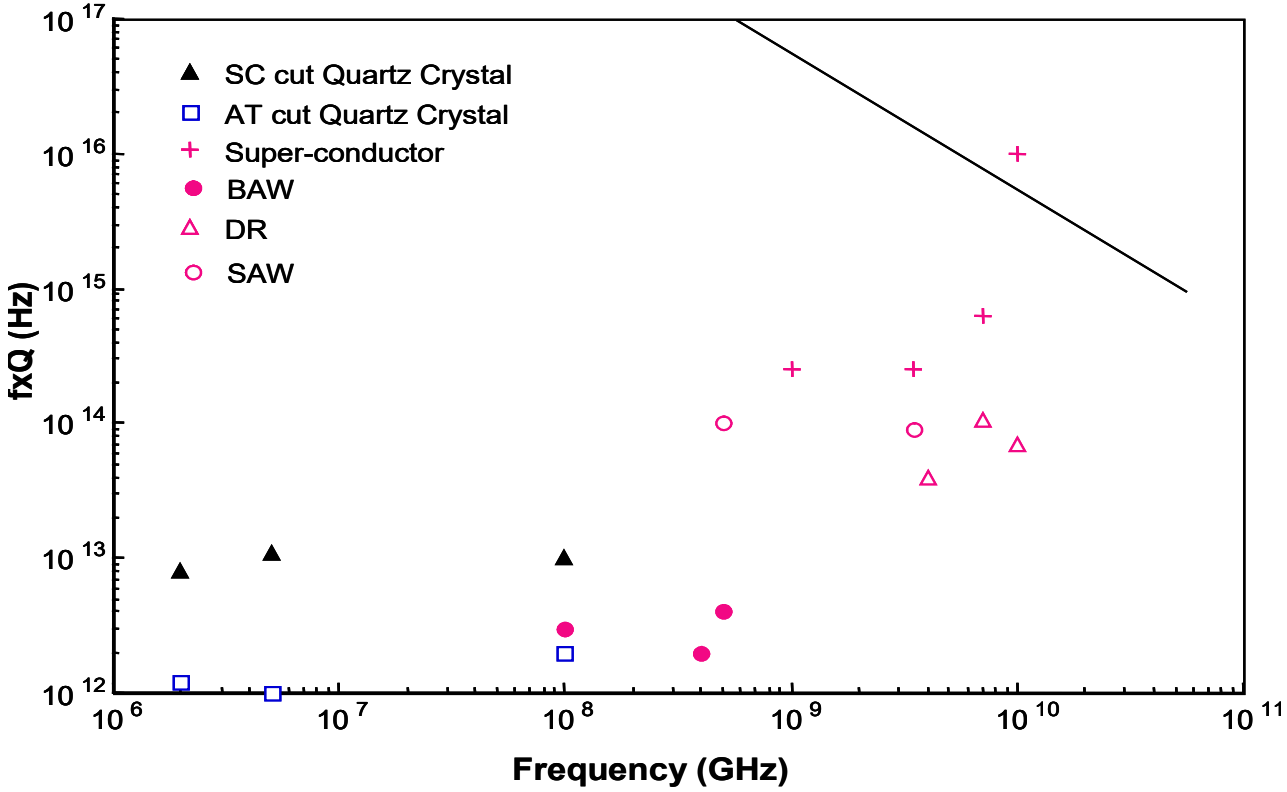

Oscillator Performance: Technologies

Resonator Technology		f_{osc}	Q_C	Phase Noise (dBc/Hz)	Stability (ppm/ C)
Quartz	BAW	<200MHz	10^5	*100MHz* : -140 @ 100Hz <-170 @10kHz	0.1
	SAW	< GHz	10^5	*1GHz* : <-130 @ 1kHz	< 2
Coaxial Cable		300MHz to 3GHz	10^2 - 10^3	*1GHz* : -70 @ 1kHz -110 @ 10kHz	100
Metallic Cavity		L-C Band	~10^3 - 10^4	≈*4GHz* : -110 @ 10kHz	100
DRO	Ceramic	L to Ku Band	~10^4	~*1GHz* : -159 @ 10kHz ~*4GHz* : -133 @10kHz ~*10GHz* : -118 @10kHz	0.1-10
	Sapphire	L to X Band	>10^5	*4.85GHz* : -138 @ 1kHz -170 @ 10kHz	NA

Courtesy: Online images, Table and view graphs from Internet

Phase Noise: Effect of Resonator Q

Effect - Low Q

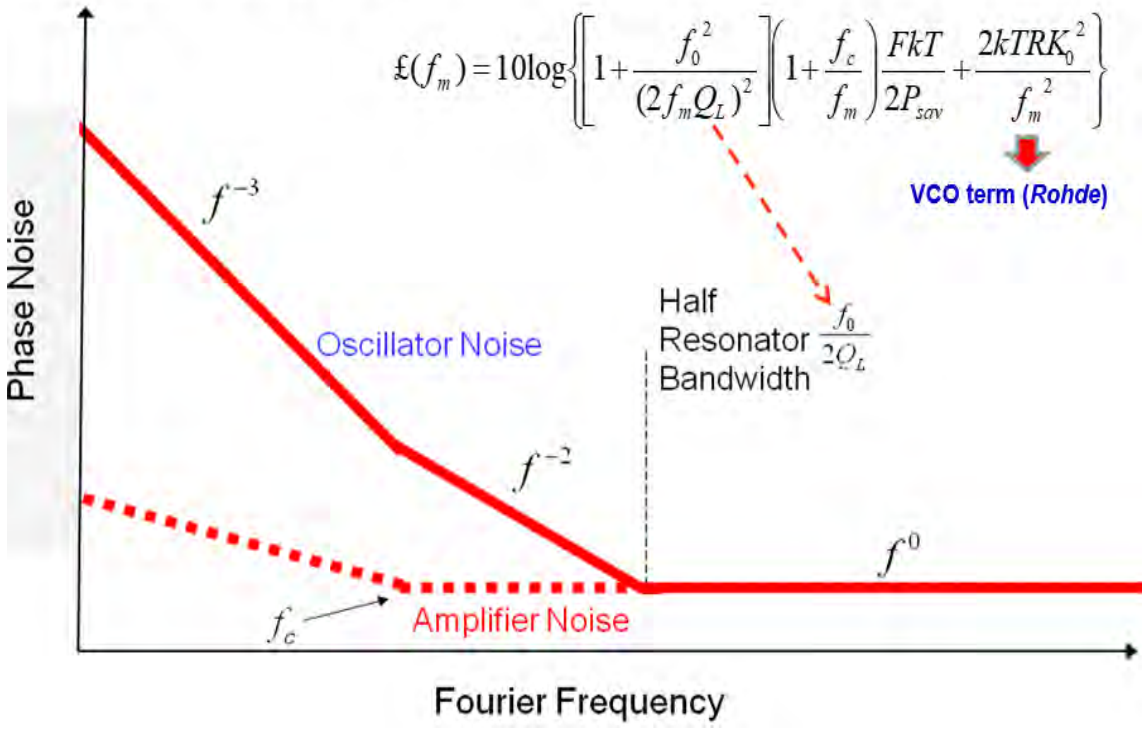

Effect - High Q

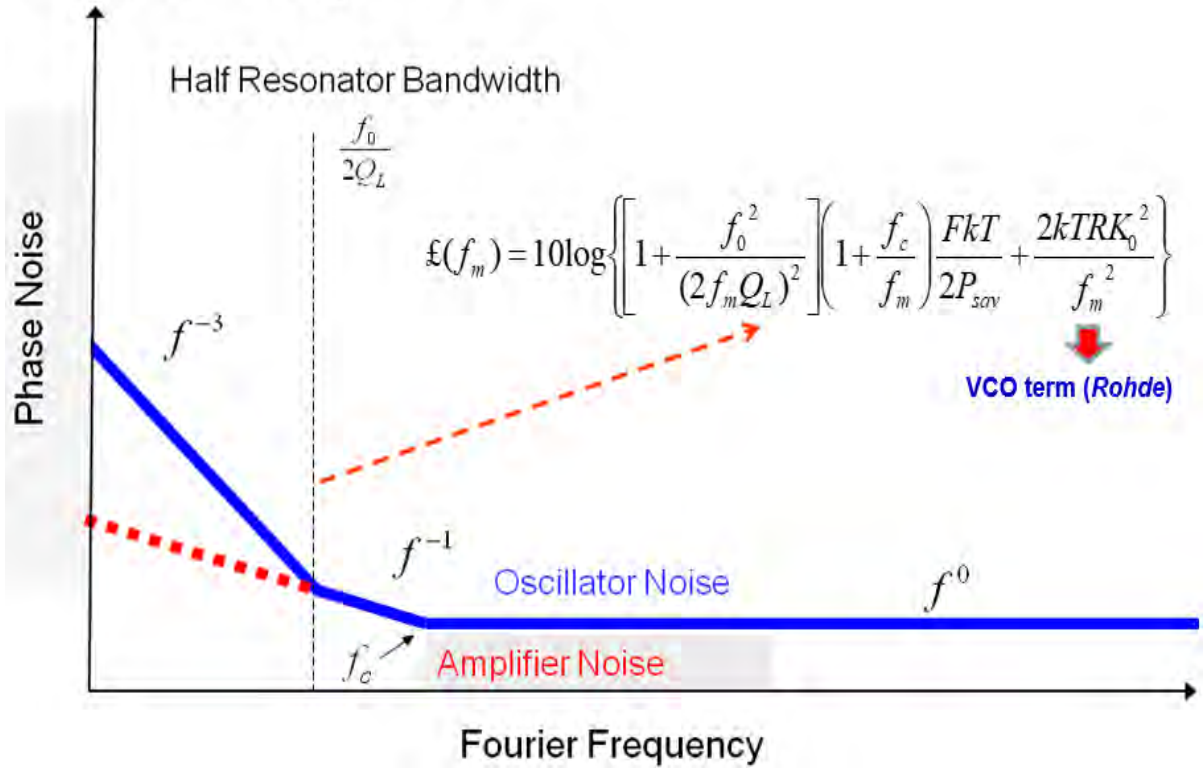

Phase Noise Reduction Techniques

- Phase Noise-Why Care ?
  - Important in Communication System and Transmitter
- Noise Reduction techniques
  - Use of multiple devices
  - Noise detection and reduction via feedback.
  - Noise enhancement (carrier nulling), amplification, and reduction via feedback and feed-forward techniques.
  - Optimum Transconductance & Impedance Matching
  - Coupled Oscillator-N-Push Topology
  - Injection-Mode-Coupling
  - Vibration Induced Noise-Isolator
  - Maximizing the Q and group delay

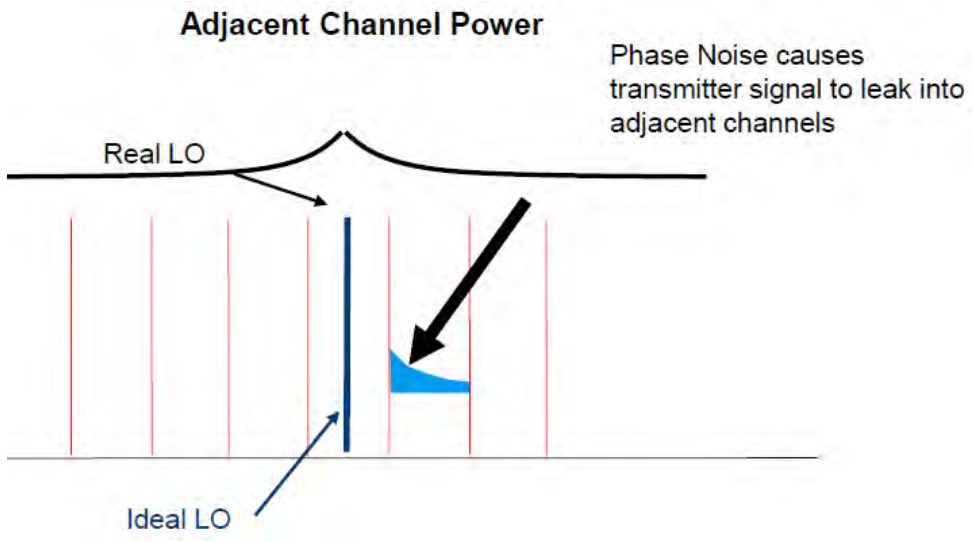

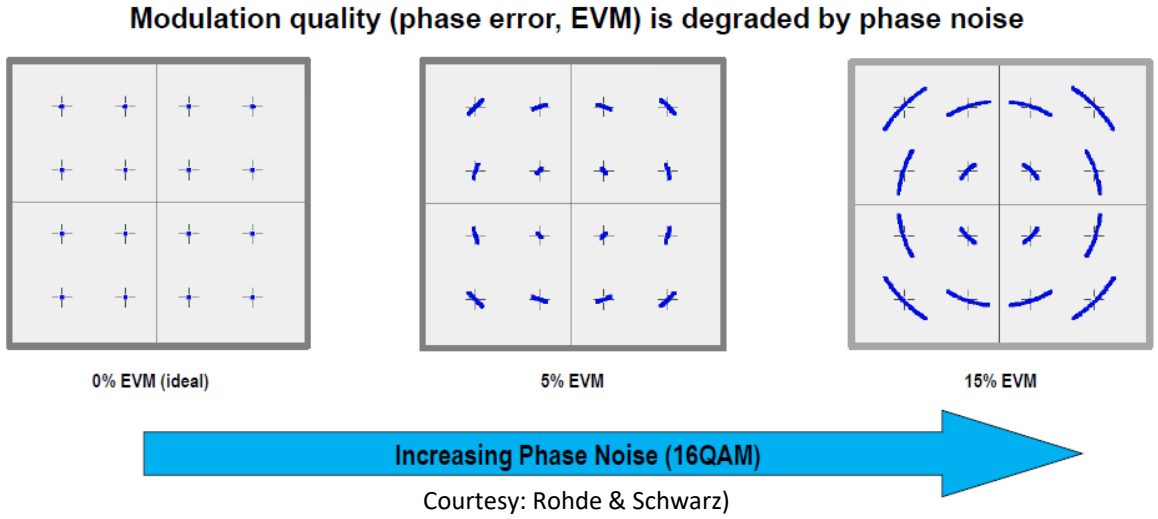

Courtesy: Rohde & Schwarz)

Phase Noise: In digital Design

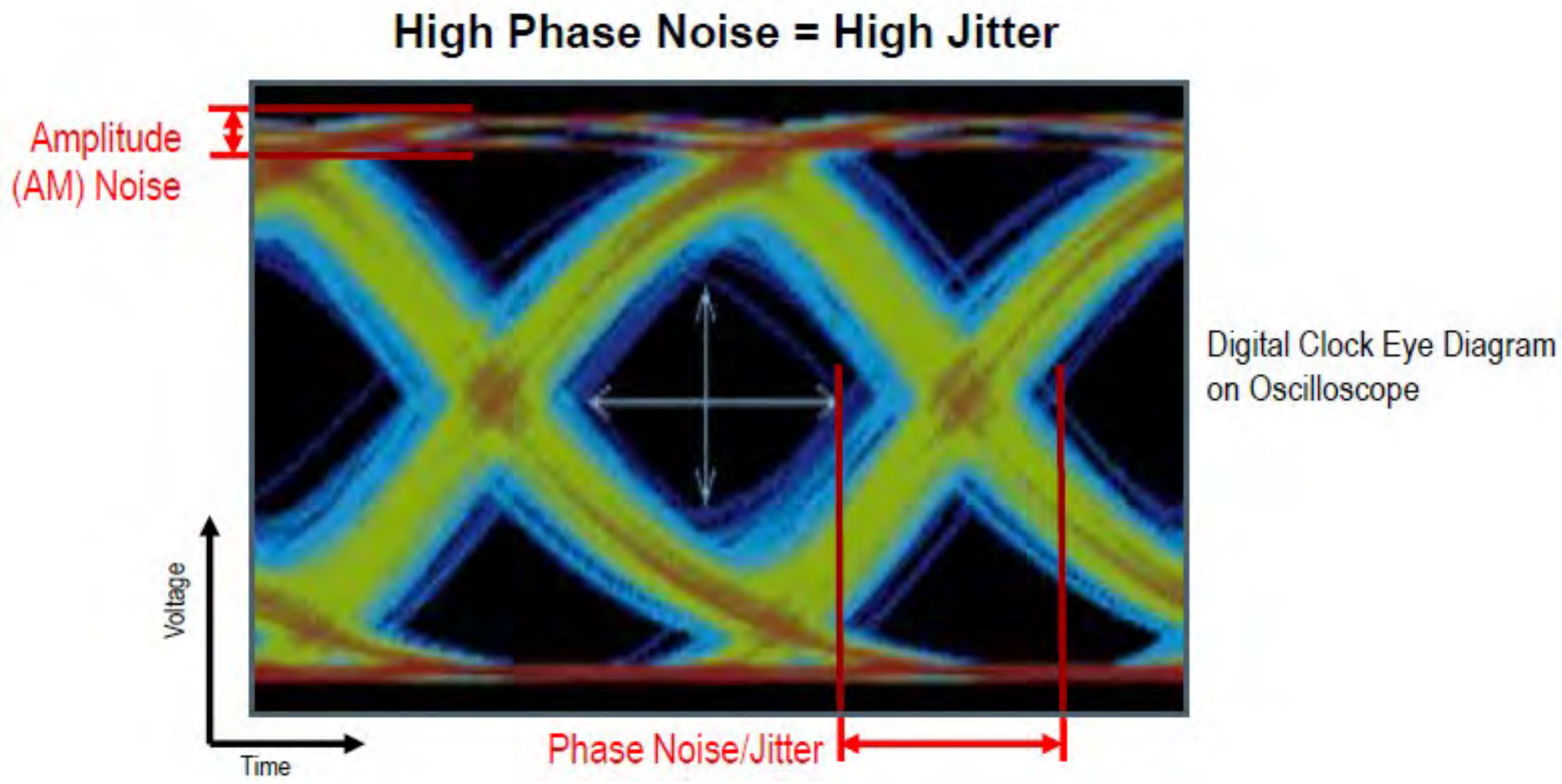

Jitter peaks can cause transmitted symbol errors which increase bit error and limit usable data rate

Courtesy: Rohde & Schwarz)

Phase Noise Reduction Techniques

Use of Multiple Devices

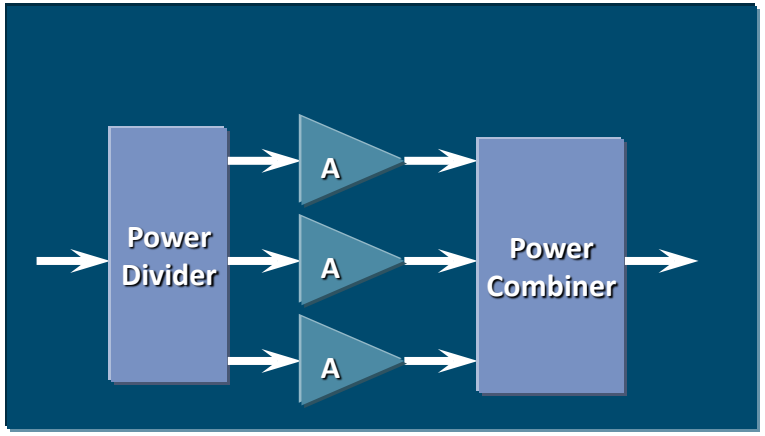

- Individual device (amplifier) noise is un-correlated.
- Net effect is a 10Log(N) decrease in flicker-of-phase noise.
- Additive (KTBF) white noise is not reduced because signal level at each amplifier is reduced by the input power divider.

Ref. Michael Driscoll, Tutorial Lecture 2018

Noise Detection and Reduction via Baseband Feedback

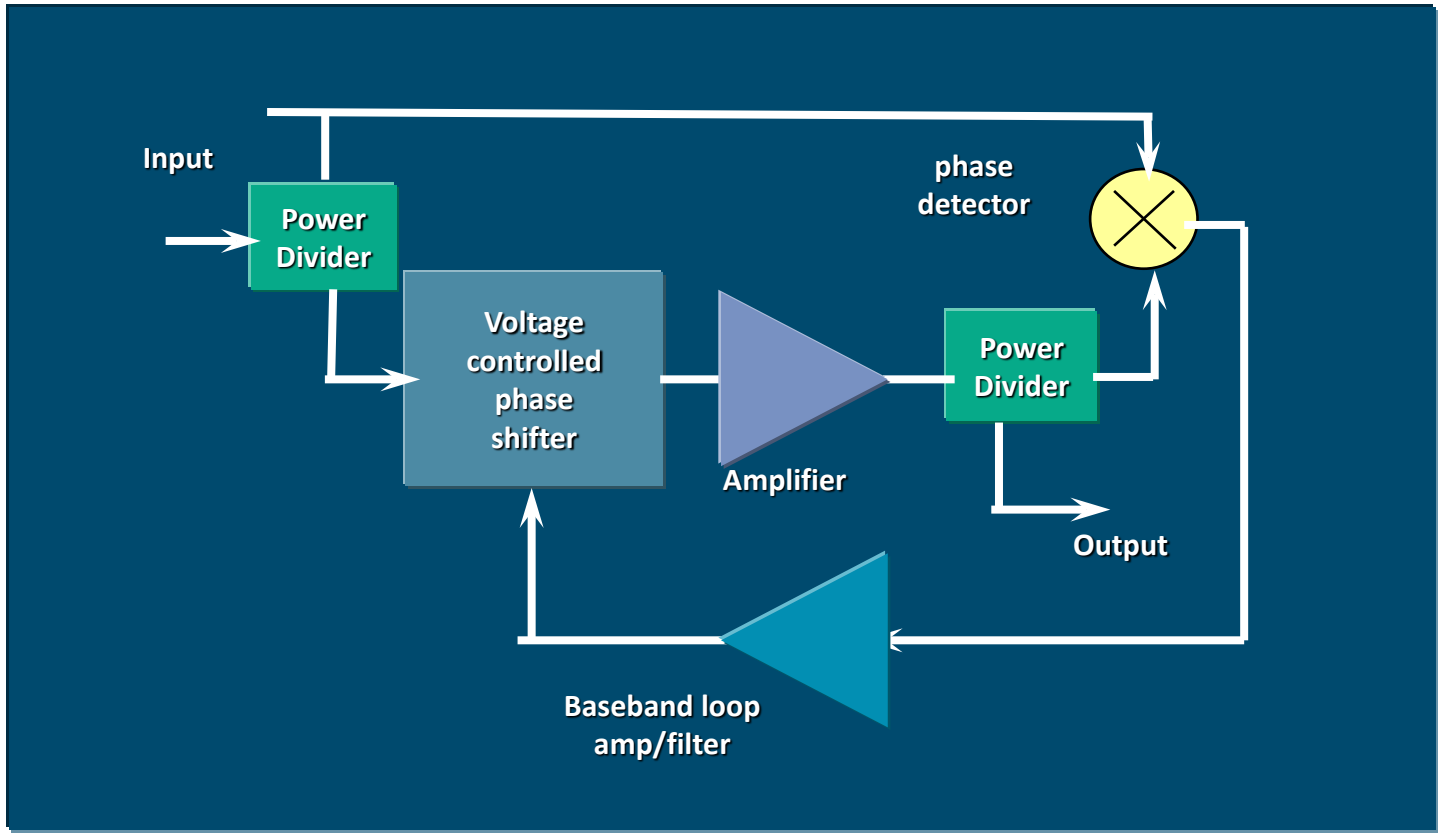

- Noise feedback used to reduce amplifier phase noise.
- Noise reduction is limited to noise of the phase detector and loop amplifier.

Phase Noise Reduction Techniques

Noise Detection/Reduction via Feedback from a delay line discriminator

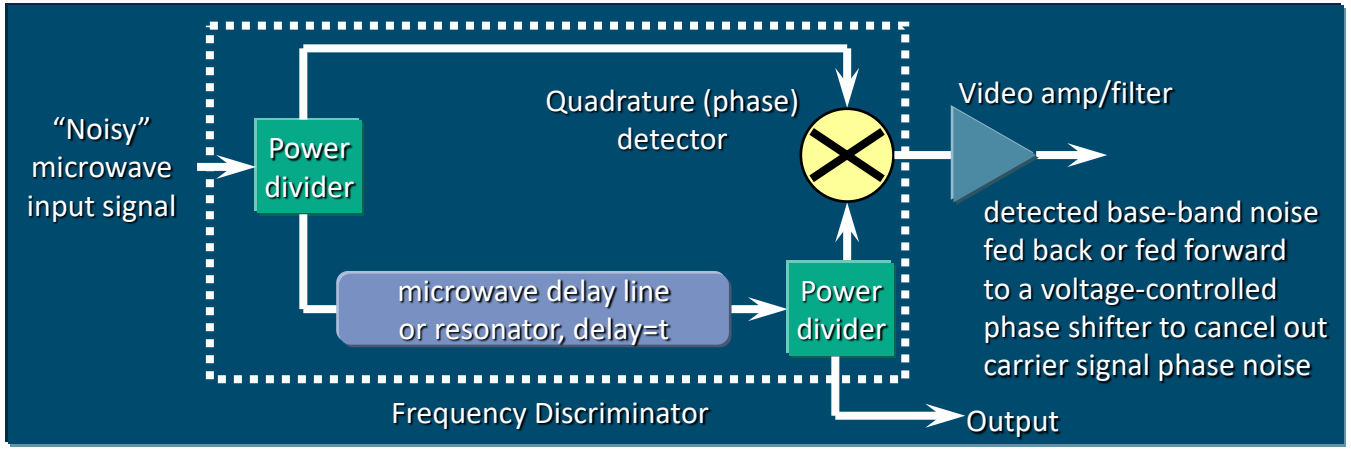

- Large delay needed to obtain high detection sensitivity.
- Large delay implies high delay line loss and/or small resonator bandwidth.
- Effectiveness (sensitivity) decreases with decreasing carrier offset.
- Carrier nulling can be used for noise enhancement prior to detection.

Ref. Michael Driscoll, Tutorial Lecture 2018

Noise Enhancement (carrier nulling), Amplification, and Reduction

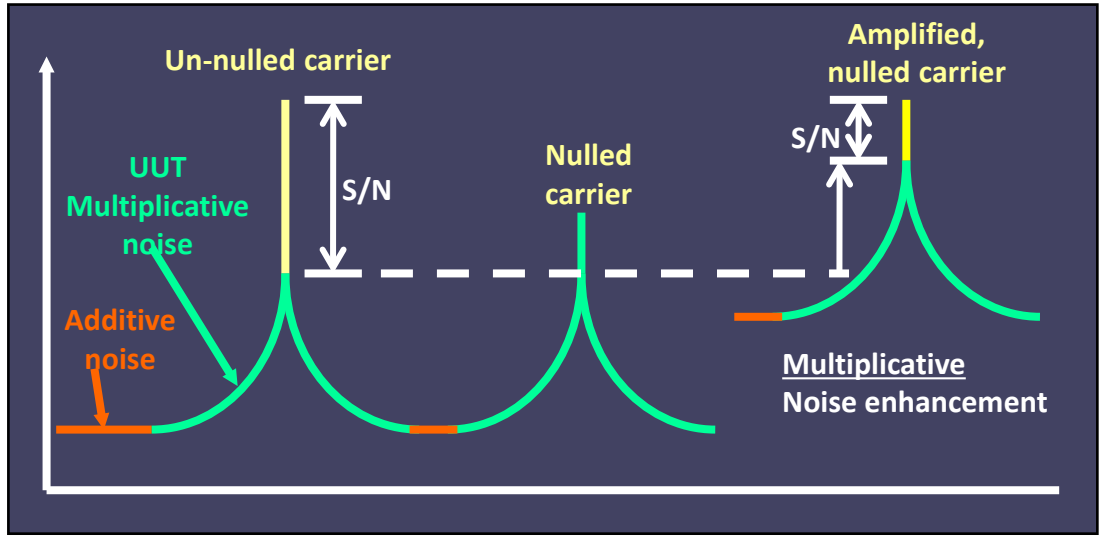

Noise reduction is normally accomplished via RF signal feed-forward or baseband detection with feedback techniques

Phase Noise: Optimum Transconductance

Noise Minimization Techniques

- Optimum Transconductance
- Impedance Matching

Influence of Transconductance

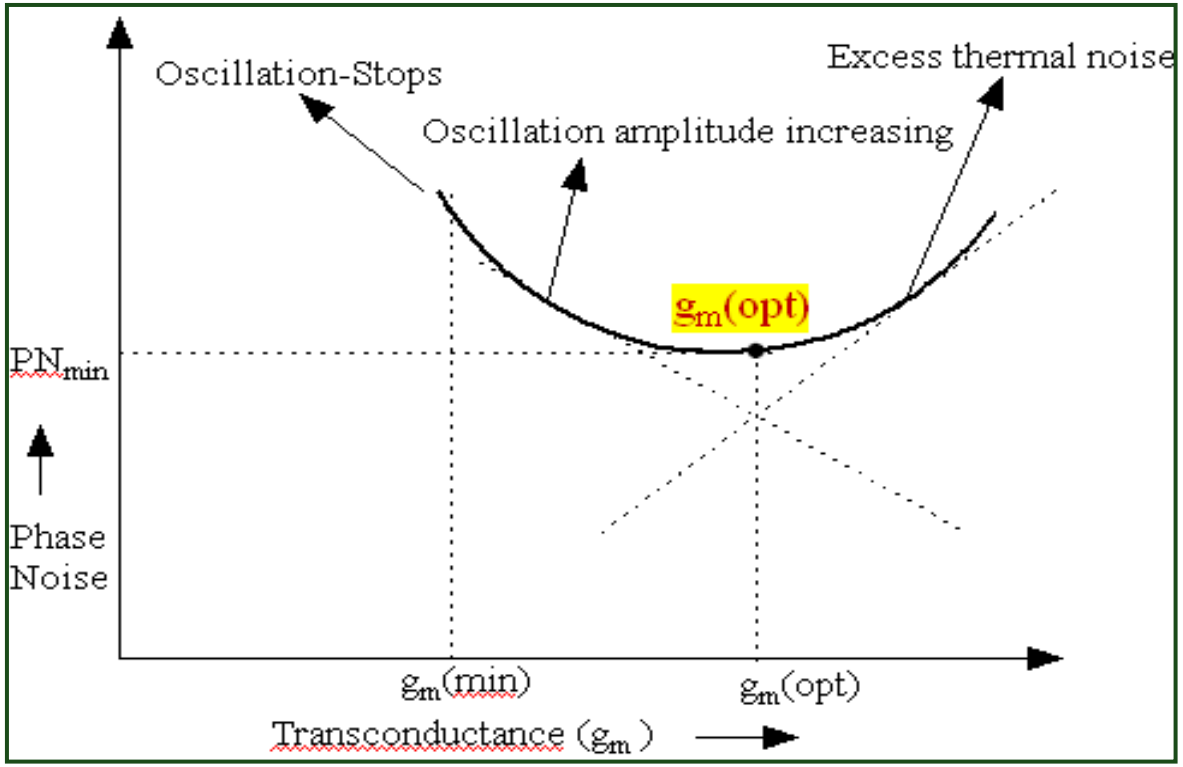

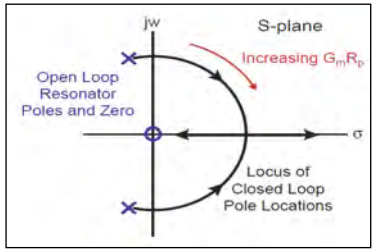

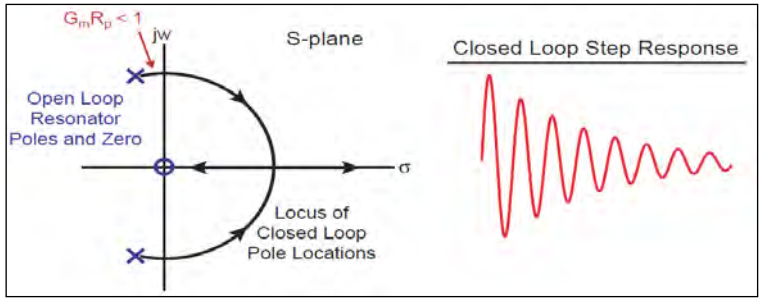

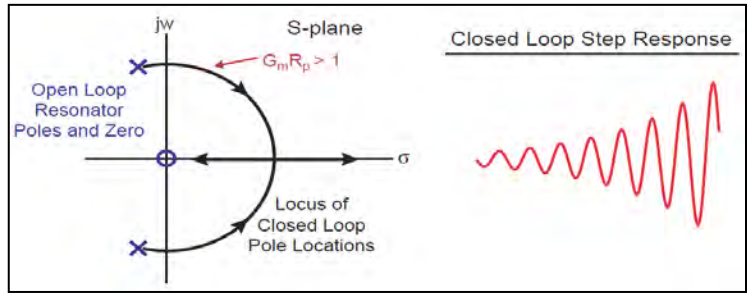

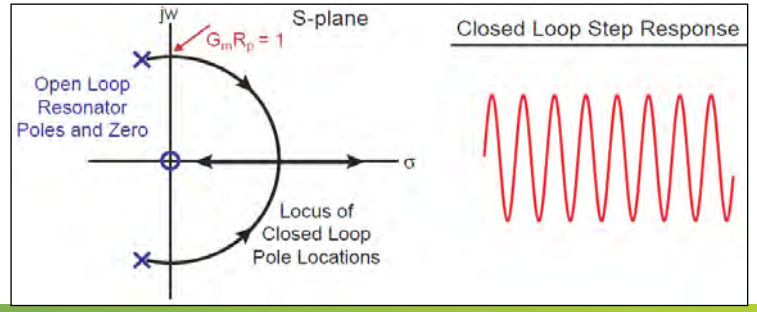

CourOnline images and view graphs tesy: from Internet

MMR Inspired Resonator

- MMR (Mobius Metamaterial Resonator)Technology
  - **Metamaterial : Artificial Composite Structure**
  - **Metamaterial Based Microwave Sensors**
  - **Metamaterial Resonator Based Oscillators**

- Möbius Technology
  - **Möbius Strips**
  - **Möbius Strips Resonator: Applications in Oscillators, Synthesizers**
  - **Möbius Resonator Based Microwave Sensors**

What are Metamaterials (MMs)?

MM: Engineered materials possessing properties that are not available in nature .
Material properties are determined by the properties of the sub-units plus their spatial distribution.

For a << l → effective medium theory.

For a ~ l → photonic effects

a_0 << a << l (Material scale order determines the properties)

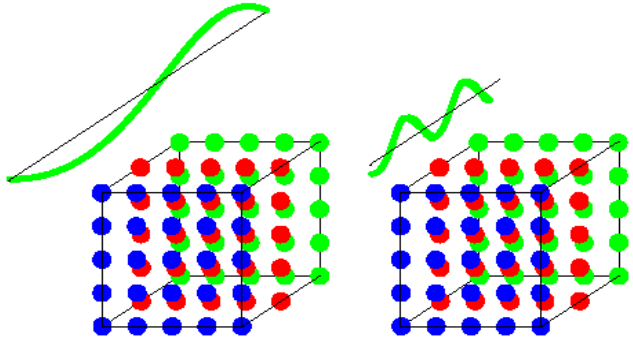

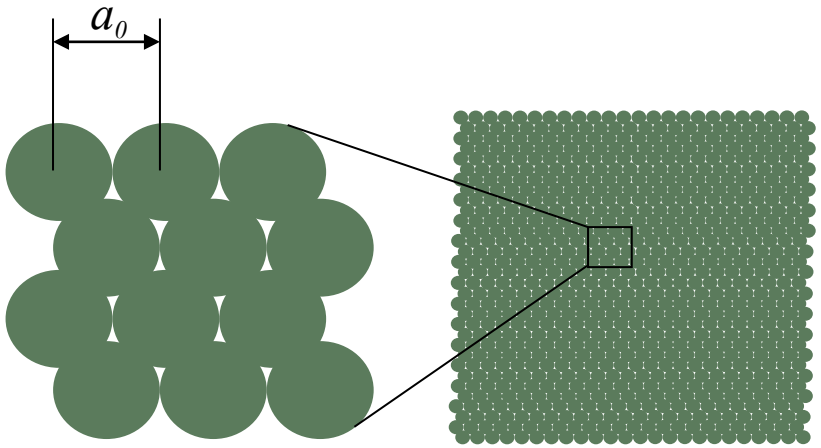

Atomic scale Atomic homogenization

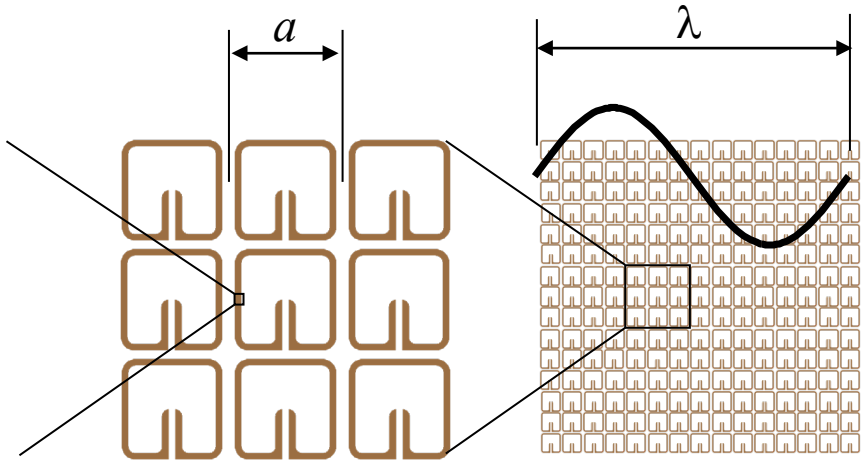

Meta-atomic scale Effective medium (second homogenization)

Courtesy: Online images and view graphs from Internet

Negative e, μ_r :Realization

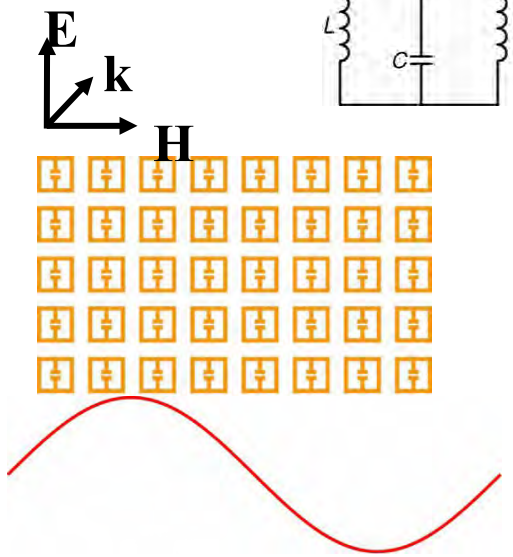

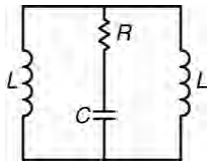

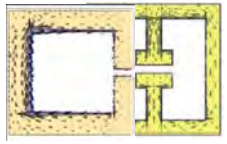

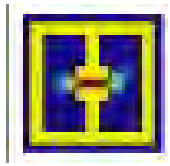

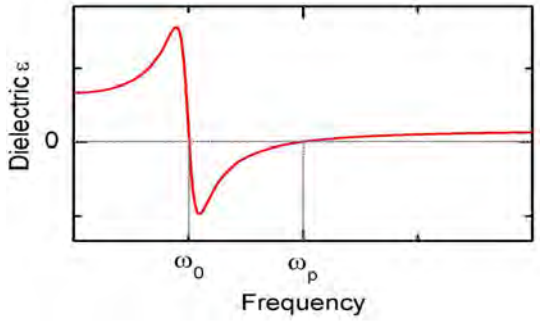

$\varepsilon < 0$ when $\omega_0 < \omega < \omega_p$

W. J. Padilla et al, Phys. Rev B 75 (2007).

$$\mu_{eff} = 1 - \frac{\frac{\pi r^2}{a^2}}{1 + \frac{2\sigma i}{\omega r \mu_0} - \frac{3}{\pi^2 \mu_0 \omega^2 C r^3}}$$

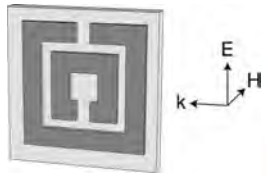

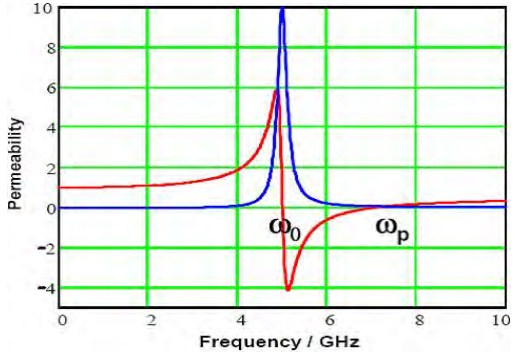

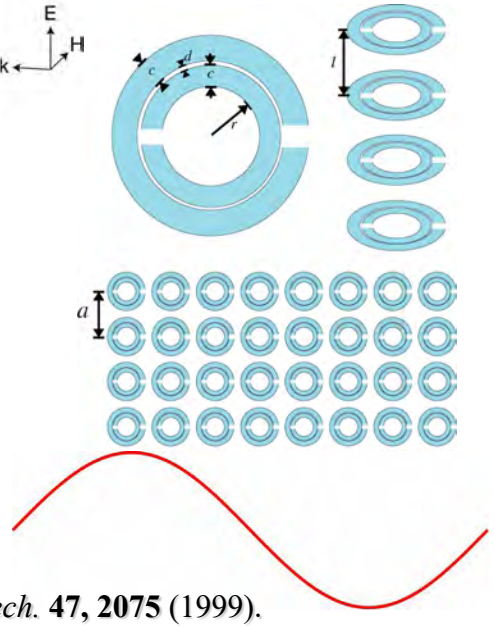

J.B. Pendry *et al.*, *IEEE Trans. Microwave Tech.* **47, 2075** (1999).

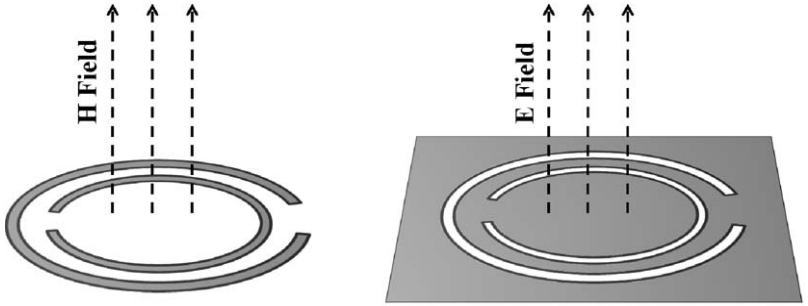

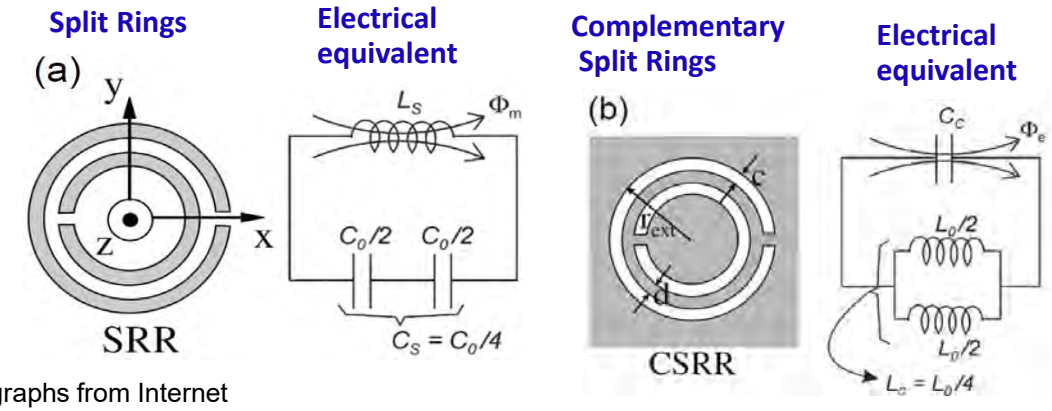

Courtesy: Online images and view graphs from Internet

Ring and Cut Wire Electrical Resonance

Array of thin conducting wires **Unit cell** **Permittivity**

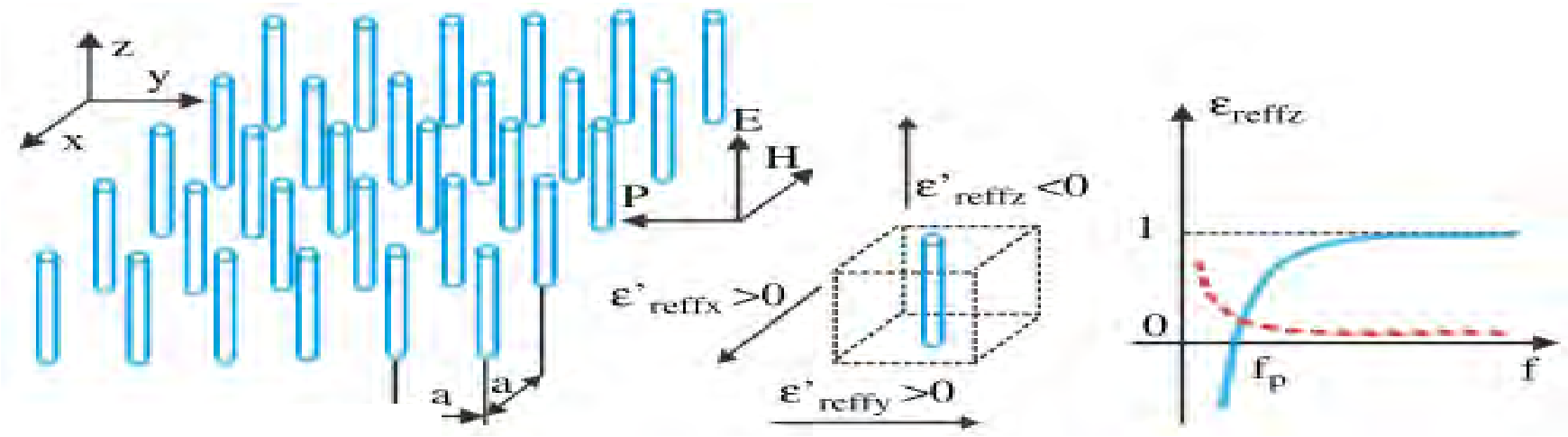

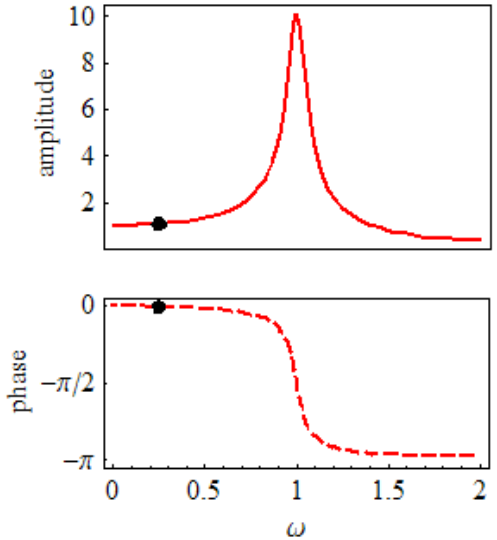

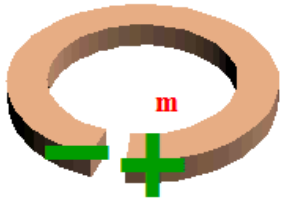

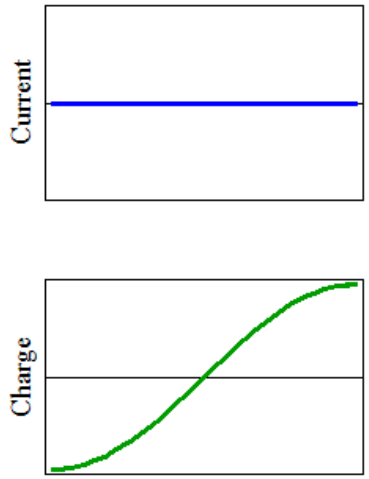

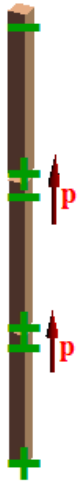

Ring and Cut Wire Electrical Resonators

Courtesy: Online images and view graphs from Internet

Tuning Electric & Magnetic Resonance

Re[μ]

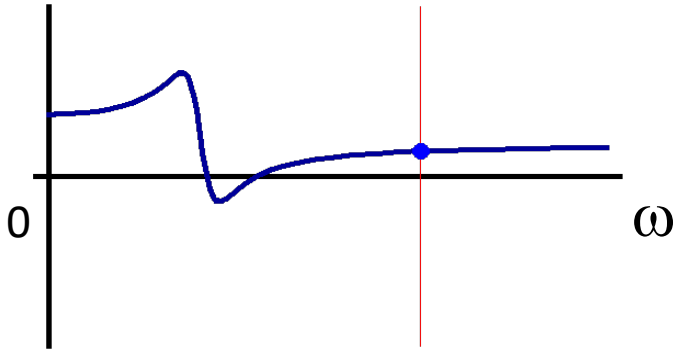

$$\omega_0 = \frac{1}{\sqrt{LC}}$$

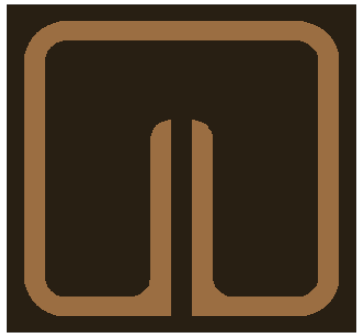

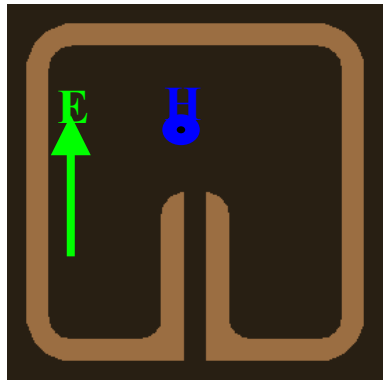

Re[ε]

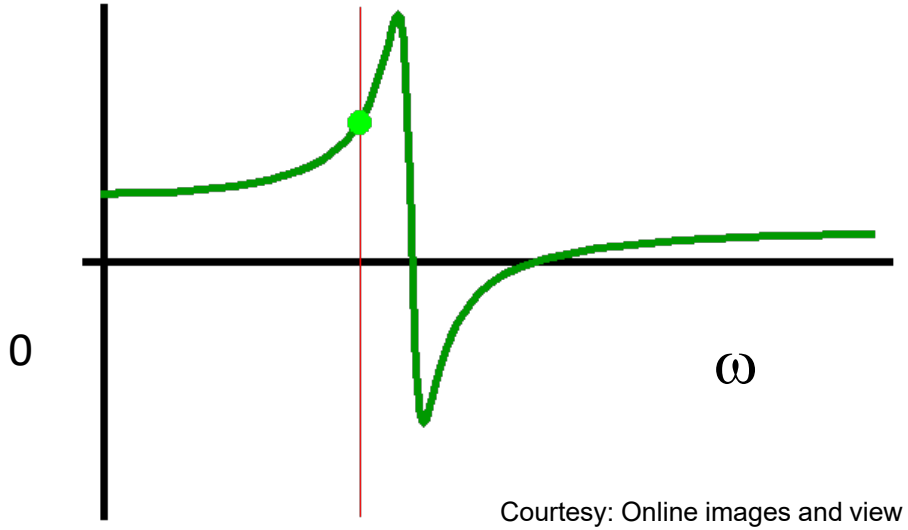

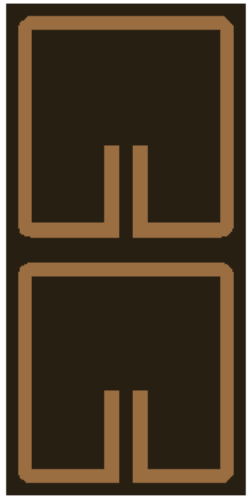

$$\omega_0 = \frac{1}{\sqrt{LC}}$$

Courtesy: Online images and view graphs from Internet

Regenerative Resonance: VCO Application

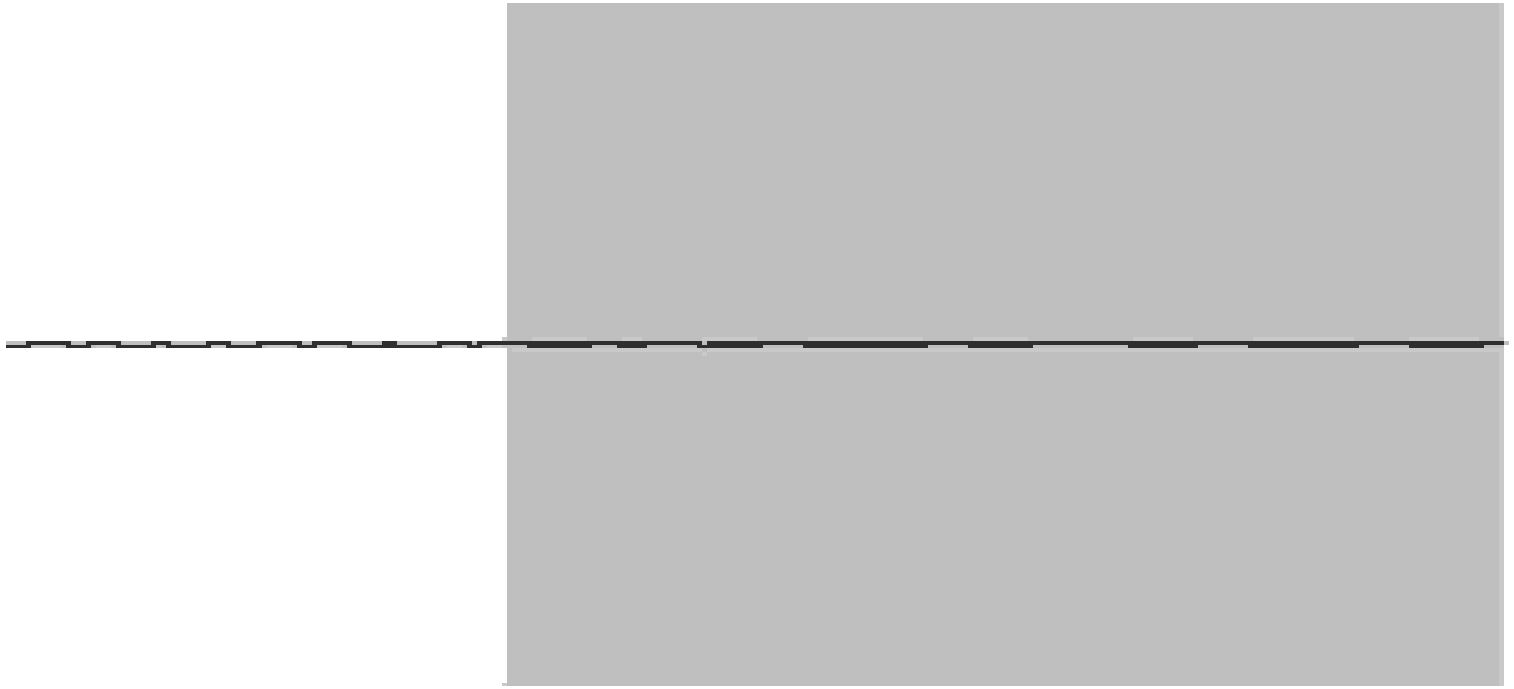

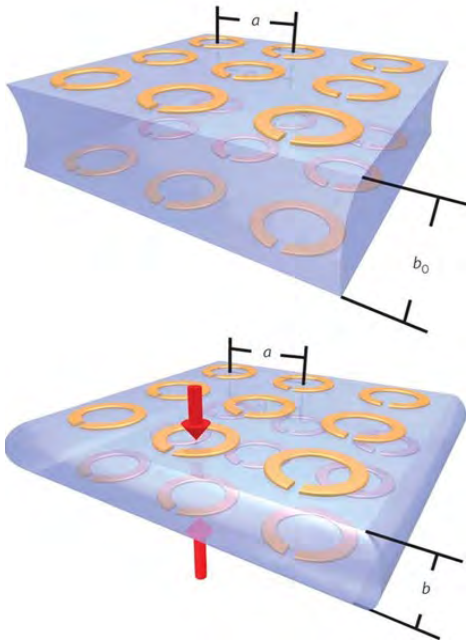

+ve Index Medium

-ve Index Medium (Evanescent Mode amplification)

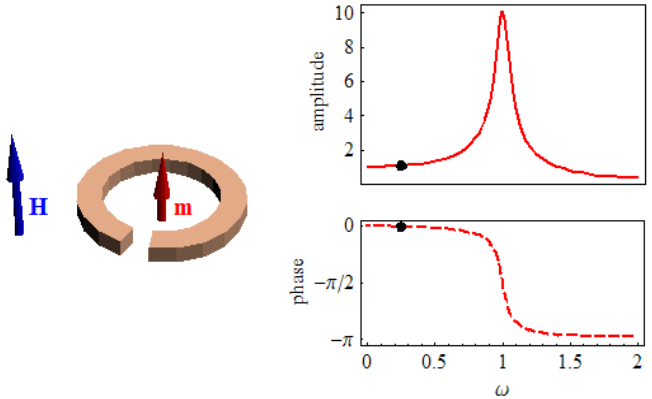

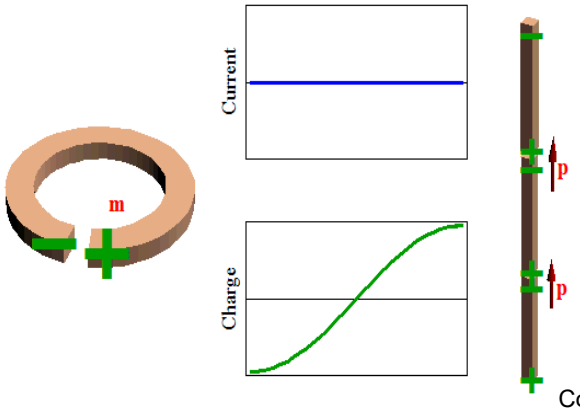

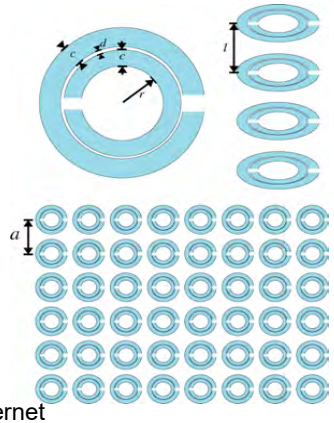

Courtesy: Online images and view graphs from Internet

Metamaterial Resonator Realization (SIW)

a. X-band

b. C-band

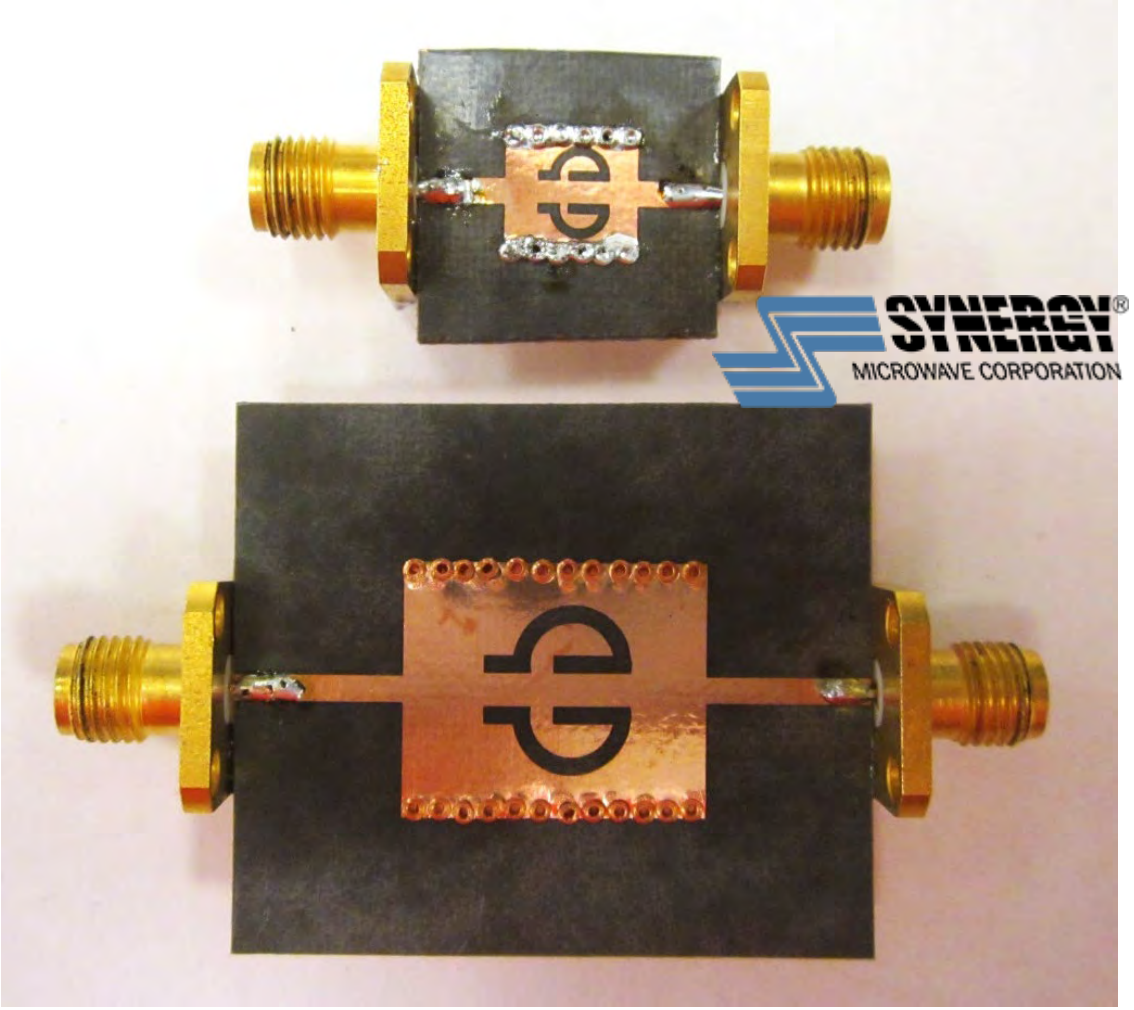

Complementary Coupled Resonator using Substrate Integrated Waveguide (SIW) Cavity

Ref.: . M. Wu, and Tatsuo Itoh , Ulrich L. Rohde, Ajay K. Poddar , "A C-band Tunable Oscillator Based on Complementary Coupled Resonator using Substrate Integrated Waveguide Cavity," *European Microwave Conference 2014.*

Metamaterial SIW Resonator Response

C-BAND

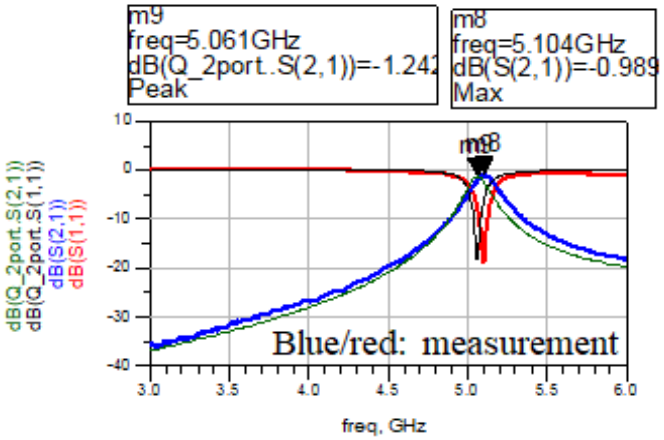

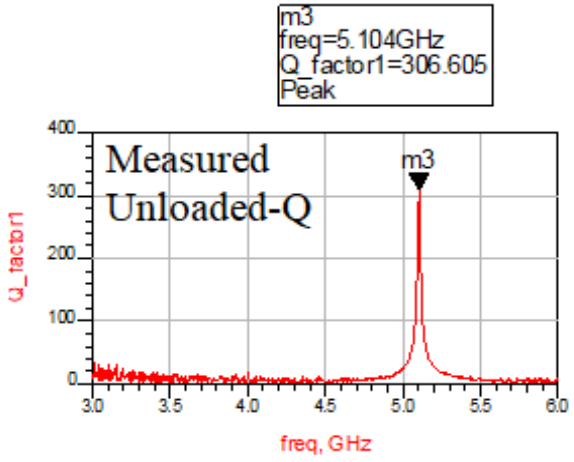

X-BAND

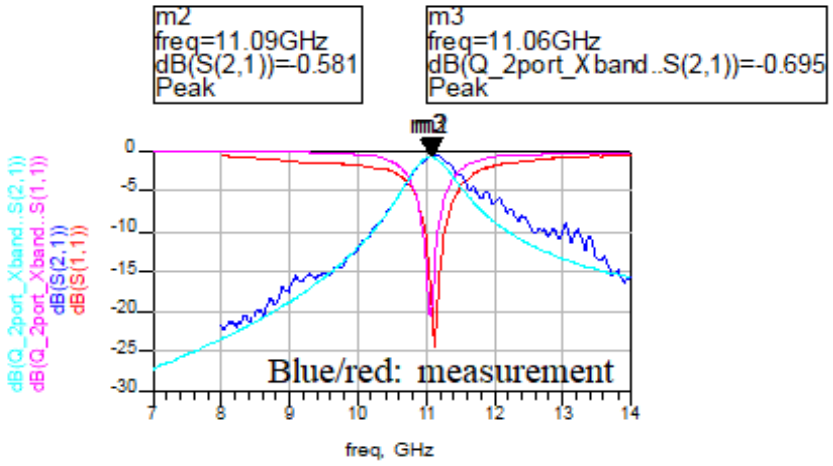

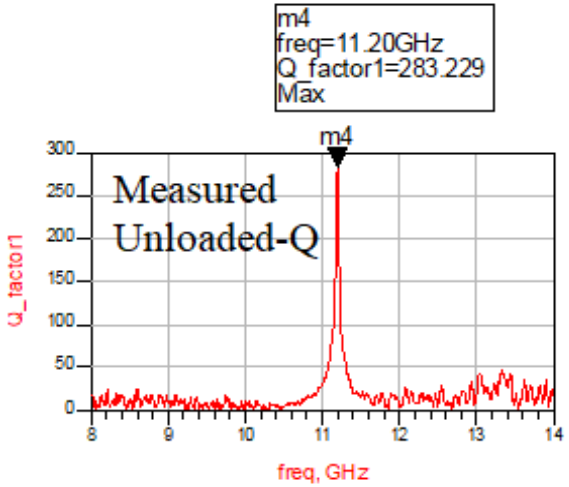

$$Q_{unloaded} = \frac{\omega_0}{2}\left|\frac{Z_{21}(\omega_0)'}{Z_{21}(\omega_0)}\right|$$

Ref.: . M. Wu, and Tatsuo Itoh , Ulrich L. Rohde, Ajay K. Poddar , "A C-band Tunable Oscillator Based on Complementary Coupled Resonator using Substrate Integrated Waveguide Cavity," *European Microwave Conference 2014.*

Complimentary Coupled Resonator (CCR)

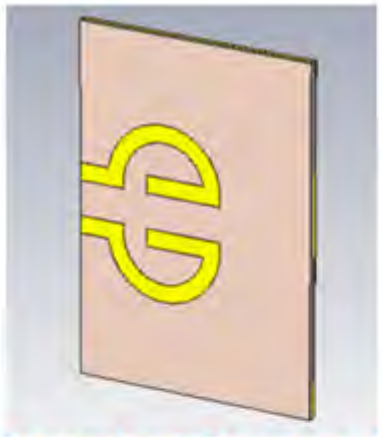

Coupled Resonator

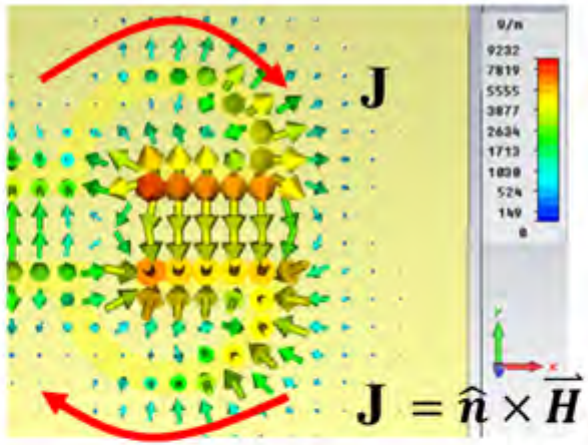

Unloaded Q of CCR

$$Q = \frac{\omega_0}{2}\left|\frac{Z_{11}(\omega_0)'}{Z_{11}(\omega_0)}\right|$$

$=270$

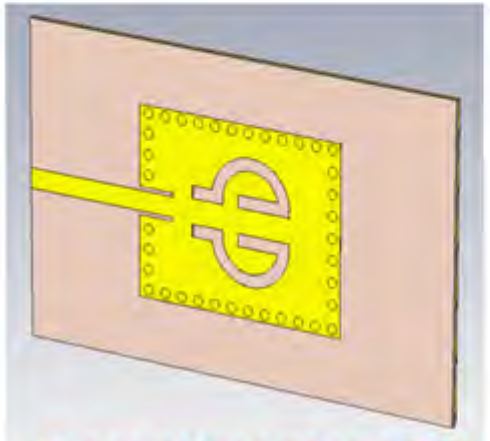

Complimentary CR

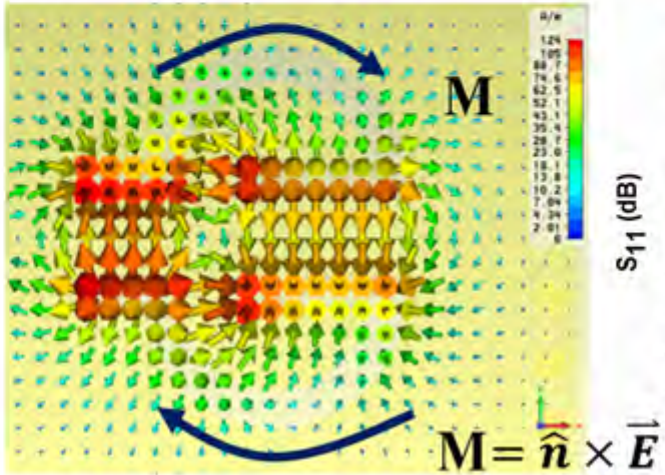

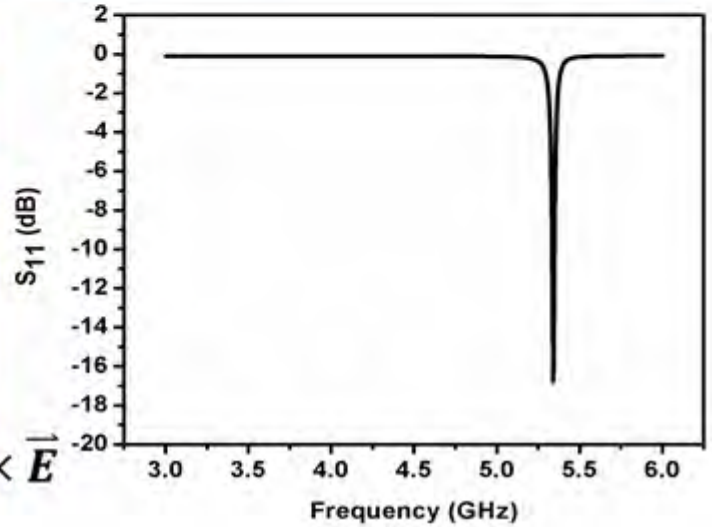

Ref.: . M. Wu, and Tatsuo Itoh , Ulrich L. Rohde, Ajay K. Poddar , "A C-band Tunable Oscillator Based on Complementary Coupled Resonator using Substrate Integrated Waveguide Cavity," *European Microwave Conference 2014.*

Tunable C-Band Oscillator Using MMR

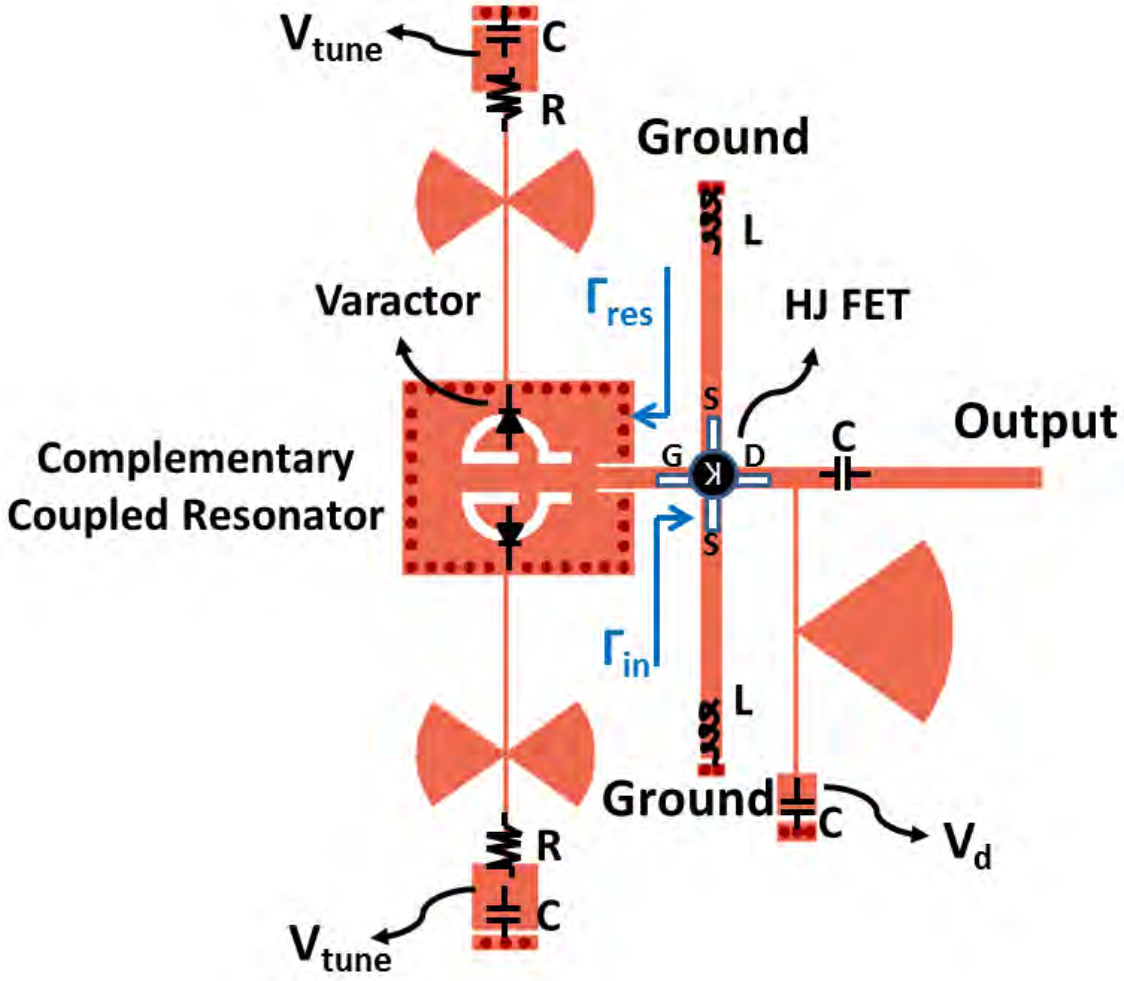

Circuit Layout

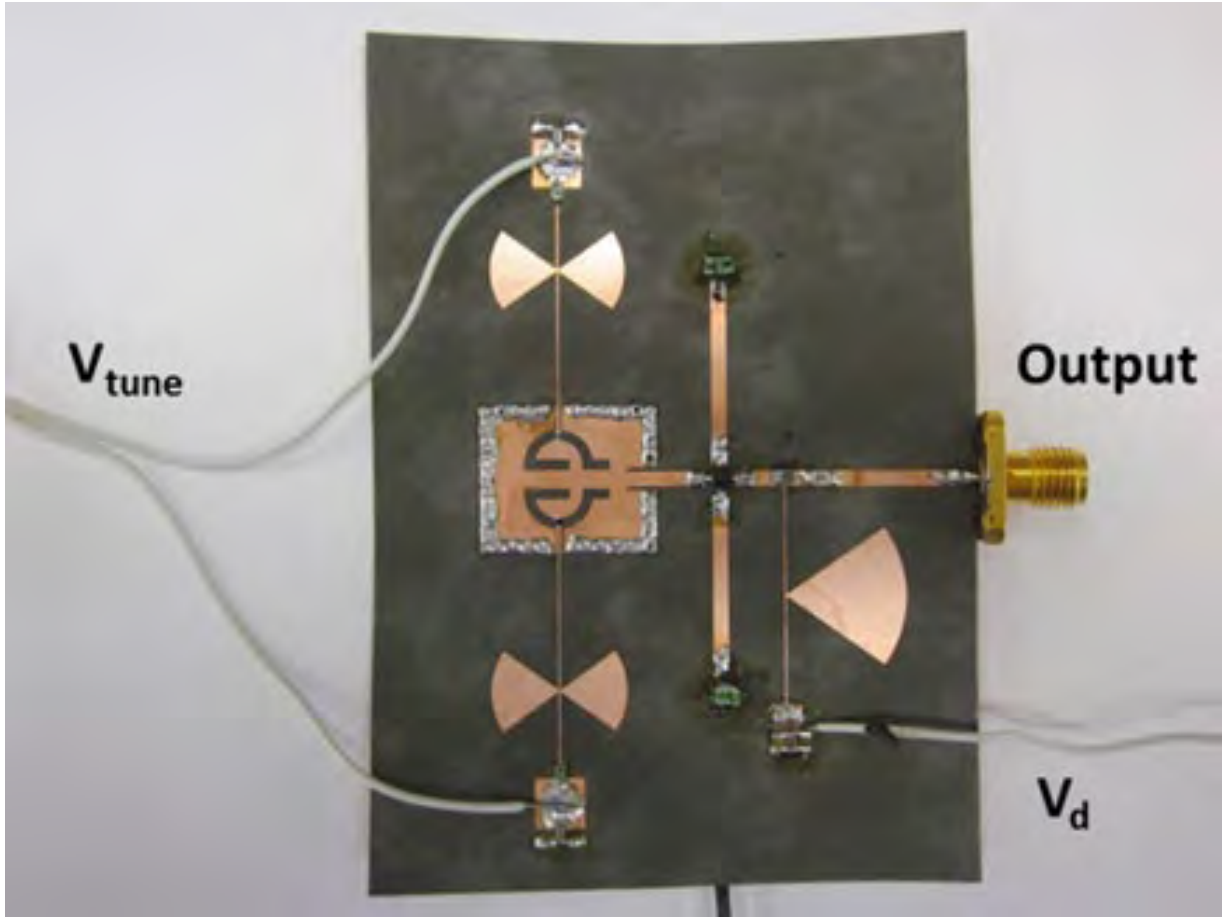

Fabricated Prototype

Ref.: . M. Wu, and Tatsuo Itoh , Ulrich L. Rohde, Ajay K. Poddar , "A C-band Tunable Oscillator Based on Complementary Coupled Resonator using Substrate Integrated Waveguide Cavity," *European Microwave Conference 2014.*

Tunable C-Band Oscillator Using MMR

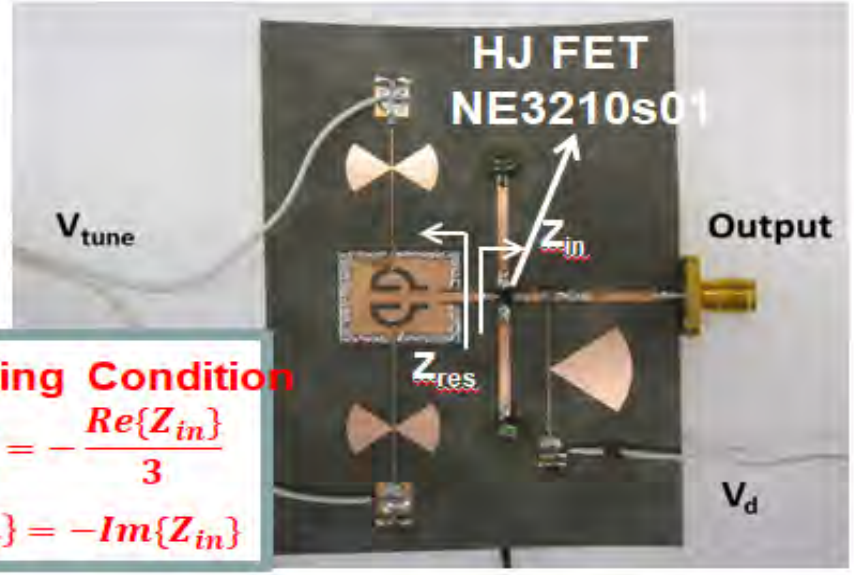

Oscillating Condition

$$Re\{Z_{res}\} = -\frac{Re\{Z_{in}\}}{3}$$

$$Im\{Z_{res}\} = -Im\{Z_{in}\}$$

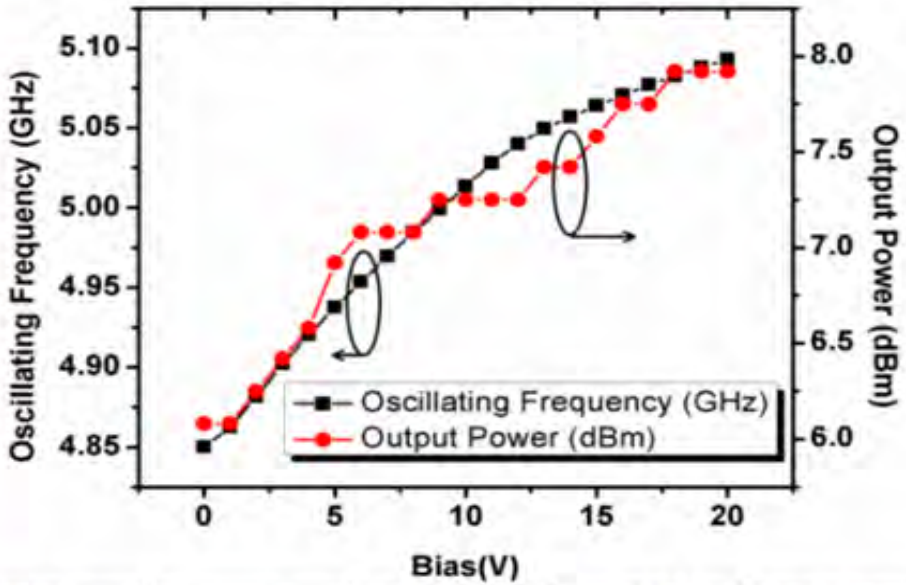

	f_0 (GHz)	f_{offset} (MHz)	PN @ 1MHz	P_{DC} (mW)	Po (dBm)	$\eta_{DC\text{-}RF}$ (%)	Tuning (%)	FOM	Technology
This Work	5.09	1	-115.2	33	8	19.12	5.15	-174.1	PCB-SIW
[1]	2.675	0.1	-105.5	168	5.33	2	0	-171.8	PCB-SIW
[2]	3.77	0.1	-99.63	161.5	10.83	7.5	0	-169.1	PCB-SIW
[3]	7.92	4644	-118	300	-3	0.166	58.5	-171.2	PCB-SWMR

[1] A dual-band oscillator with reconfigurable cavity-backed complementary split-ring resonator," in IEEE MTT-S 2012, pp. 1–3.
[2] CCR Oscillator IEEE MTT-S 2013, [3] SIW Oscillator IEEE MTT-S 2014

Active CCR for *X*-band Oscillator

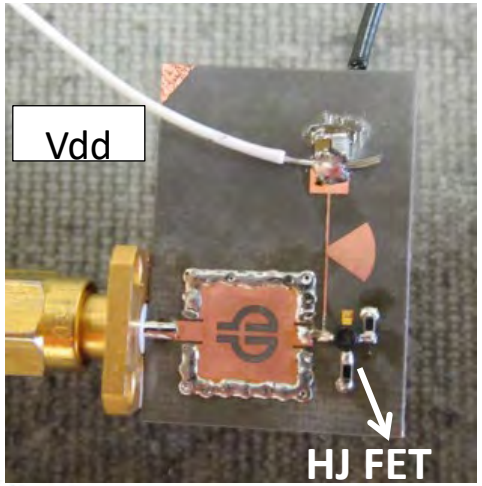

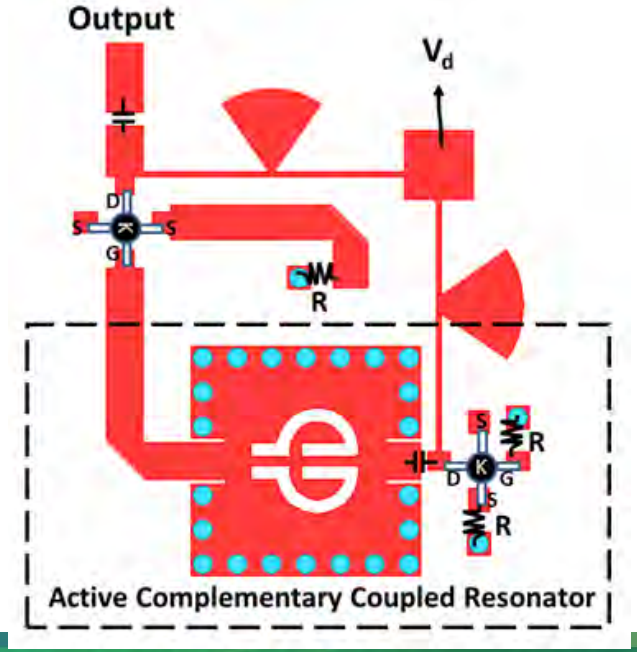

Footprint=1 square inch

Vdd	0V	0.65V	1V	1.2V
Unloaded Q	130.7	95.6	706.3	1913.1
Vdd	1.4V	1.6V	1.8V	2.0V
Unloaded Q	3390	7249	21172	6938.5

Oscillator Summary

	Oscillating Frequency	Output Power	Phase Noise@1MHz	FOM
Simulation	10.01GHz	0.043dBm	-137.9dBc	-203.54
Measurement	9.9285GHz	0.83dBm	-123.5dBm/Hz	-191.52

Ref. C. M. Wu, and Tatsuo Itoh, Ulrich L. Rohde, Ajay K. Poddar,, "A C-band Tunable Oscillator Based on Complementary Coupled Resonator using Substrate Integrated Waveguide Cavity," *European Microwave Conference 2014.*

Möbius Twist Metamaterial: Graphene

Graphene

- Single layer of graphite, exhibits mechanical properties like planar paper or plastic with large bulk modulus, easily bent and wrap into carbon nanotubes without deformation
- This unique characteristic qualifies to use Graphene as a promising material to build Möbius metamaterial strips for the applications in developing microwave and optical components for modern communication systems.

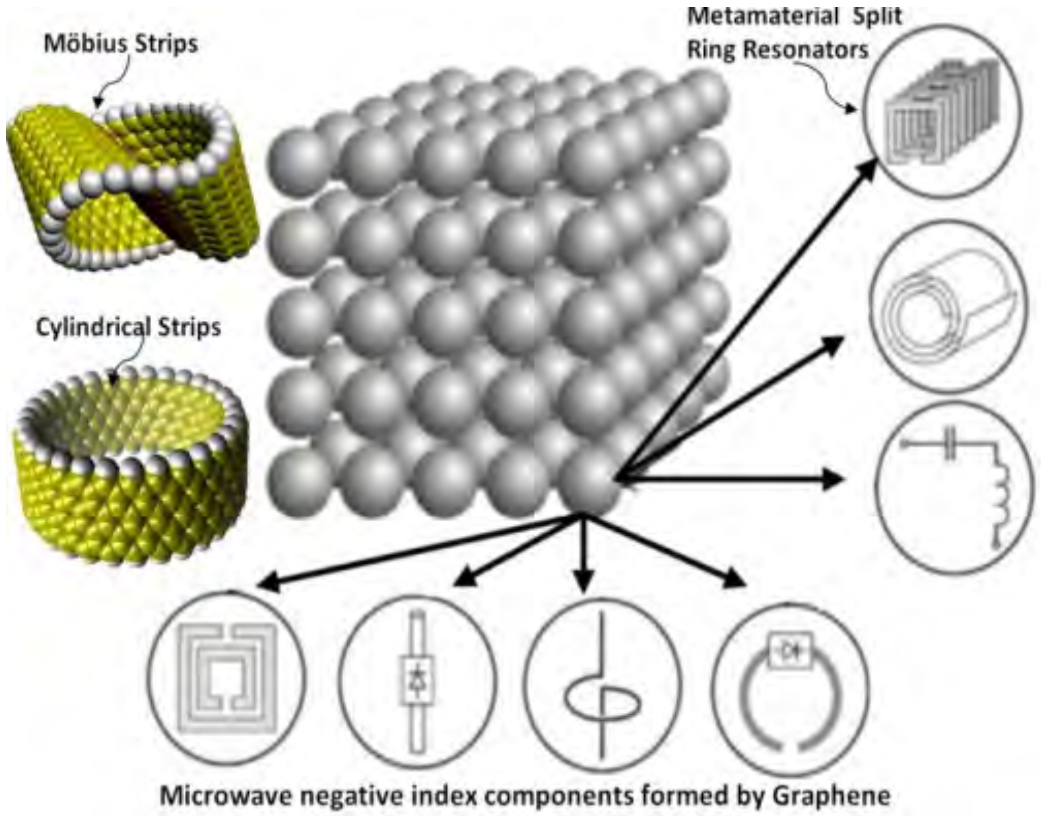

Figure shows the Metamaterial Möbius strips formed Graphene nano-ribbons behave as a topological insulator and possess topology-induced thermal and magnetic properties.

Ref. : Wang[1] investigated the stability and total magnetic moment (TMM) of Möbius strips with fixed length and different widths, the Möbius strips formed by Graphene nanoribbons found extraordinarily stable. These unique magnetic properties make the Möbius strips Graphene building blocks in spintronic devices.

Typical Möbius Strip Surface

- A typical Möbius is a surface with only one side and only one boundary component, the mathematical property of being non-orientable.
- The concept of the Möbius strips is based on the fact that a signal coupled to a strip shall not encounter any obstruction when travelling around the loop and the loop shall behave like an infinite transmission line, therefore exhibit large group delay resulting improved Q-factor.
- Challenge: 3-D structure not easily amenable for planar integrated circuit solution

➢ **Möbius Resonator Based Oscillator presents several advantages in comparison with conventional planar resonator for a given size :**

- high Q-factor and improved selectivity
- easy integration in MIC/MMIC technologies
- small dimensions and weight
- multi-band characteristics
- relatively insensitive to EMI and EMC

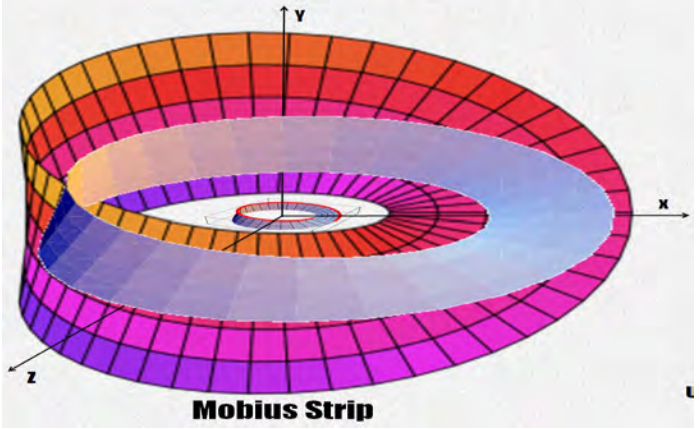

Courtesy: Online images and view graphs from Internet

Ref. A. K. Poddar, U.L. Rohde, D. Sundarrajan", Real Time Signal Retention Device using Co-planar Waveguide (CPW) as Mobius strip", 2013 IEEE MTT-S Digest, pp. 1-3, June 2013

Split Ring Resonator: Möbius Twist !

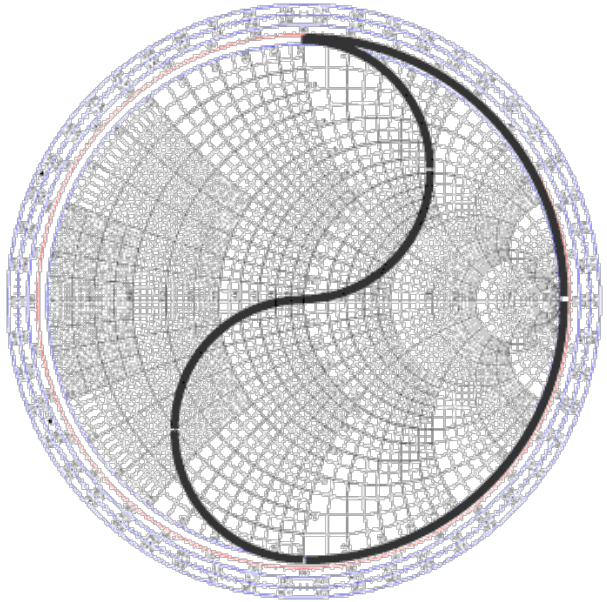

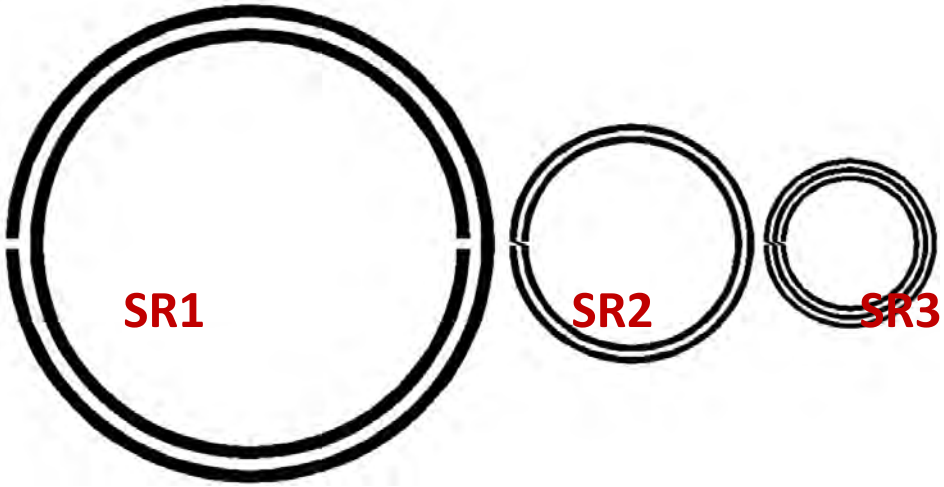

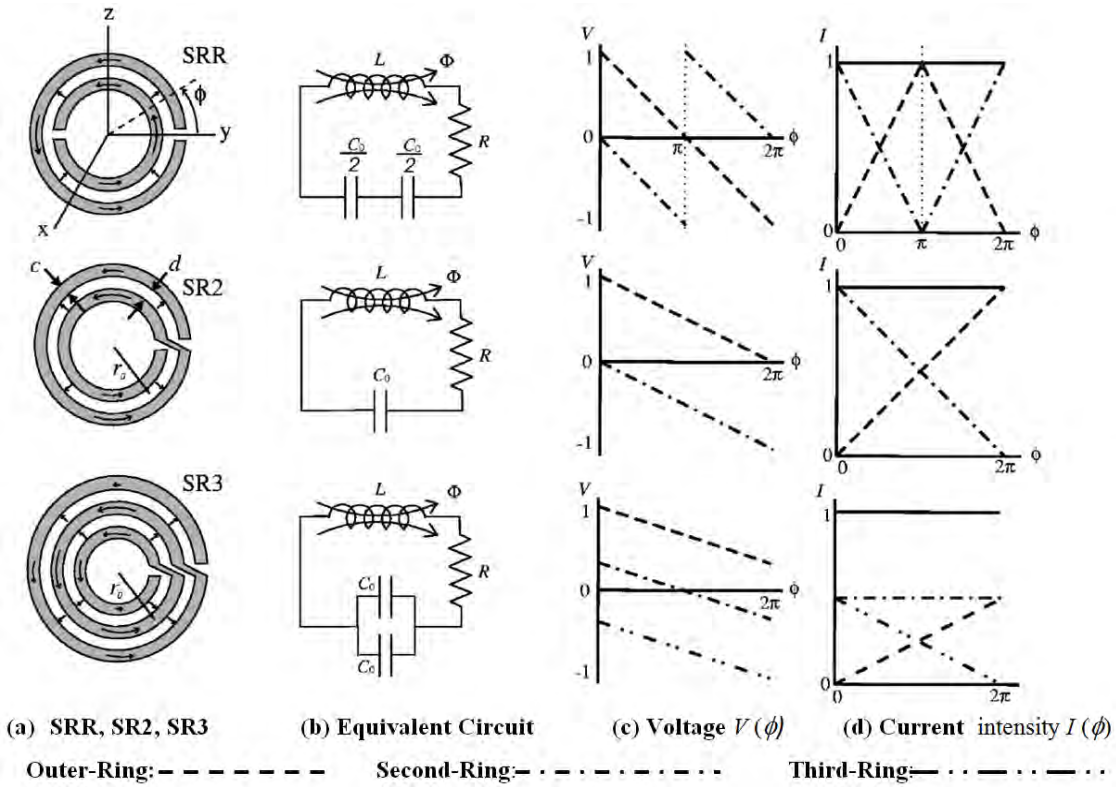

Figure: A typical comparison layout: (a) SR1 (b) SR-2, and (c) SR-3 (same resonance frequency, the reduction factors are about 50% and 65% with respect to the original SRR), SR-2 and SR-3 are promising topology for Möbius-Loop

Courtesy: Tao, online images and view graphs from Internet

Metamaterial Resonator

Dual-Band Resonator Oscillator using Metamaterial resonator

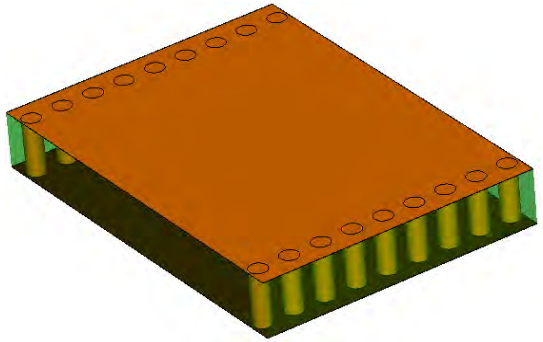

SIW Cavity

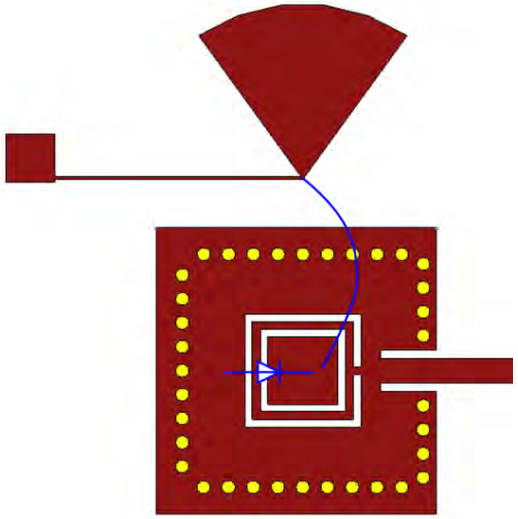

Reflective cavity resonator

Ref. A Dual-band Oscillator with Reconfigurable Cavity-Backed Complementary Split-Ring Resonator (T. Itoh, IMS2012)

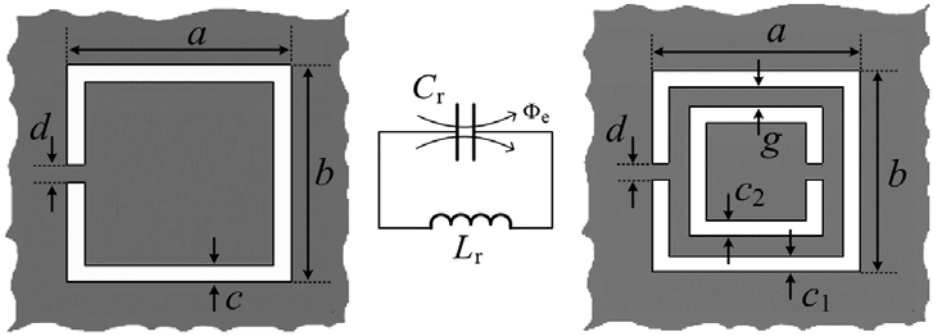

Single- and Double-Ring CSRR

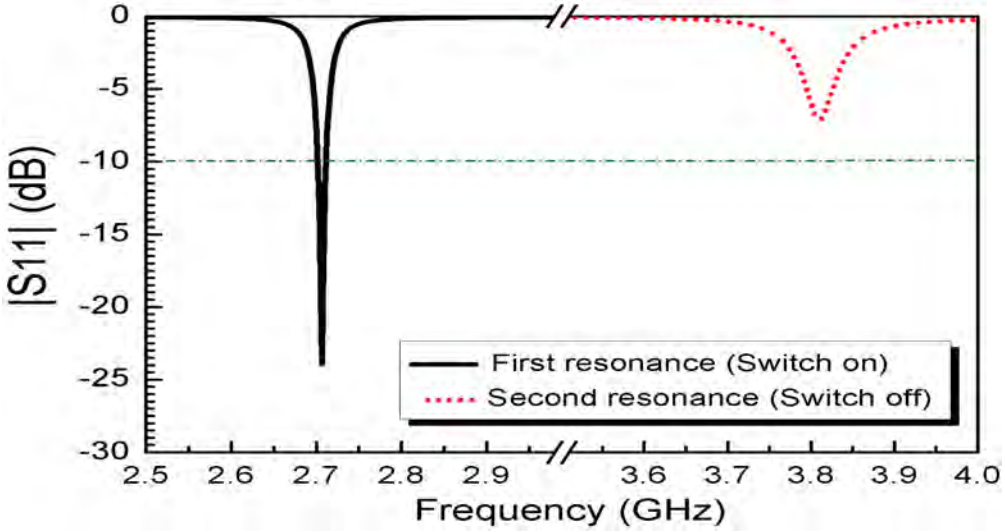

The resonance frequencies can be adjusted by changing the split length, as well as the length and width of the ring slots of the CSRR.

Emerging Technologies : Signal Sources

Dual-Band metamaterial Resonator Oscillator

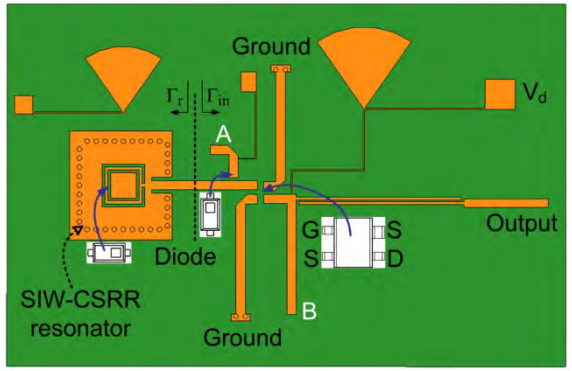

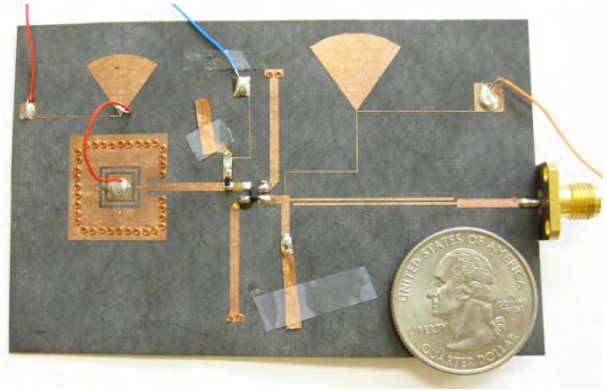

Substrate: Rogers 5880 substrate

Active Component:
Avago ATF-34143 low noise pHEMT

Diode: MADP-017015-1314 & MADP-008120-12790T

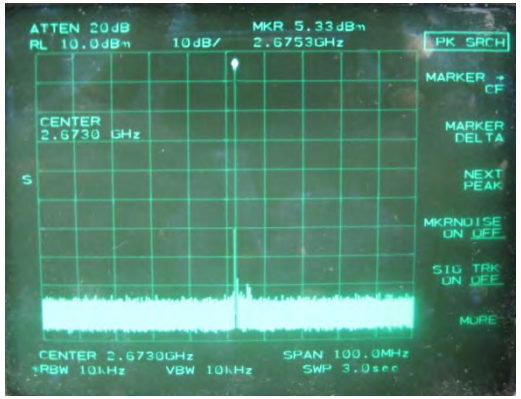

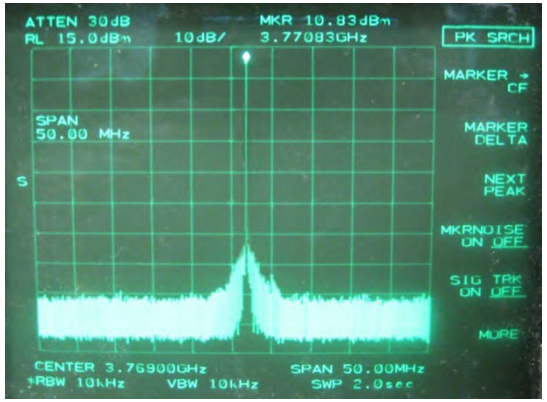

A Dual-band Oscillator with Reconfigurable Cavity-Backed Complementary Split-Ring Resonator, I(T. Itoh, MS2012)

Practical Applications: Möbius Strips Resonator

Möbius ring resonator exhibits a topological half-twist transformation divides into half-integral and integral normal mode indices. The eigenfunctions of the Möbius resonator form an orthogonal basis set; presents an interesting possibility for the design of high Q-factor resonator for the application in tunable oscillators, and filter circuits.

Printed Möbius Metamaterial Resonator

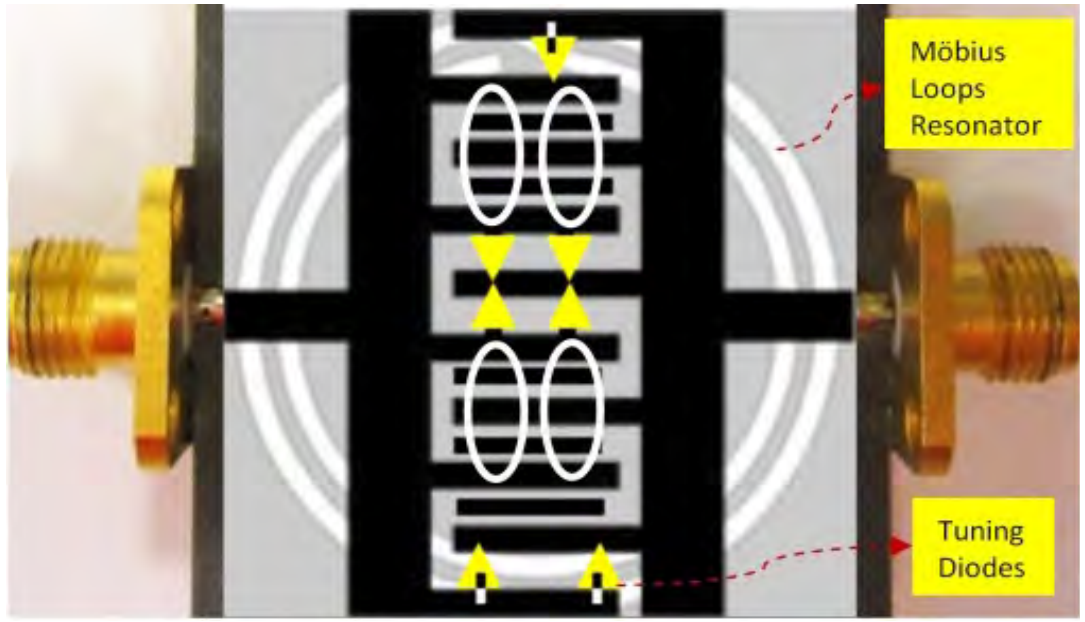

SYNERGY® MICROWAVE CORPORATION

Lumped Model

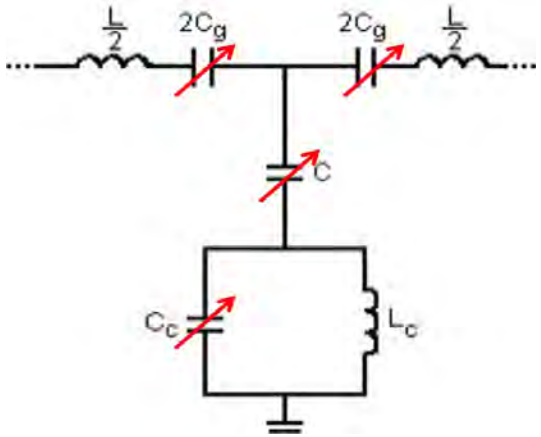

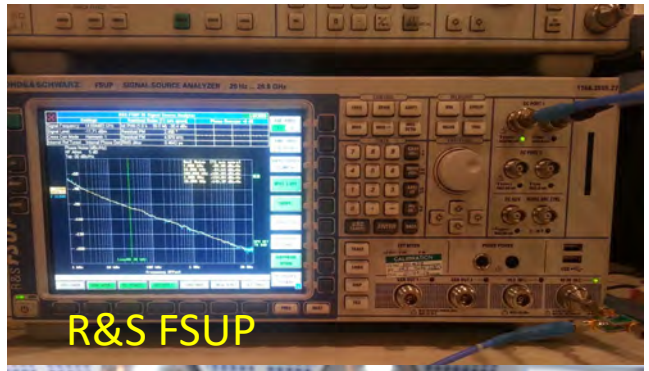

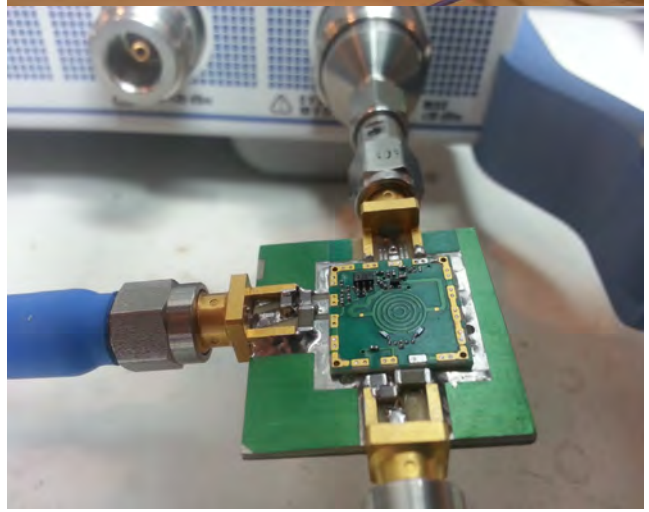

U. L. Rohde, A. K. Poddar, "Möbius Metamaterial Strips Resonator: Tunable Oscillators for Modern Communication Systems", Part 1-3, **Microwave journal**, Jan 2015

Non-Planar/Planar Möbius Strips Resonator

Connecting Minds. Exchanging Ideas.

Non-planar Möbius resonator Filter

Dual-Mode [1]

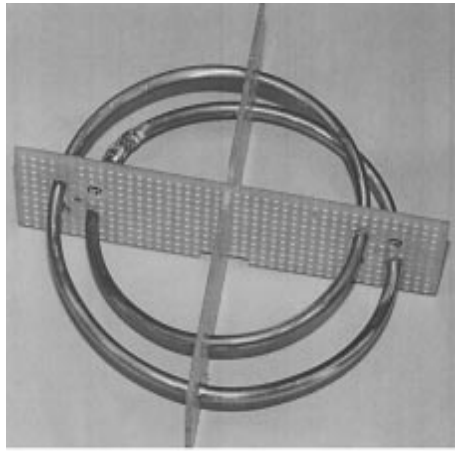

Quad-Mode [2]

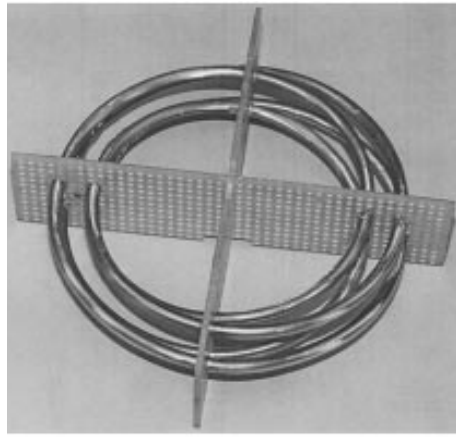

Planar Möbius resonator filter [3]

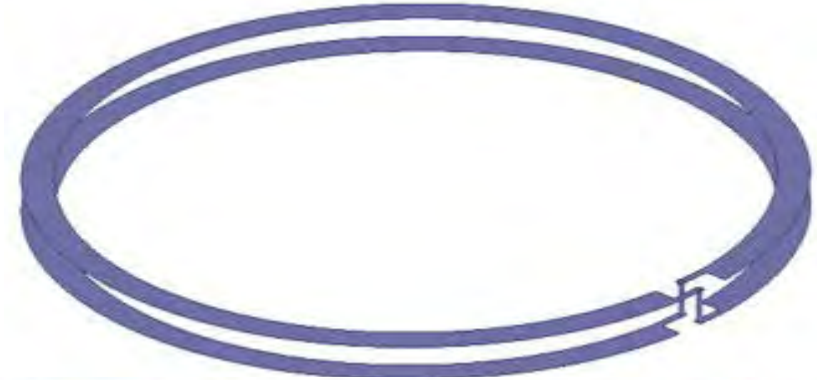

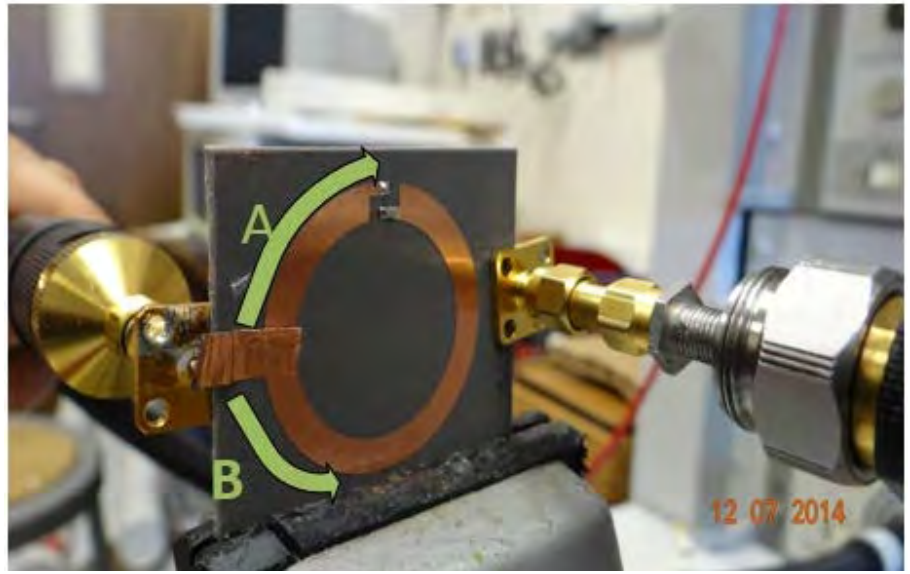

[1] J. M. Pond, “Mobius Dual Mode Resonators and Bandpass Filter”, IEEE. Trans. of MTT Vol. 48, No.12, Dec 2000, pp 2465-2471.
[2] J. M. Pond, et.al. "Band-pass Filters Using Dual-Mode and Quad-Mode Mobius Resonators," IEEE Trans on MTT vol.49, pp.2363-2368, Dec.2001.
[3] K. Dhwaj , H. Lee, L. Jiang, and T. Itoh, “Transmission-Line Equivalent and Microstrip Structure for Planar Mobius Loop Resonator, IMS 2015

Printed Resonator-Fabrication

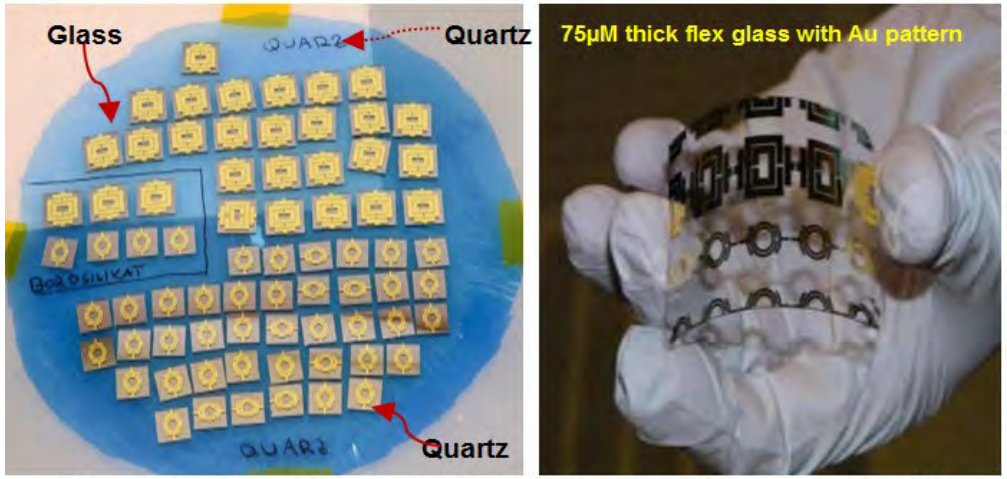

Photos of metamaterial inspired SRR fabricated on glass/quartz material

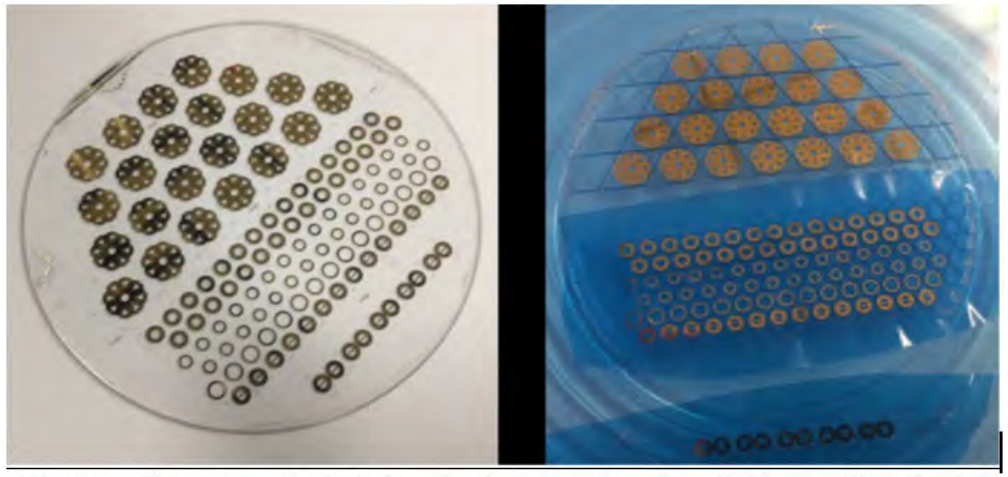

Photos of metamaterial inspired resonator for high quality factor resonator tank applications, fabricated on glass/quartz material

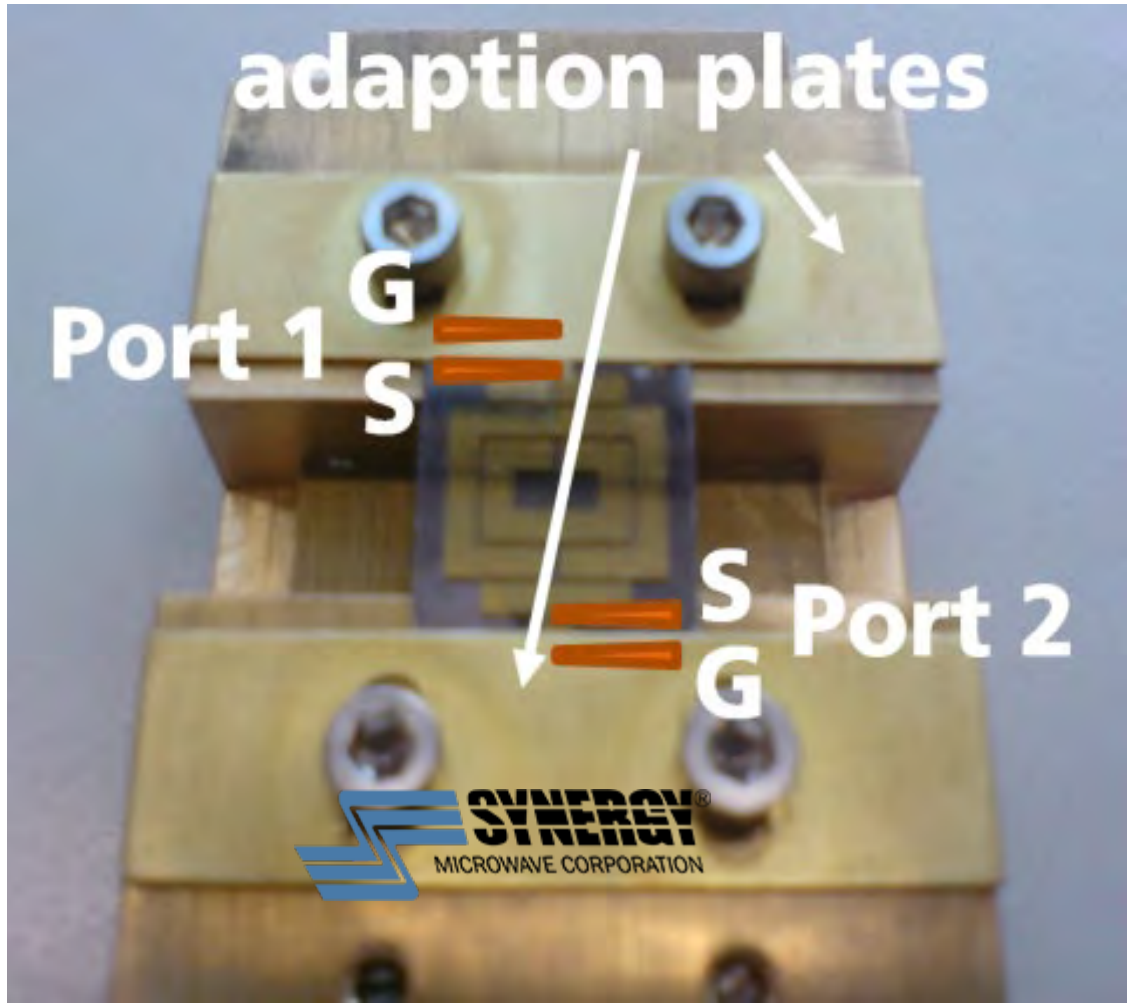

GSG probe configuration for the measurement of S parameter

Tunable Möbius Resonator VCO

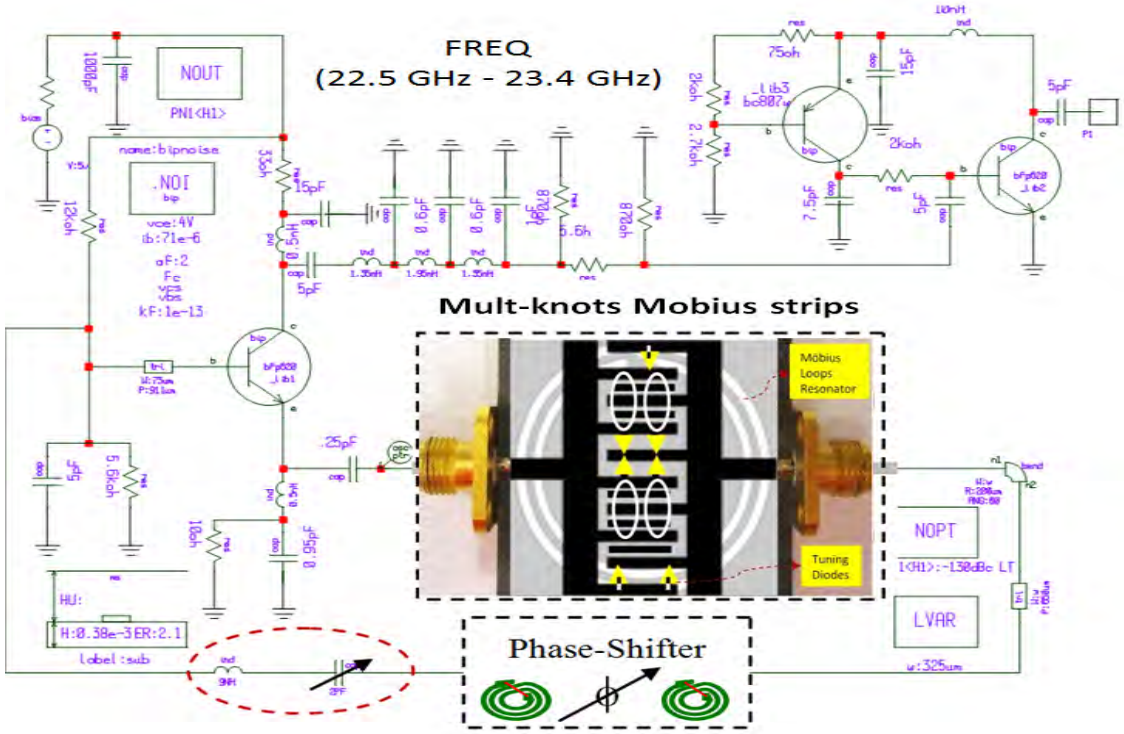

EMPIMC : Evanescent Mode Phase Injection Mode-Coupled

Figures show the typical circuit schematic, injection locking scheme, and phase perturbation dynamics.

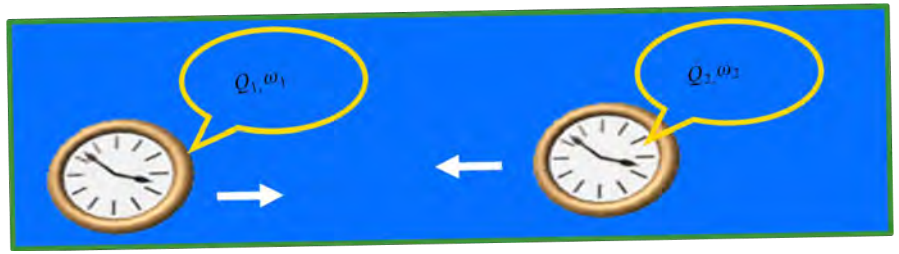

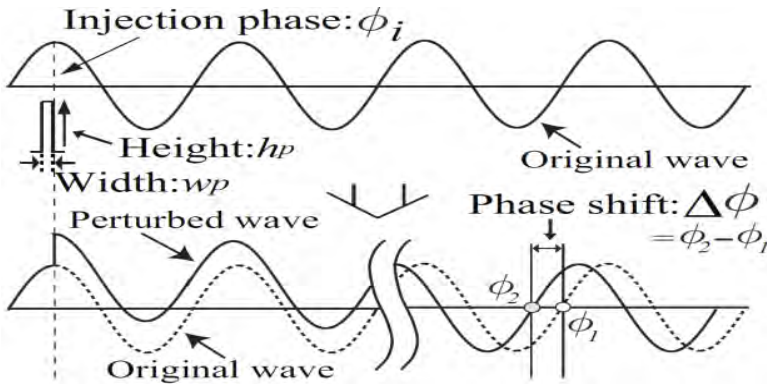

3rd Harmonic Injection

Phase shift due to impulse perturbation at ϕ_i.

$$Q_L = \frac{\omega_0}{2}\left|\frac{d\varphi(\omega)}{d\omega}\right|_{\omega=\omega_0} = \frac{\omega_0}{2}\tau_d; \quad \tau_d = \left|\frac{d\varphi(\omega)}{d\omega}\right|_{\omega=\omega_0} \quad \tau_d = \frac{d\varphi(\omega)}{d\omega}\bigg|_{\omega=\omega_0} = \frac{\varphi(\omega_0+\Delta\omega)-\varphi(\omega_0-\Delta\omega)}{2\Delta\omega}$$

where $\varphi(\omega)$ is the phase of the oscillator's loop transfer function at steady state and τ_d *is the group delay of the metamaterial Möbius strips resonator.*

Ref. U. L. Rohde, A. K. Poddar, "Möbius Metamaterial Strips Resonator: Tunable Oscillators for Modern Communication Systems", Part 1-3, **Microwave journal**, Jan 2015

Möbius Strips: Rotator Wave Oscillator

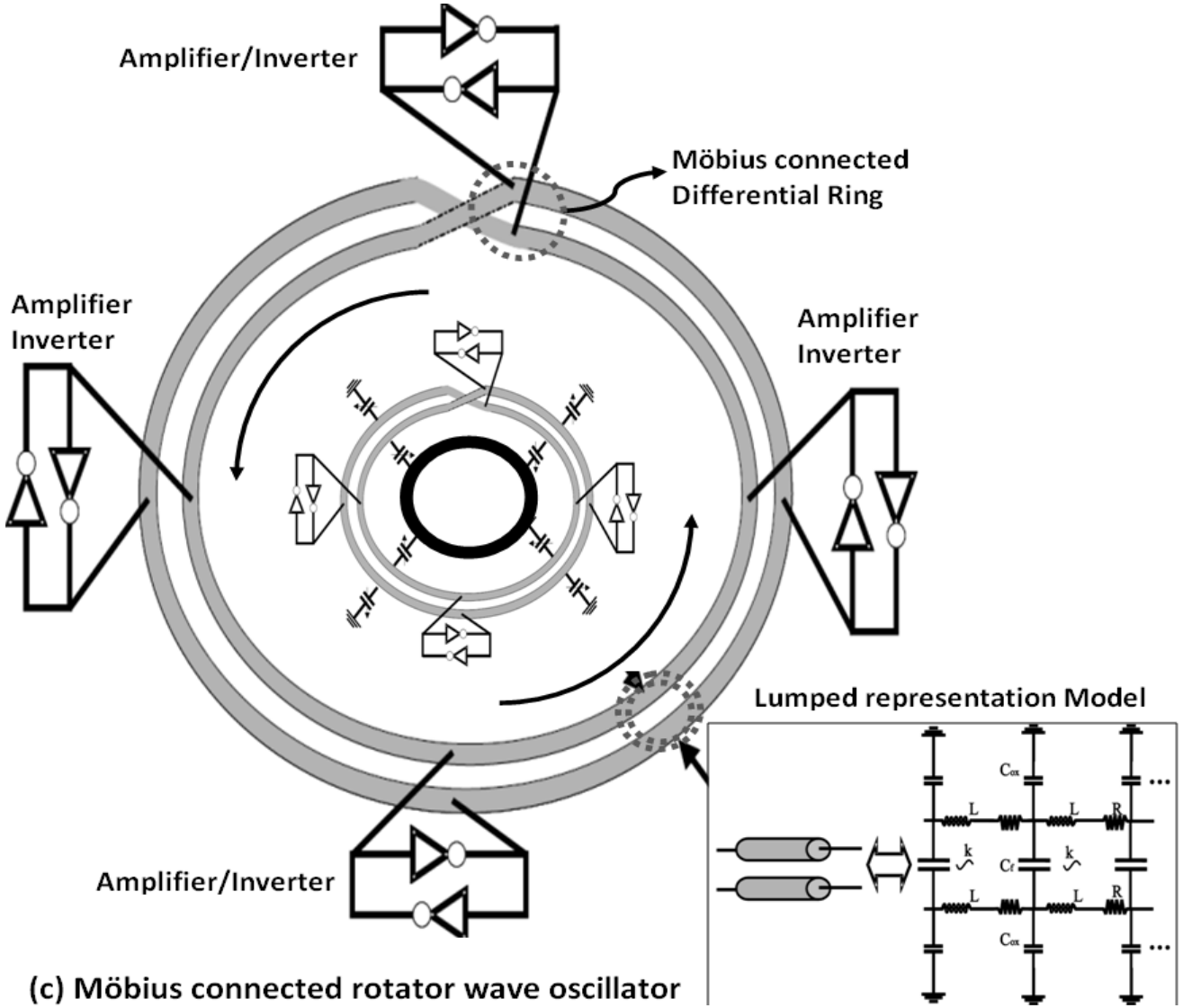

The resonator coupling coefficient 'β_j' depends upon the geometry of the perturbation:

$$\beta_j = \left[\left(\frac{\int \varepsilon E_a . E_b \, dv}{\sqrt{\int \varepsilon E_a^2 dv \int \varepsilon E_{bd}^2 dv}}\right)_e + \left(\frac{\int \mu H_a . H_b \, dv}{\sqrt{\int \mu H_a^2 dv \int \mu H_b^2 dv}}\right)_m\right]$$

where E_a and H_a are the electric and magnetic fields produced by the Möbius strip, and E_b, H_b are the corresponding fields due to perturbation or nearby adjacent resonator, subscript 'e' and 'm' are the electrical and magnetic coupling.

RWO:
Clocking applications

Ref. John wood, RTWO Arrays: anew clock technology, IEEE JSSC, vol. 36, pp. 1654-1665, 2001

Möbius Strips: Rotator Wave Oscillator

Size: 3.1" × 1.34" × 0.788" inches

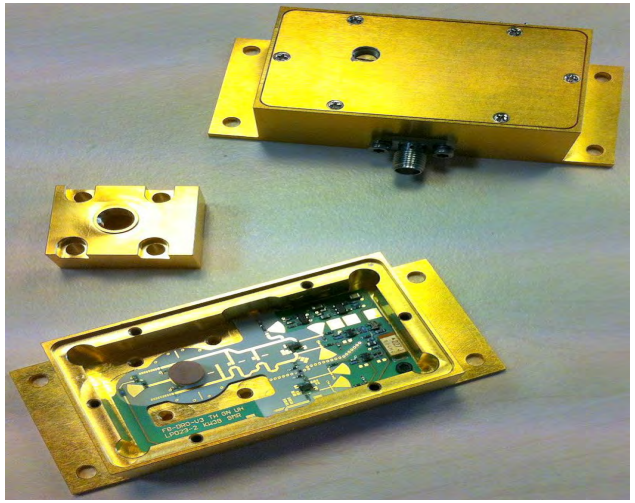

Connectorized 3-D Disc resonator based 10.24 GHz Oscillator 5V, 80 mA

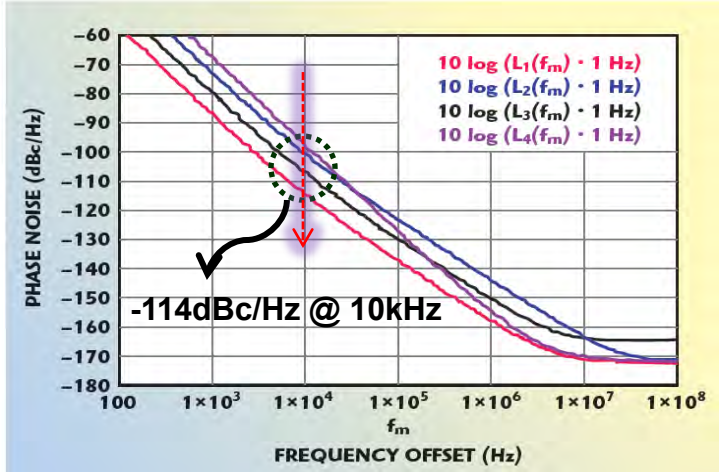

0.5"x 0.5" inches

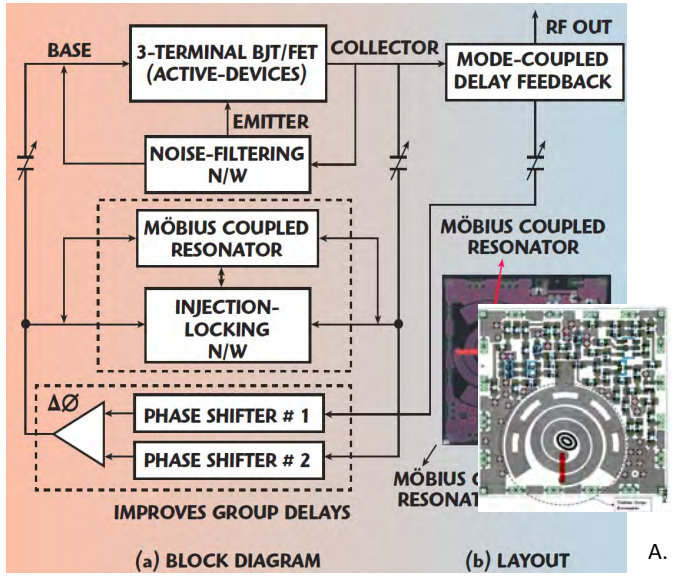

Printed Möbius Resonator Based 10.24 GHz Oscillator with DC bias of 5V, 30 mA

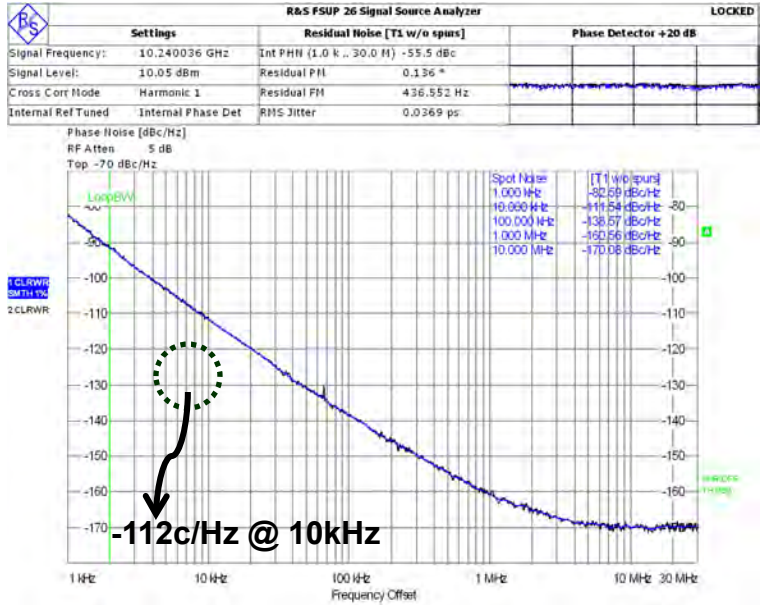

A. K. Poddar, "Slow Wave Resonator Based Tunable Multi-Band Multi-Mode Injection-Locked Oscillators" Dr.-Ing.-habil Thesis, BTU Cottbus, Germany, 2014

High Performance 10.24 GHz Synthesizer

R&S FSUP 26 Signal Source Analyzer							LOCKED
Settings		Residual Noise [T3 w/o spurs]		Phase Detector +20 dB			
Signal Frequency:	10.239955 GHz	Int PHN (100.0 .. 30.0 M)	-74.2 dBc				
Signal Level:	7.9 dBm	Residual PM	15.735 m°				
Cross Corr Mode	Harmonic 1	Residual FM	468.955 Hz				
Internal Ref Tuned	Internal Phase Det	RMS Jitter	0.0043 ps				

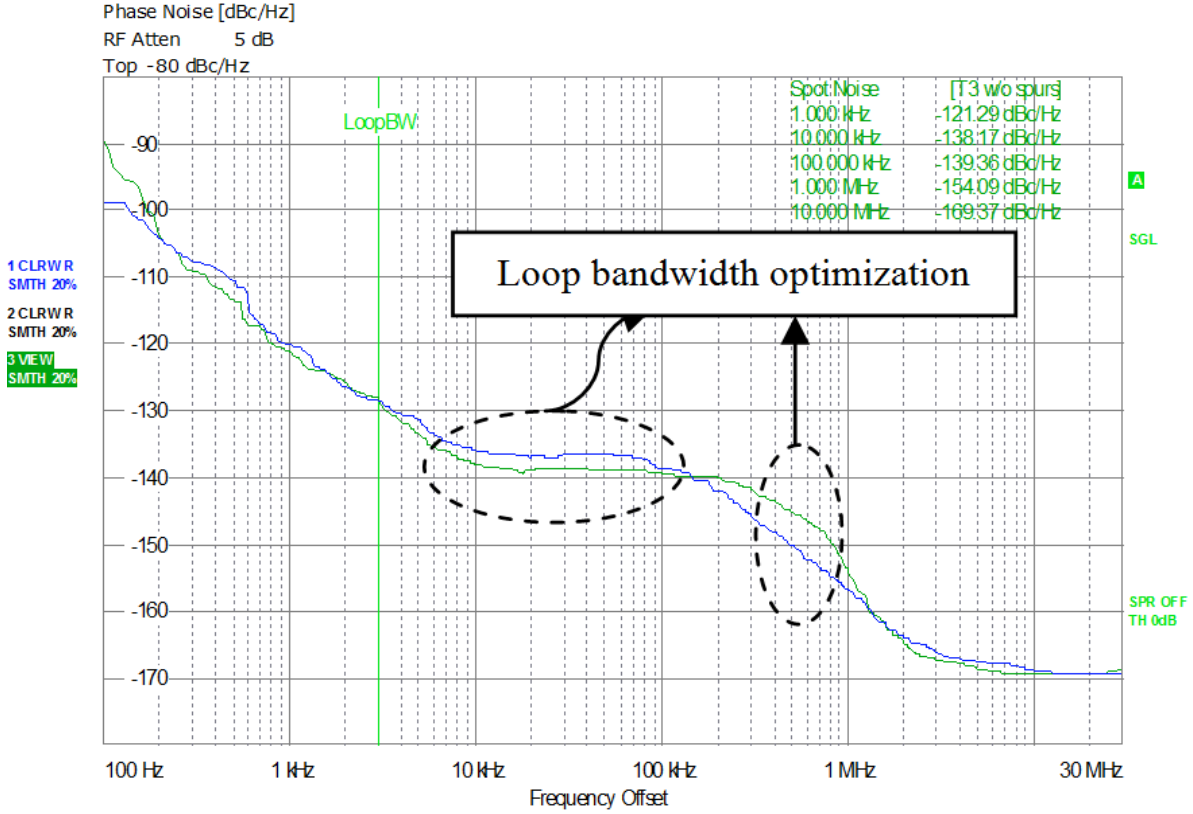

A typical measured phase noise plot of the 10.24 GHz synthesized signal source

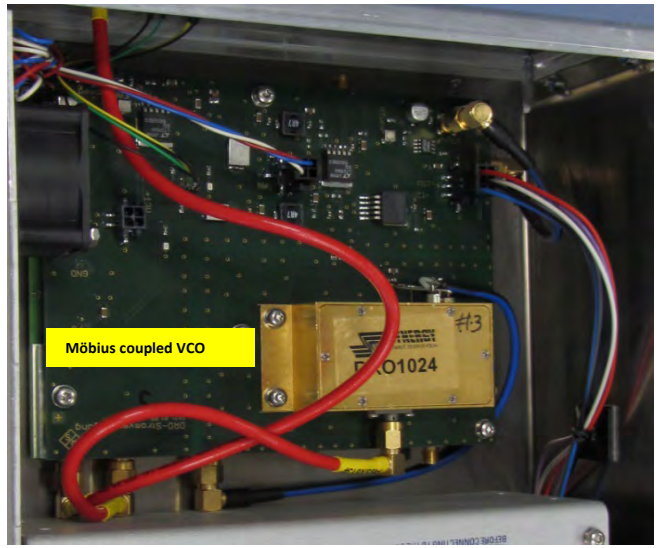

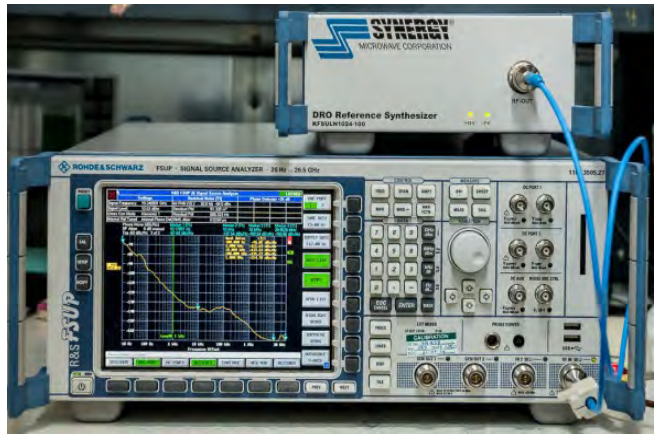

R&S FSUP 50: PN measurements

Emerging Technology: Mobius Resonator

Plot of unloaded Q-factor of printed resonators

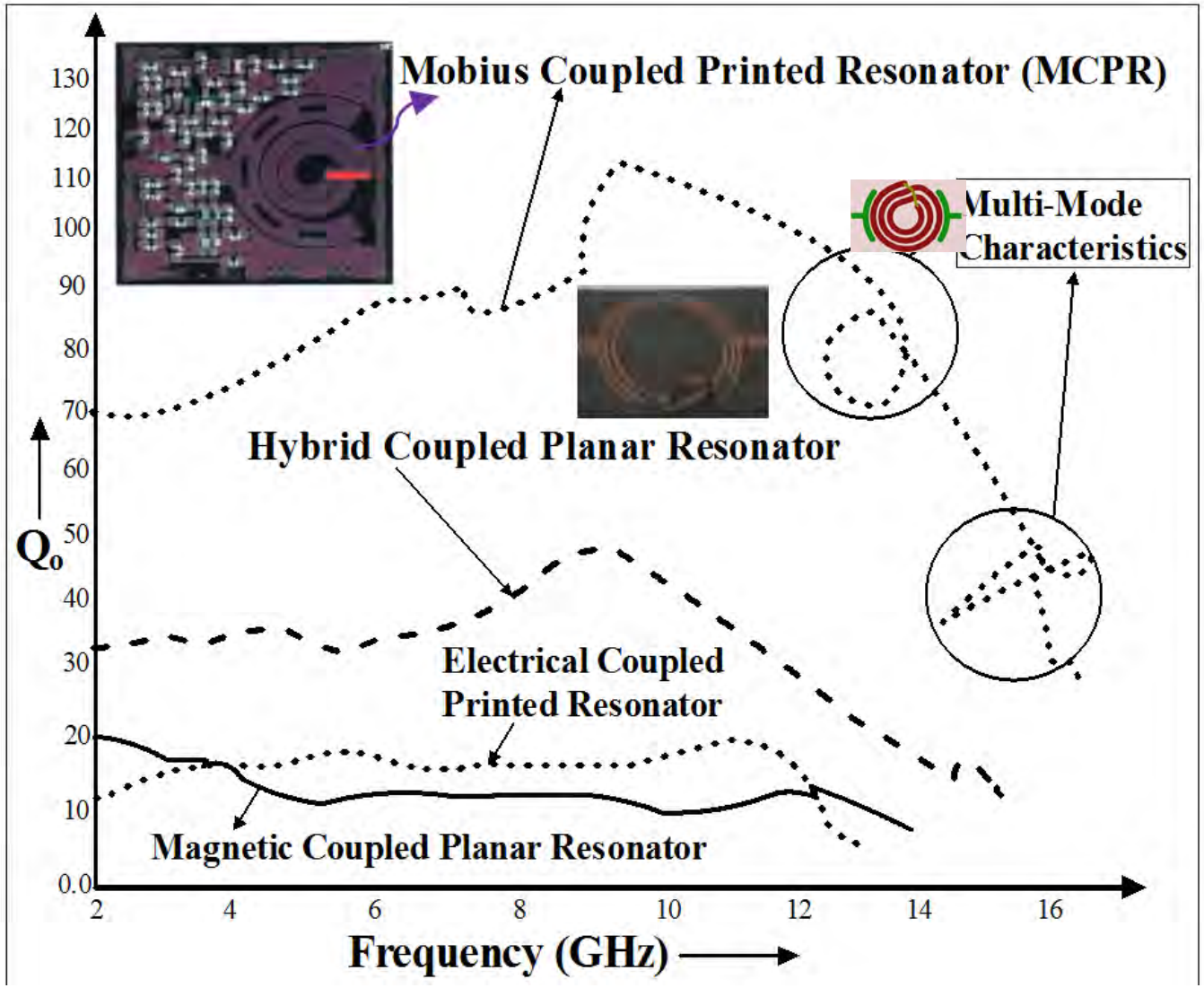

Mobius Resonator

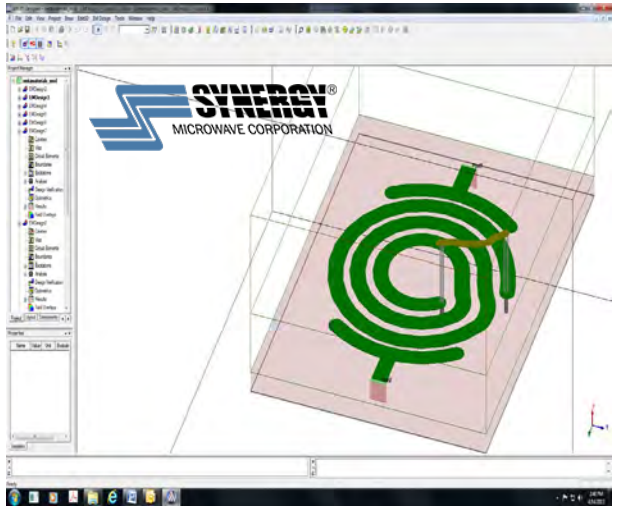

Mobius resonator VCO

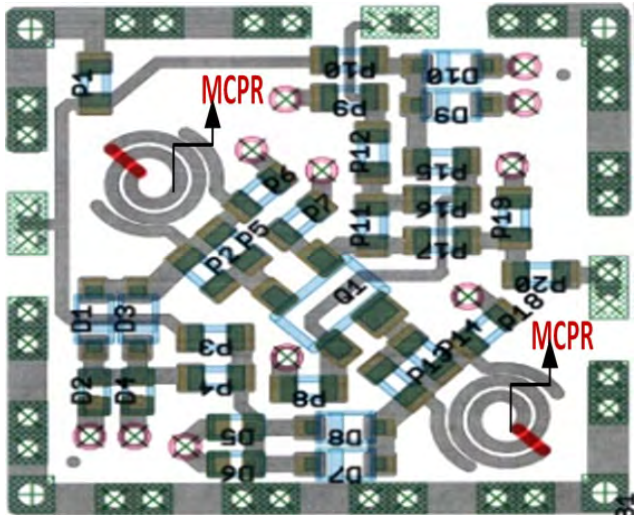

Emerging Technologies : Printed VCOs

The coupling coefficient 'βj' depends upon the geometry of the perturbation, and it can be given by

$$\beta_j = \left[\left(\frac{\int \varepsilon E_a E_b \, dv}{\sqrt{\varepsilon E_a^2 dv \int \varepsilon E_{bd}^2 \, dv}} \right)_{\text{electrical-coupling}} + \left(\frac{\int \mu H_a H_b \, dv}{\sqrt{\int \mu H_a^2 \, dv \int \mu H_b^2 \, dv}} \right)_{\text{magnetic-coupling}} \right]$$

where E_a and H_a are, respectively, the electric and magnetic fields produced by the square loop ring resonator, and E_b, H_b are the corresponding fields due to the perturbation (d≠0) or nearby adjacent resonator (second square loop resonator).

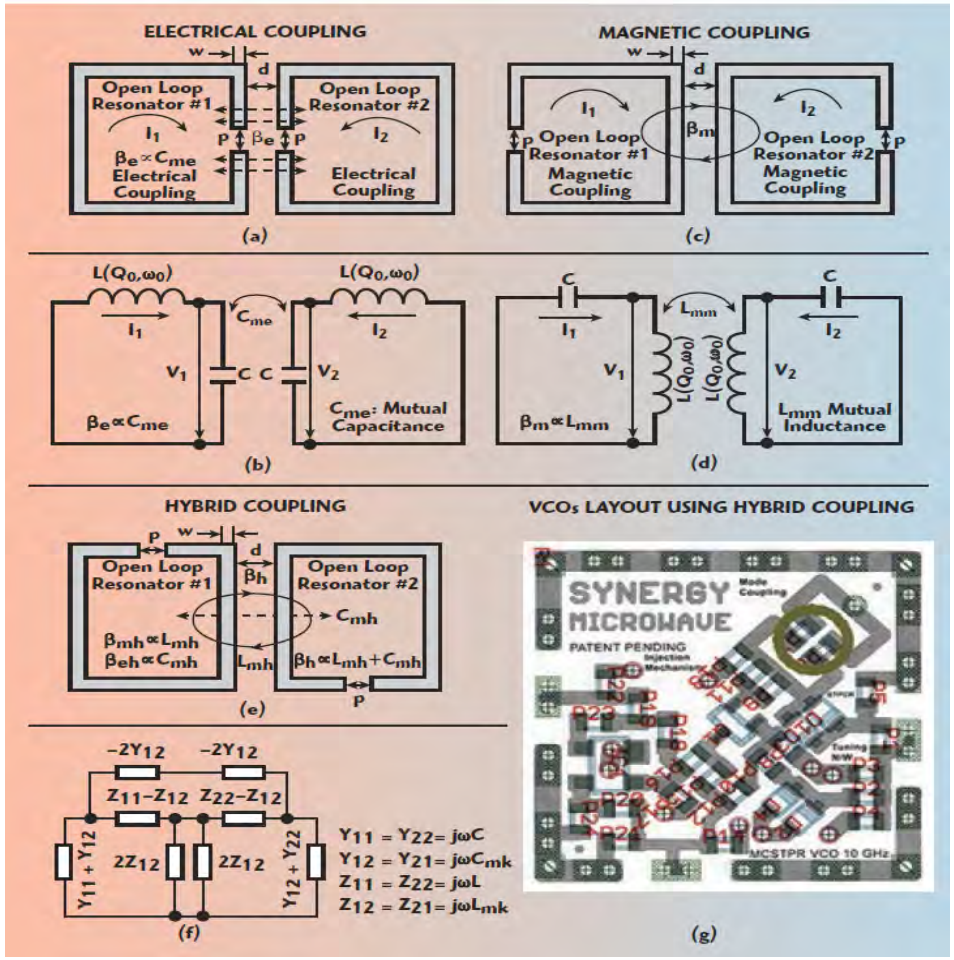

Typical simplified structure of open loop microstrip line coupled resonator networks: (a) electrical coupling, (b) equivalent lumped model of electrical coupling, (c) magnetic coupling, (d) equivalent lumped model of magnetic coupling, (e) hybrid coupling, (f) equivalent lumped model of hybrid coupling and (g) layout of VCO using electric and magnetic coupling.

Emerging Technologies : VCO Solutions

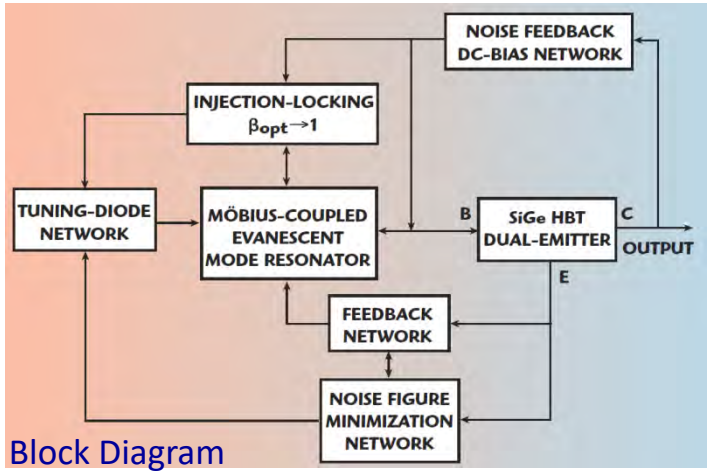

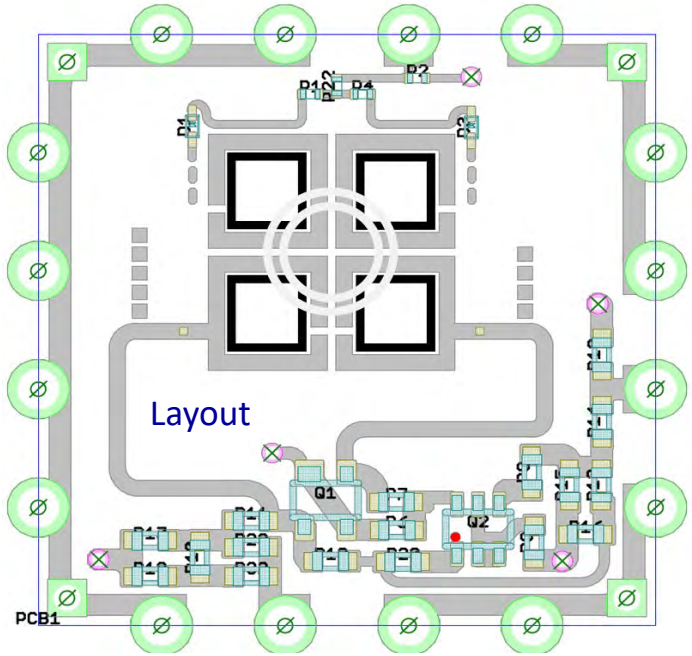

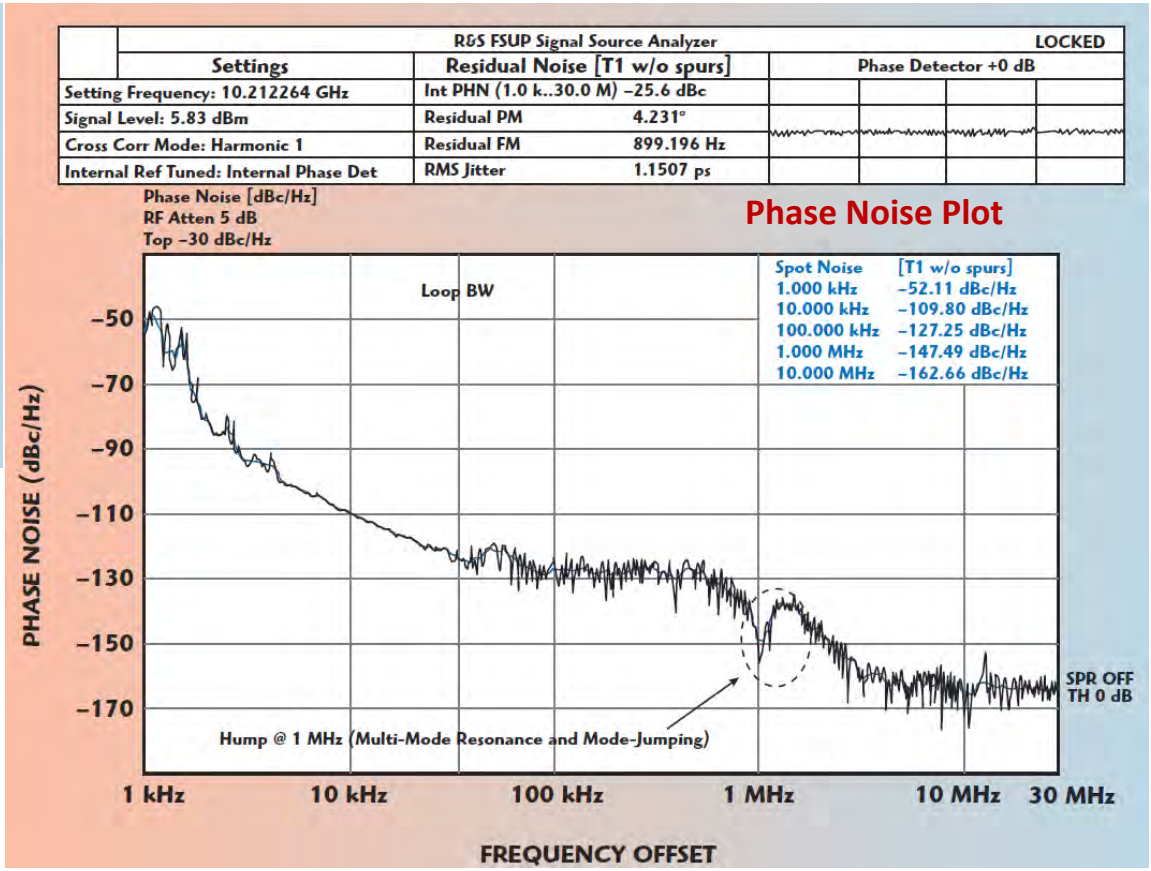

Figures : show the typical block diagram, layout, and measured phase noise plot of the 10.2 GHz oscillator using a SiGe HBT active device were fabricated on Rogers substrate material with a dielectric constant of 2.2 and thickness of 20mils (microstripline/stripline) for the validation of the approach.

Emerging Technologies : VCO Solutions

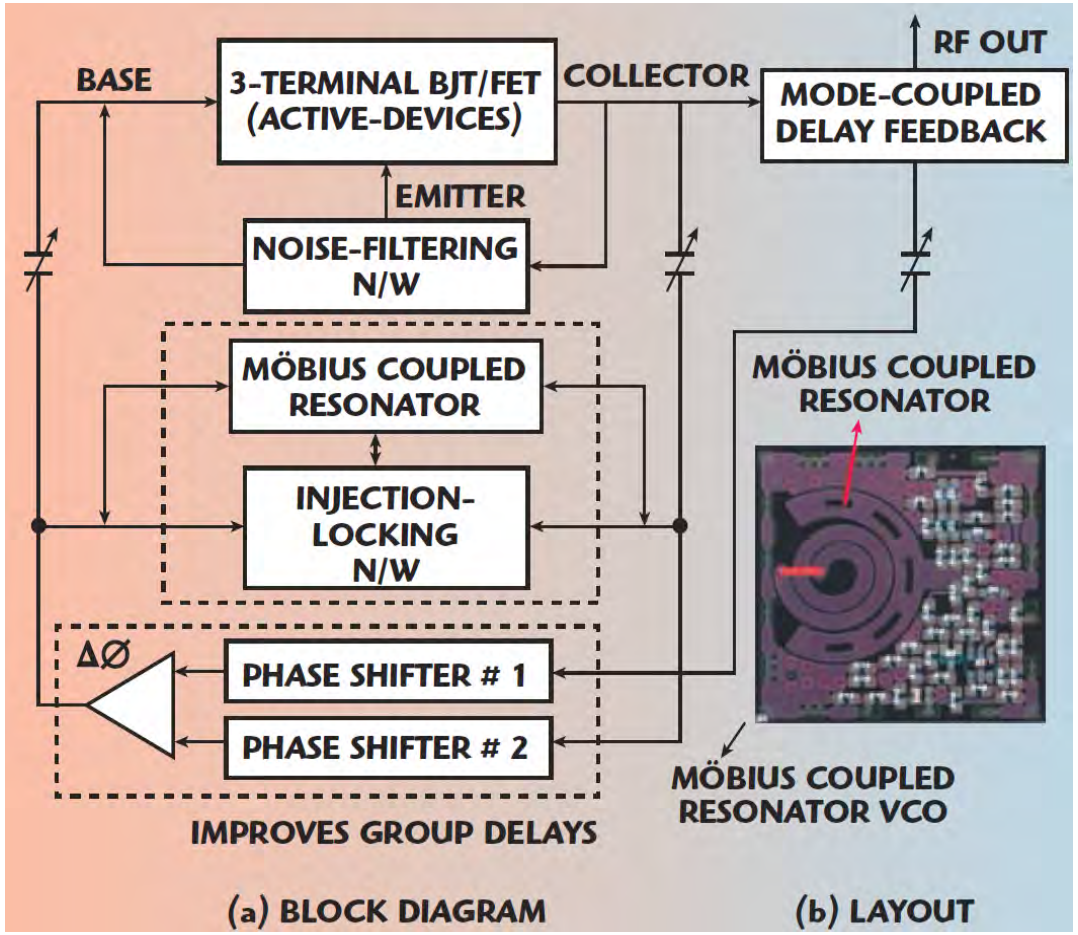

Shows the typical block diagram 10 GHz Möbius coupled resonator VCOs using a SiGe Hetro-junction-Bipolar-transistor (HBT) active device, built on 20mils substrate material

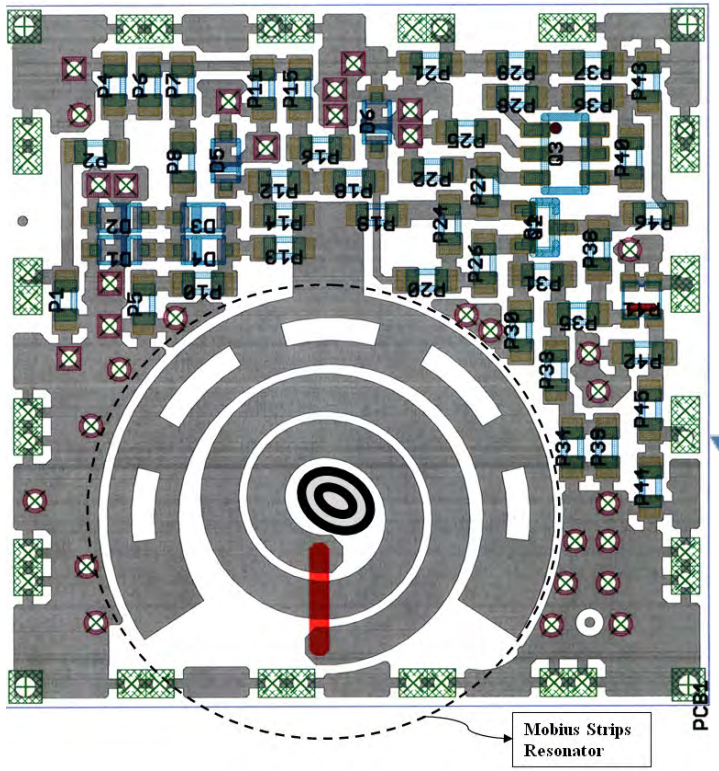

Shows the layout of 10 GHz oscillator (depicts the phase-injection-mode-locked) Möbius strips resonator (PCB layout is done with 22 mil substrate thickness with 2.22 dielectric constant, 0.75x0.75x0.18 inches)

Phase Noise Plots

Measured phase noise plot of the 10 GHz oscillator using: hybrid coupled resonator, Möbius coupled resonator, mode-locked Möbius coupled resonator network.

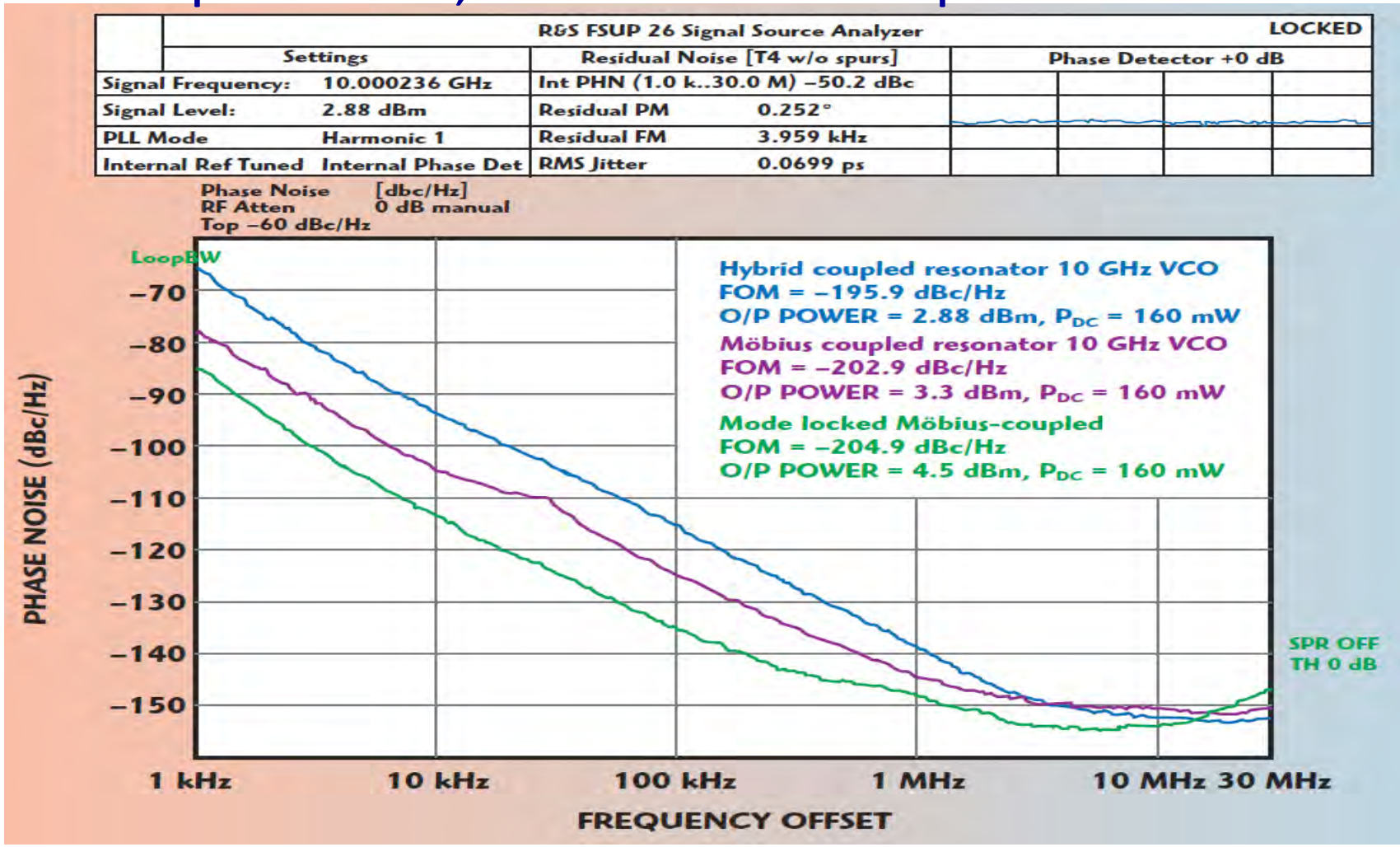

Low Cost Synthesizer

Figure Shows a high performance wideband synthesized signal sources for modern communication systems: the typical PCB Layout of 2-8 GHz Configurable Synthesizer Module

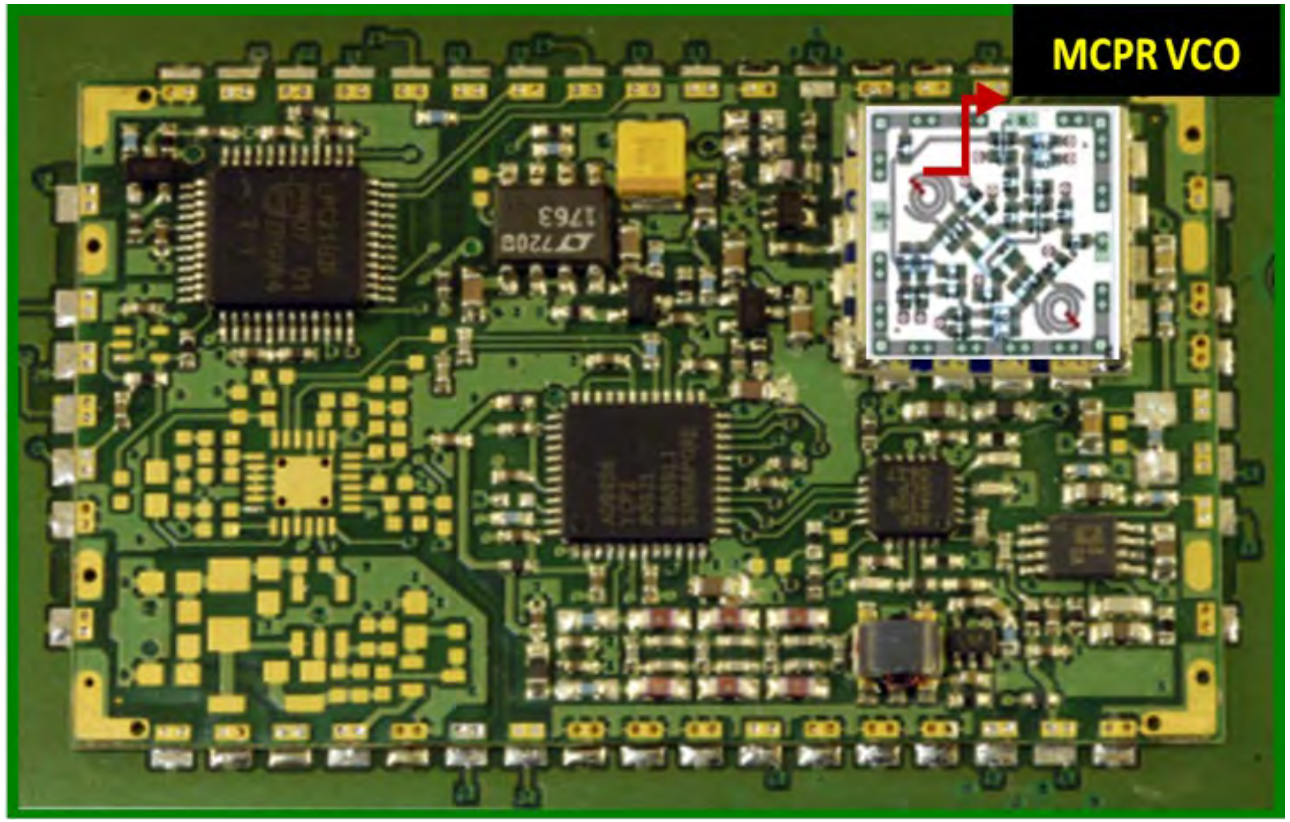

Figure Shows a typical layout of Möbius Coupled planar resonator (MCPR) VCO (2-8 GHz)

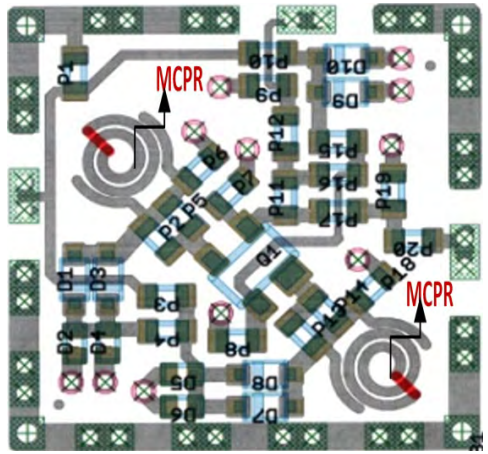

SYNERGY® MICROWAVE CORPORATION

Ex. 12 GHz Printed Resonator VCO

$$\frac{d}{dm}\left[10\log\left\{\left[1+\frac{f_0^{\,2}}{(2f_mQ_0)^2m^2(1-m)^2}\right]\left(1+\frac{f_c}{f_m}\right)\frac{FkT}{2P_0}+\frac{2kTRK_0^2}{f_m^2}\right\}\right]=0\Rightarrow m_{opt}=0.5$$

$$m=\frac{Q_L}{Q_0}\cong\left[\frac{2}{(1+\beta_e)}\right]_{electrical}\cong[2(1+\beta_m)]_{magnetic}\cong\left[\frac{2(1+\beta_{mh})}{(1+\beta_{eh})}\right]_{hybrid}\qquad m_{opt}\to0.5\Rightarrow[\beta_e]_{opt}<<1,\quad[\beta_m]_{opt}\to1,\quad 0<[\beta_h]_{opt}<1$$

For low phase noise applications, m_{opt} and β_{opt} should be dynamically tuned and must converge in the vicinity of $m_{opt}\cong0.5$ and $0<\beta_{opt}<1$, respectively, for best phase noise performances over the operating frequency band.

Phase Noise Plot: DC Noise Feedback and Mode-Coupling

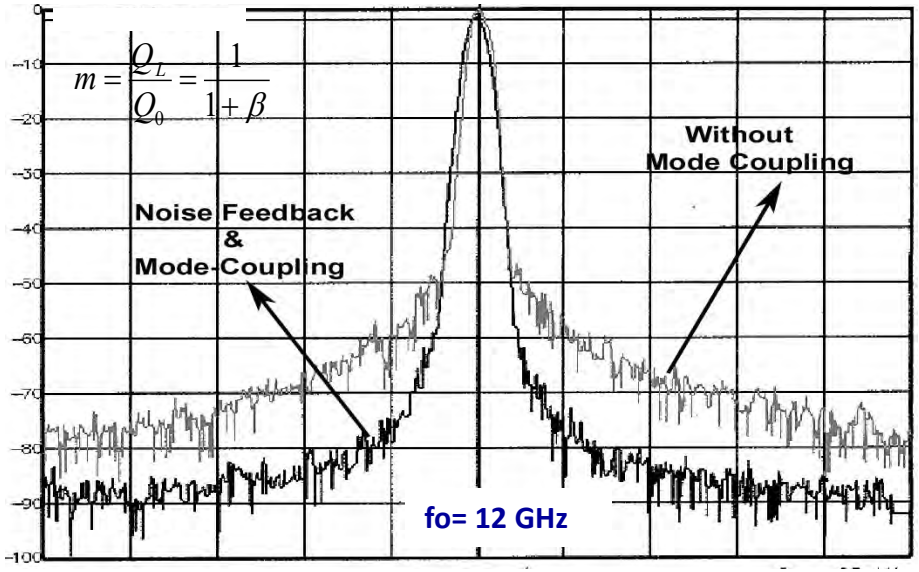

Measured Phase Noise

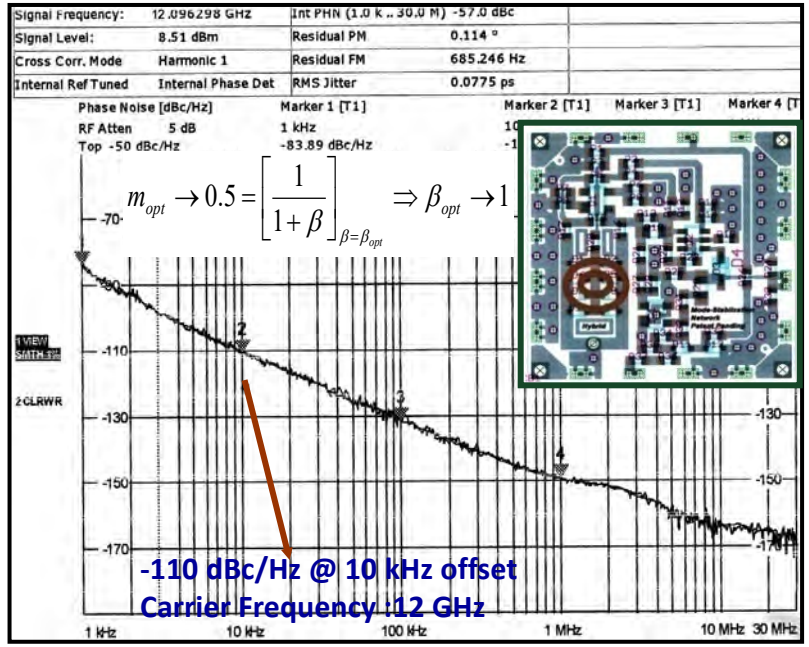

Dielectric Resonator (DR)

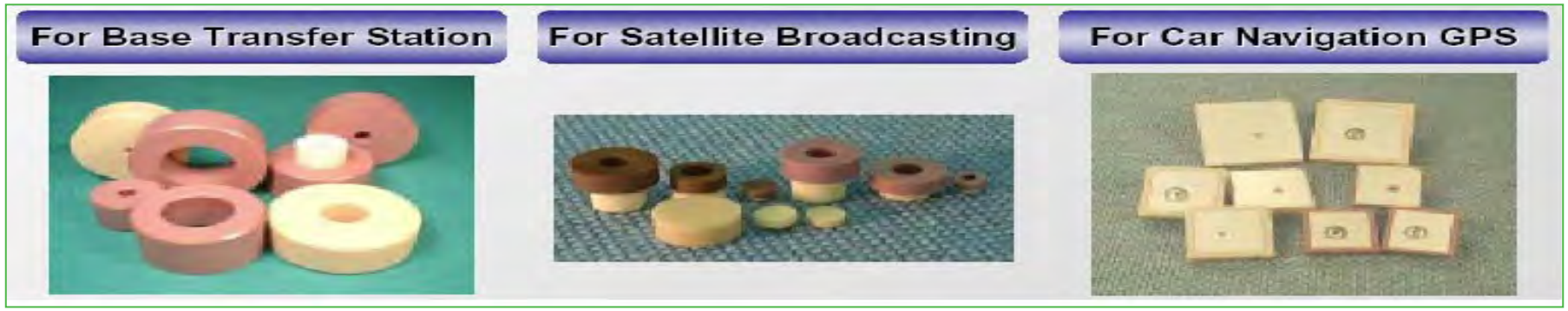

Tunable High Q Resonator: Coupled DRs

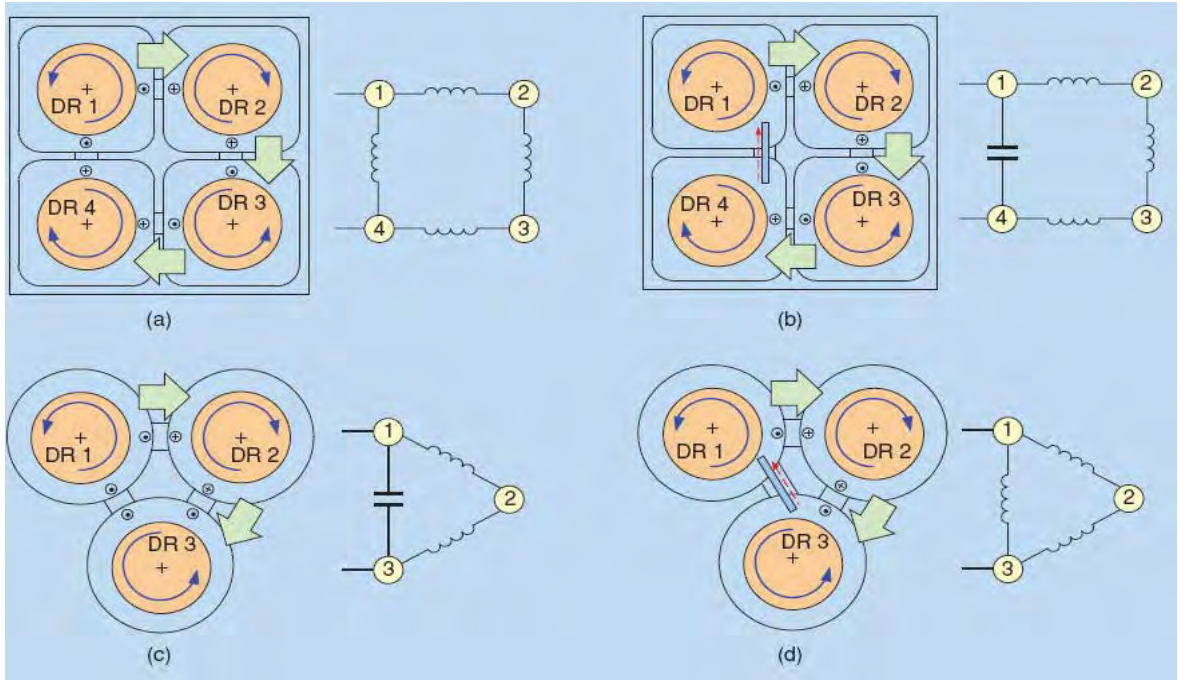

3-D Field Distribution of DRs

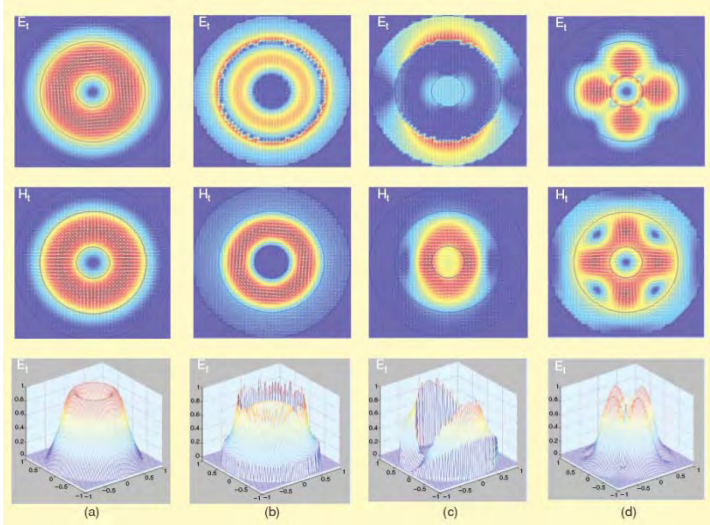

(a) TE_{01}, (b) TM_{01}, (c) HE_{11}, and (d) HE_{21} modes.

Dielectric Resonators Uses

Dielectric Resonator Modes

High Q Modes → Filtering & Oscillation

Low Q Modes → Radiating Purposes

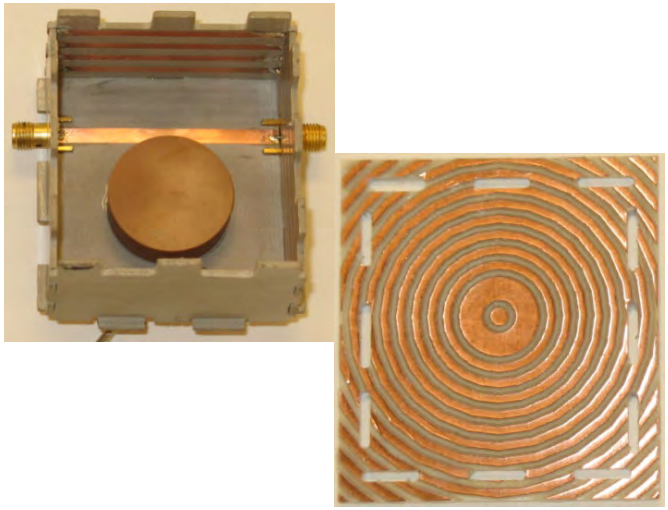

Dielectric Resonator Antenna & Oscillator

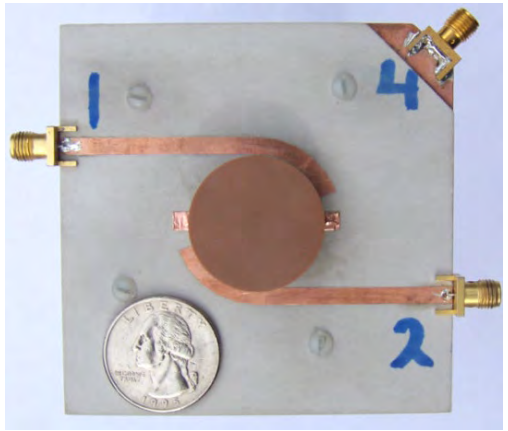

Dual Band Dielectric Resonator Antenna & Filter

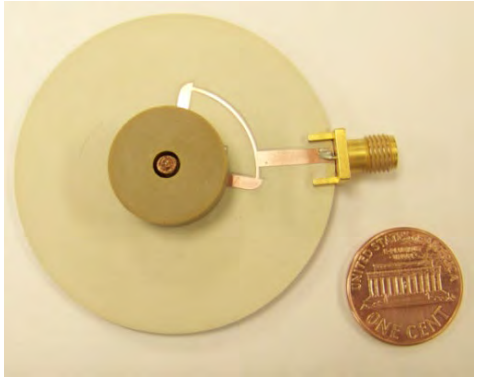

Dual Band Dielectric Resonator Antenna

Photos: courtesy of Laila Salman PhD Thesis

DR Resonator Coupling Mechanism

Excitation Techniques

Aperture Coupling

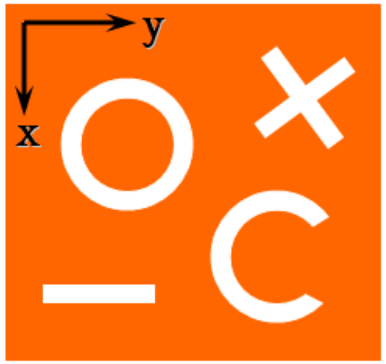

Probe Coupling

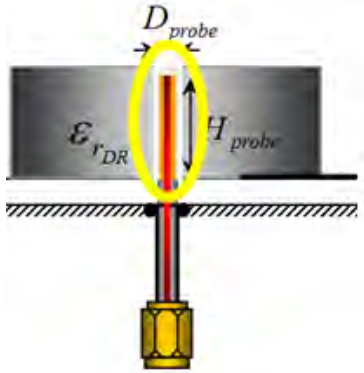

Microstrip Line

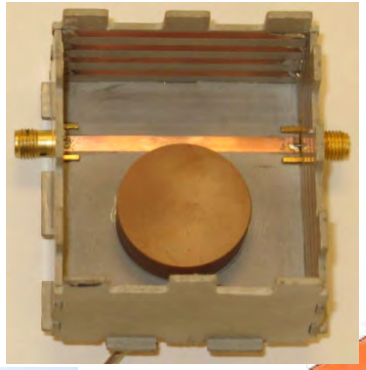

Dielectric Image Guide Coupling

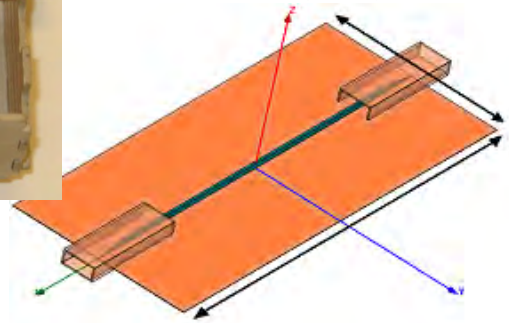

Coplanar Coupling

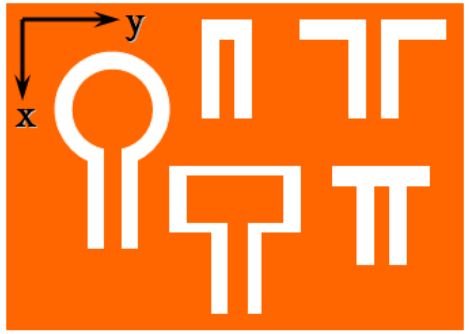

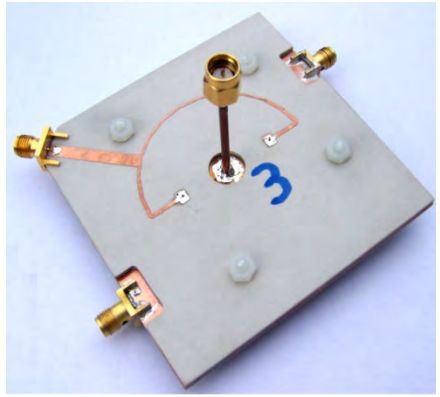

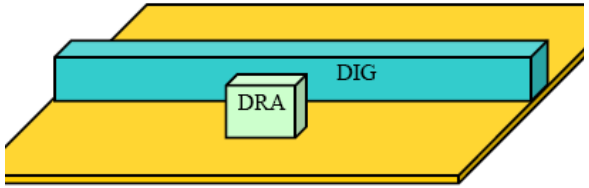

Photos: courtesy of Laila Salman PhD Thesis

Dielectric Resonator Oscillator

Dielectric Resonators

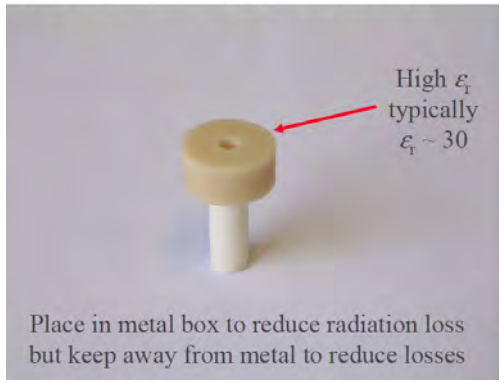

DRO circuit

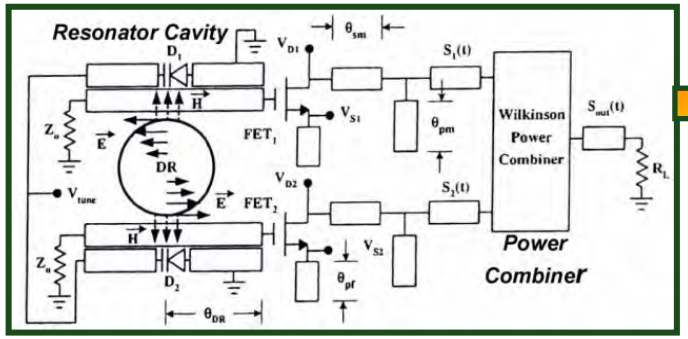

EM field coupling

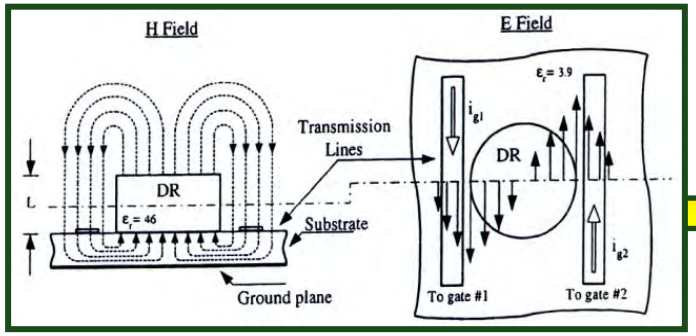

Disadvantages:

- Sensitive to Vibration
- Power-Hungry
- Not Integrable
- Not Concurrent

5 GHz DRO

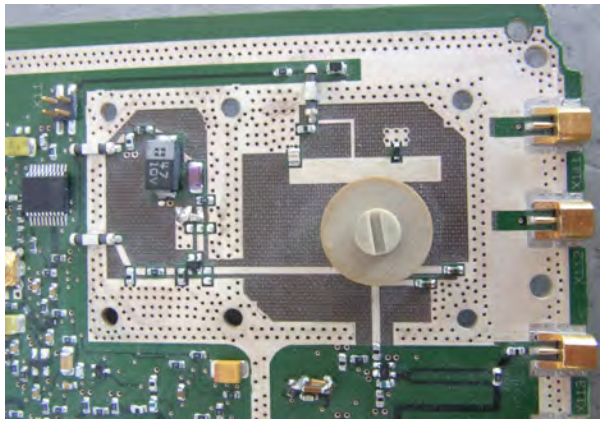

Practical Ex: 12 GHz VCO

12 GHz DRO circuit

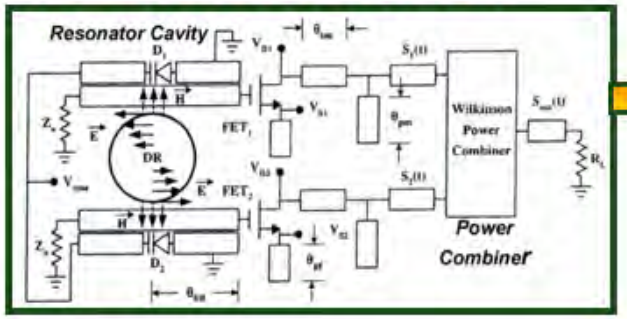

EM field coupling

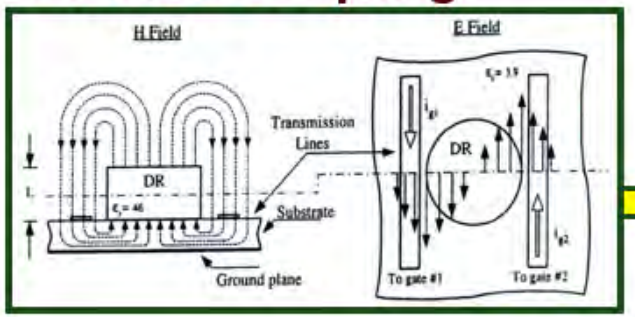

Disadvantages:

- Sensitive to Vibration
- Power-Hungry
- Not Integrable
- Not Concurrent

12 GHz Planar VCO Circuit

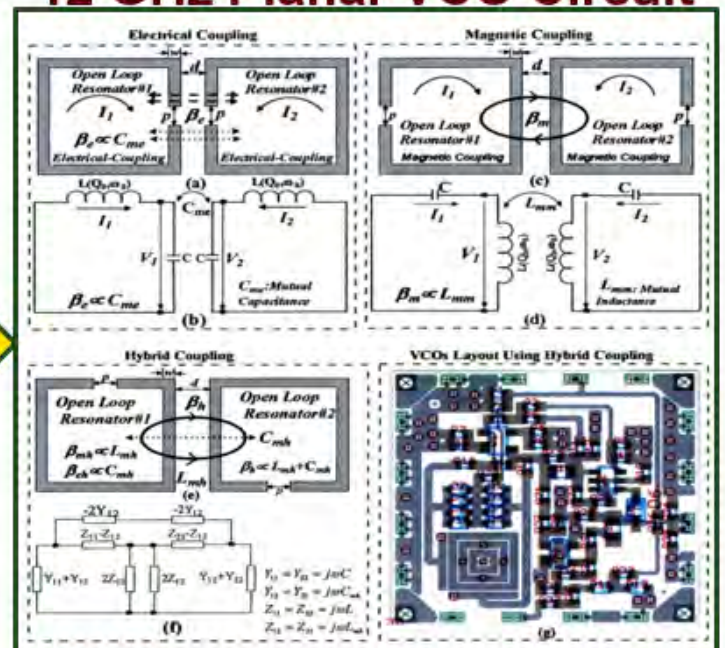

PROS:

- ✓ Reconfigurable VCO
- ✓ Integrable Alternatives
- ✓ Unified Layout

CONS:

- ✓ Mode-Jumping
- ✓ Sub-Harmonics
- ✓ Complex approach

DR

Although DR has been widely used as high performance signal sources, design communities have recently endeavored to replace DR with a state-of-the art active printed coupled resonator for low phase noise applications in MMIC process !!!

Dielectric Resonator Oscillator

Schematic of Low Phase Noise 3.8 GHz DRO

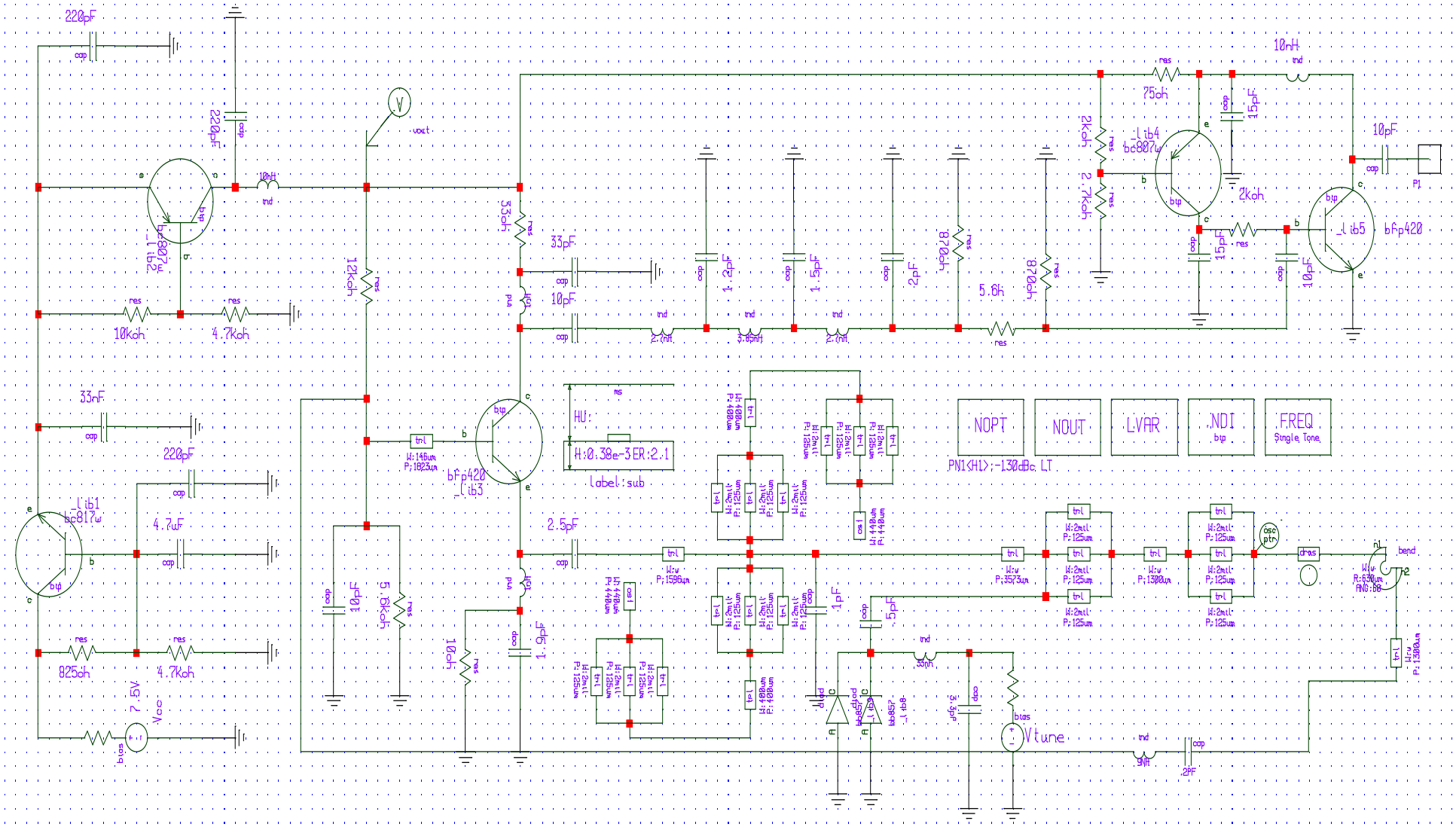

Injection-Locked 3.8 GHz DRO

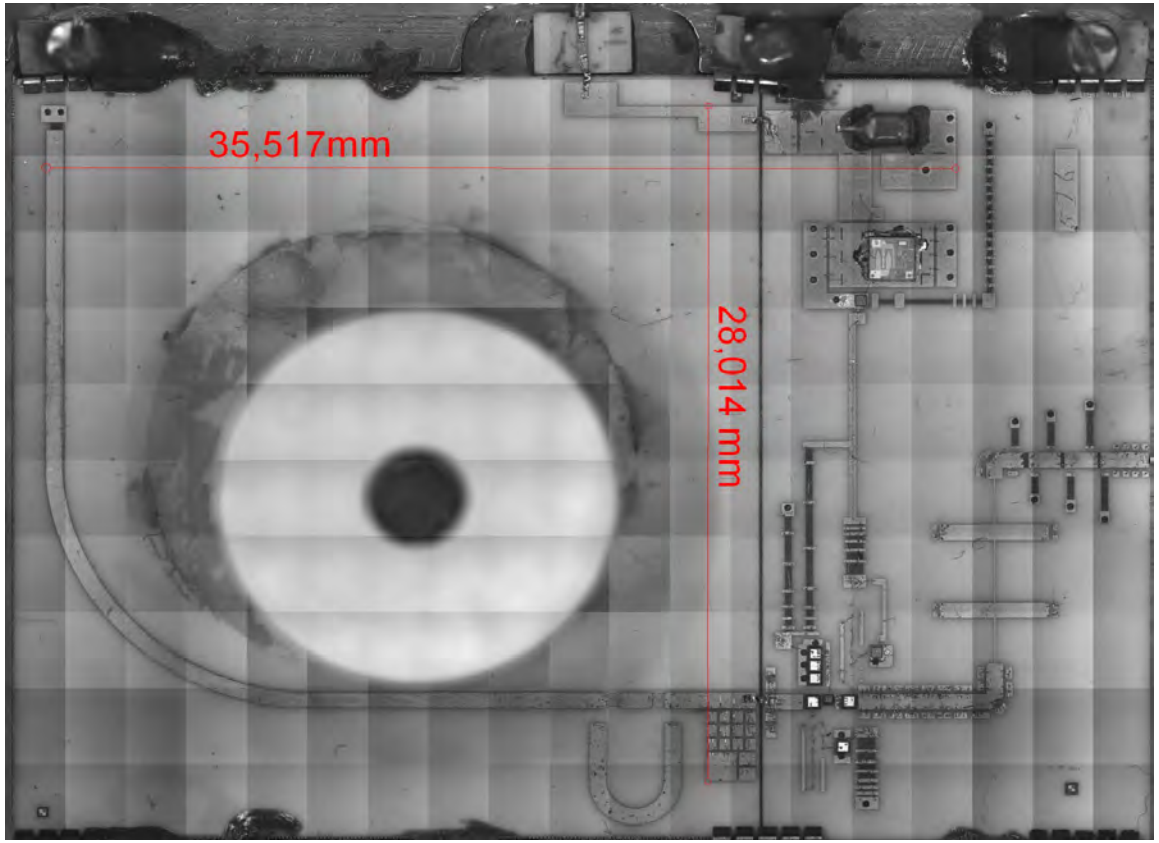

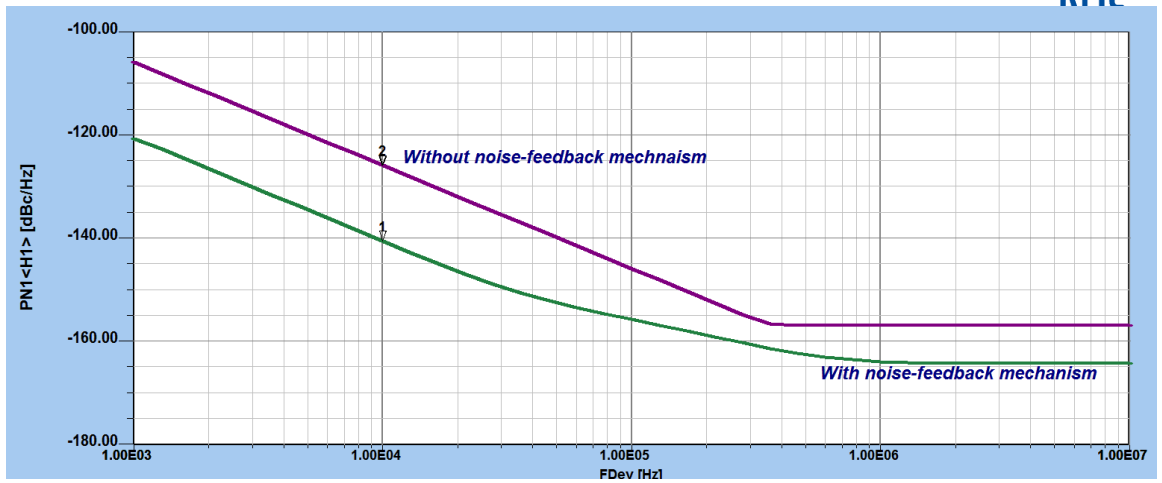

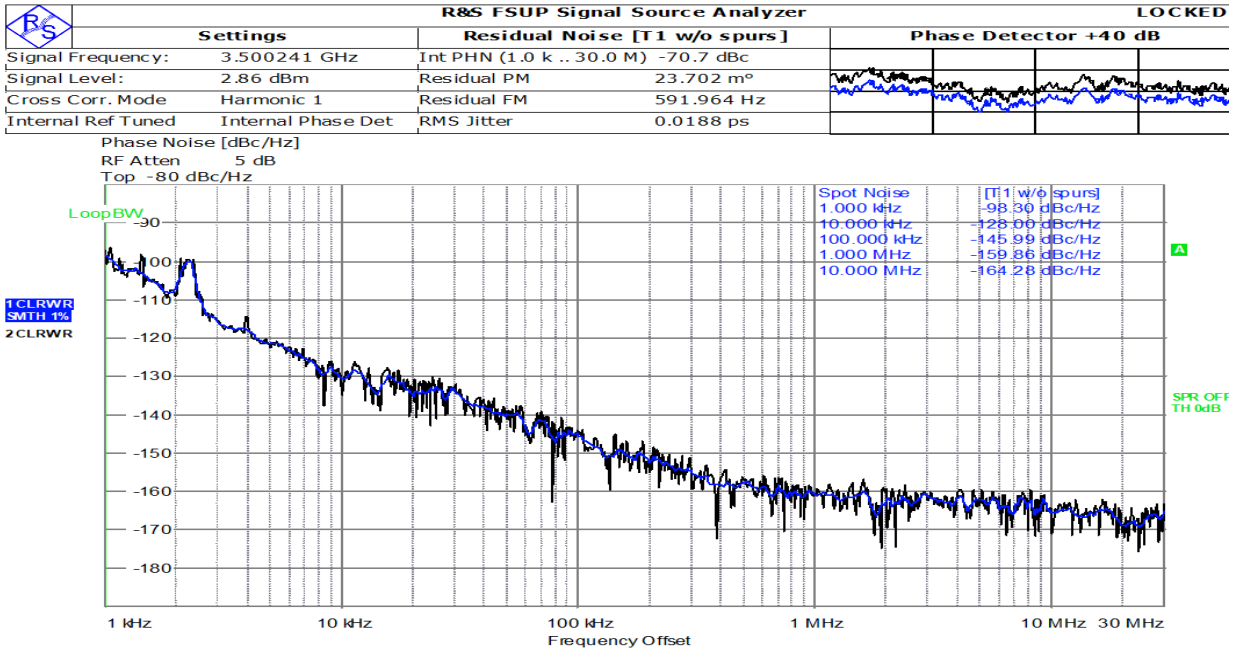

Recent Publications on DRO: 12.8 GHz

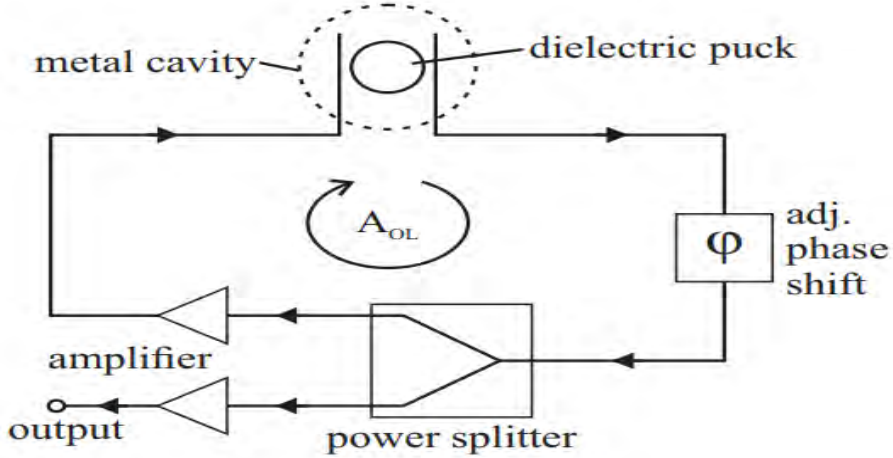

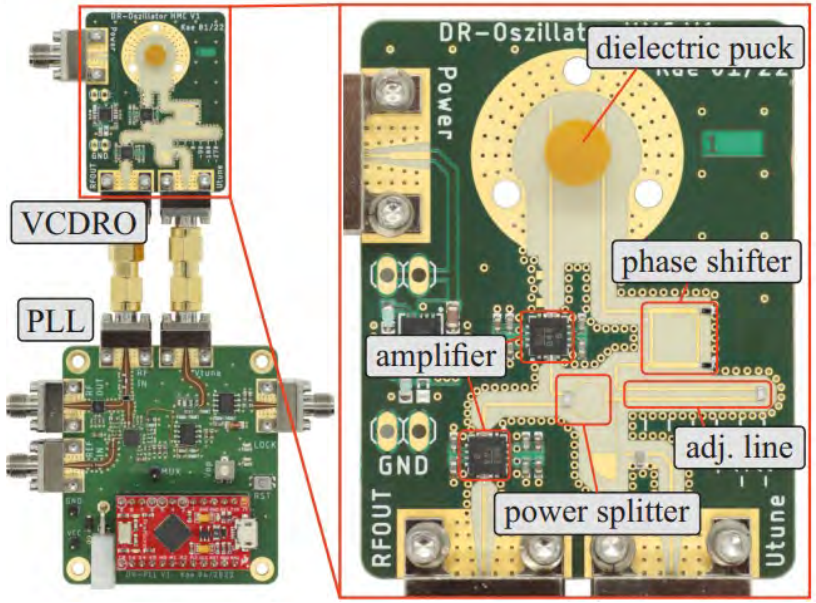

Fig. Left: Realized VCDRO with PLL stabilization (cavity removed).
Right: Detailed construction of the VCDRO [1].

Ref 1: Robin Kaesbach, Marcel van Delden, Thomas Musch, "A Fixed-Frequency, Tunable Dielectric Resonator Oscillator With Phase-Locked Loop Stabilization", **Proceedings of 2022 Asia-Pacific Microwave Conference**, pp. 728-730

MEASURED PHASE NOISE OF THE DRO IN OPEN-LOOP OPERATION

Δf	100 Hz	1 kHz	10 kHz	100 kHz
L (dBc/Hz)	−44.7	−76.7	−107.2	−134.2

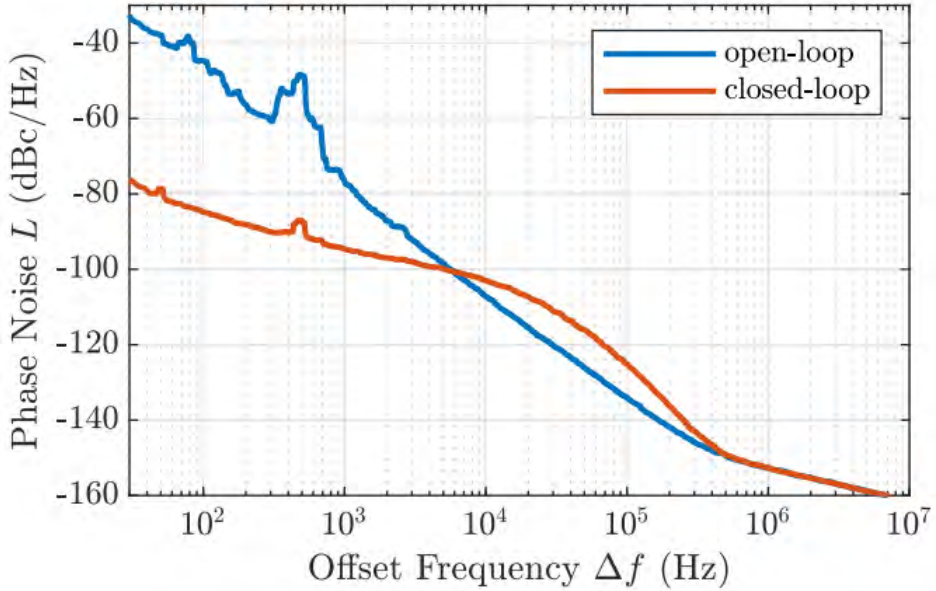

Fig. Measured phase noise of the DRO in open- and closed-loop operation at 12.8 GHz [1].

Recent Publication on mmWave Osc. 45.8GHz

Ref.1: Enrico Lia et al., "Novel mm-Wave Oscillator Based on an Electromagnetic Bandgap Resonator", IEEE MWTL, Vol. 33, No. 6, pp. 863-866, June 2023

Fig. 1 block diagram of the MMIC VCO [Ref.1].

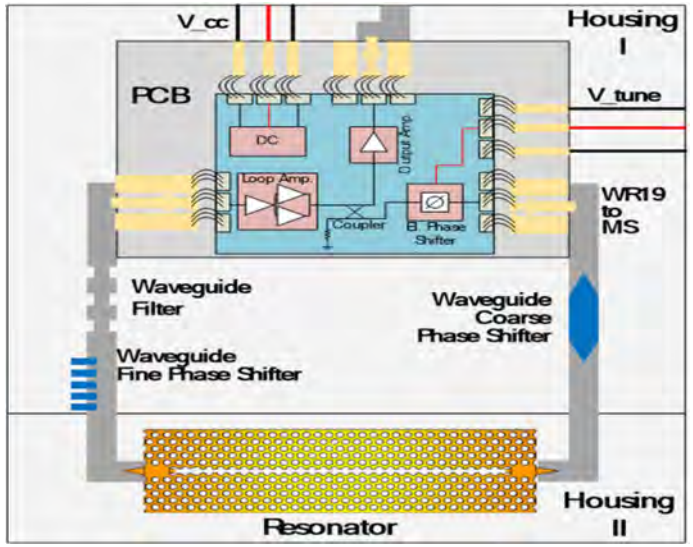

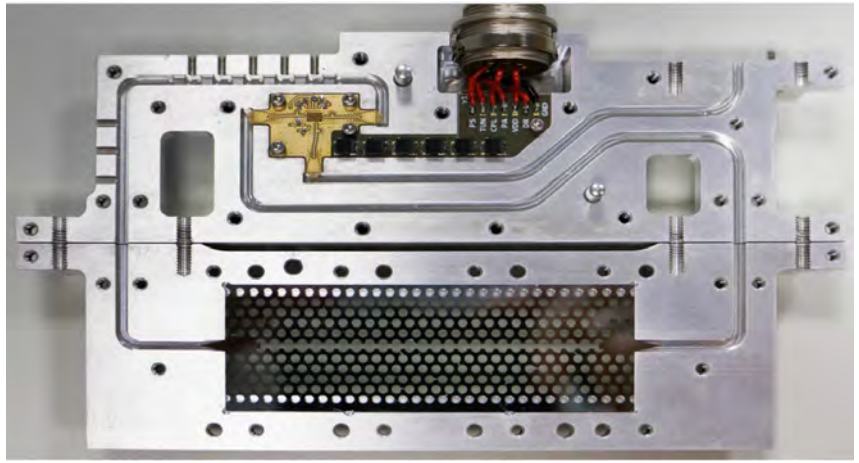

Fig. 3 MMIC VCO assembly in its housing (top half removed) [Ref,,].

Fig. 2. (a) EBG resonator with its dimensions and variable periodicity (an) along the x-axis. (b) Gaussian envelope of the resonant mode achieved by linearly increasing the reflection from the center to the outer unit cells [Ref.1]

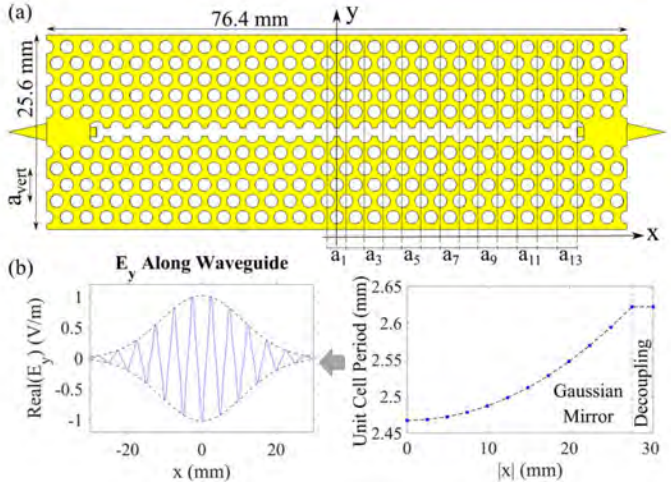

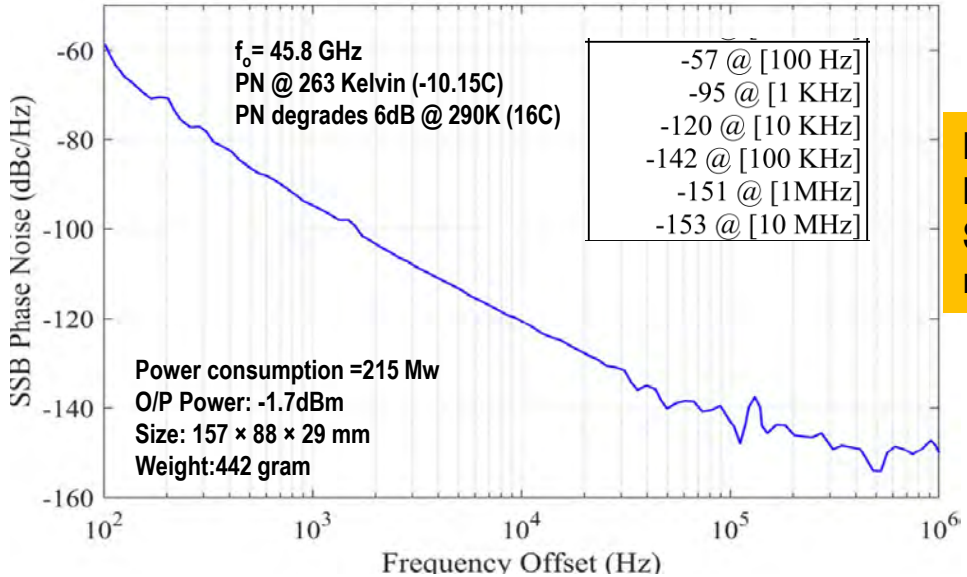

Fig. 4 Measured SSB phase noise [Ref.1]

Recent Publications on DRO: 12.8 GHz

Ref. 1: D. Trofimowicz, P. Kant, E. Lia, J. J. Michalski, Push-Push Oscillator Based on Packaged Space Qualified Components Operating at 11.8 GHz, **2022 Proceedings of the 52nd European Microwave Conference**, pp. 139-142

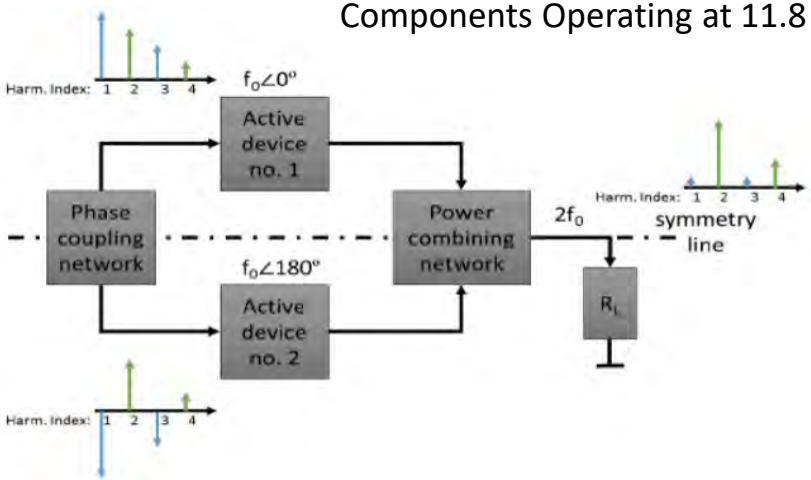

Fig. Layout of the push-push oscillator including resonant tank (left), two transistor circuits (middle) and the power combining circuit (right) [Ref.1].

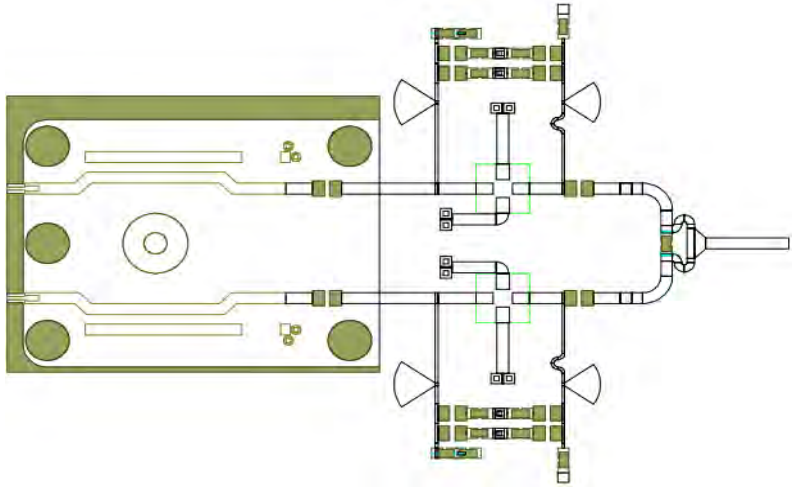

Fig. Layout of the push-push oscillator including resonant tank (left), two transistor circuits (middle) and the power combining circuit (right) [Ref. 1]

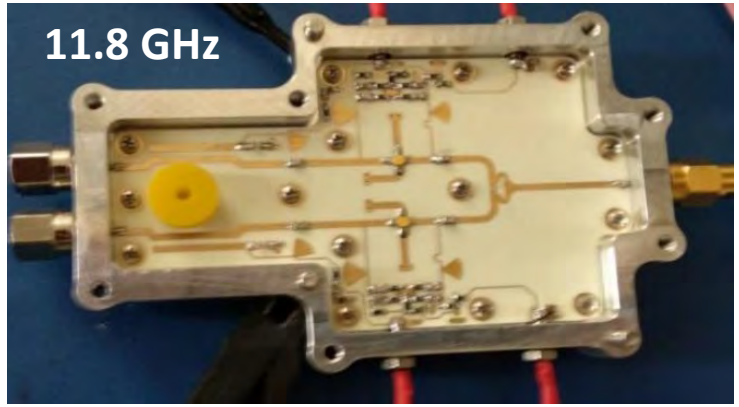

Fig. Assembled model of the DRO operation at 11.8 GHz [Ref.1]

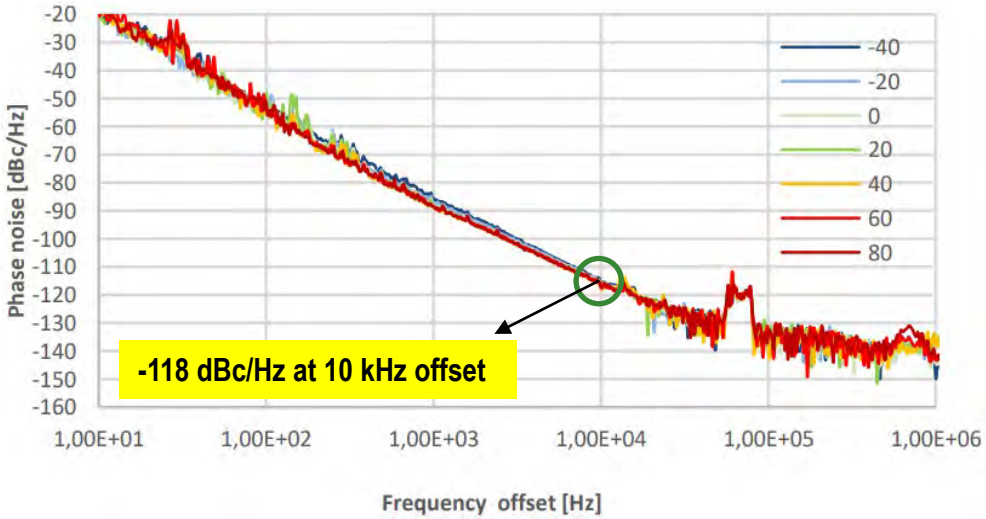

Fig. Temp. measurements of the DRO in temperature range of -40 °C to +80 °C [Ref.1]

DRO: SMD VCO Solutions

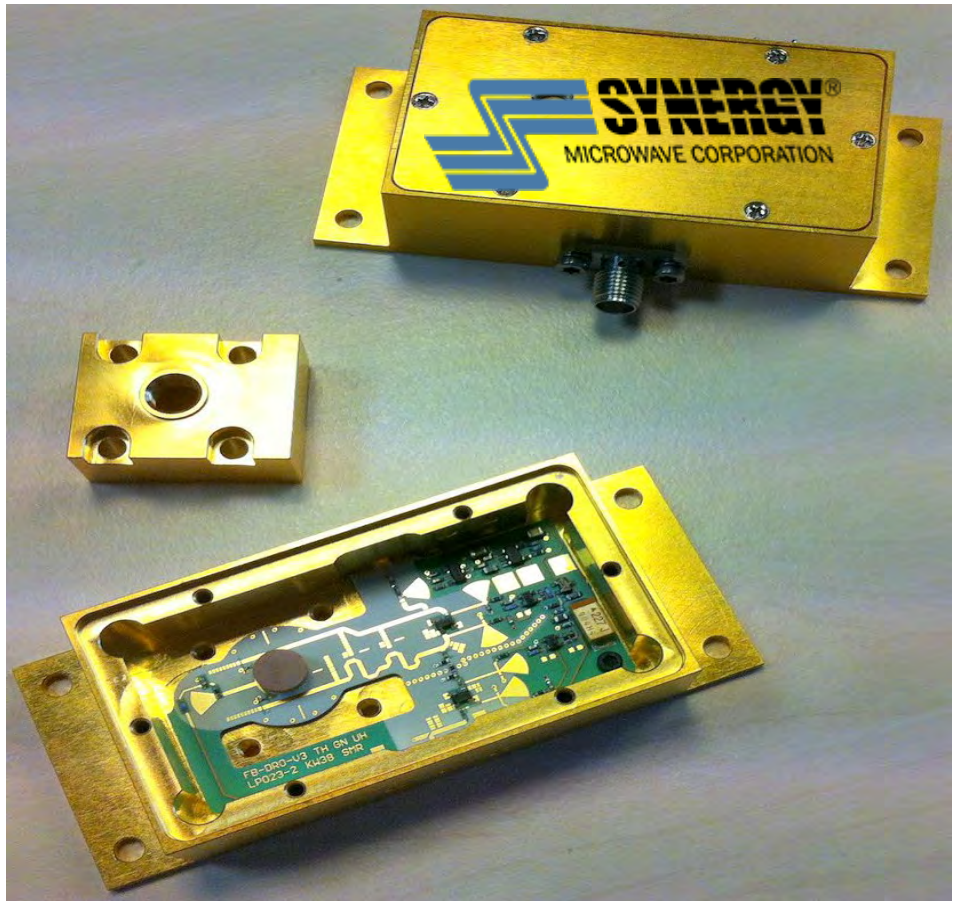

The actual package size is approximately 3.1" × 1.34" × 0.788," including mounting flaps.

Compact SMD version 10 GHz n 0.5"x 0.5" square package size with (5V, 30 mA) power consumption

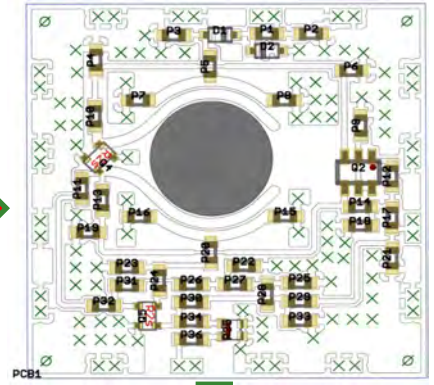

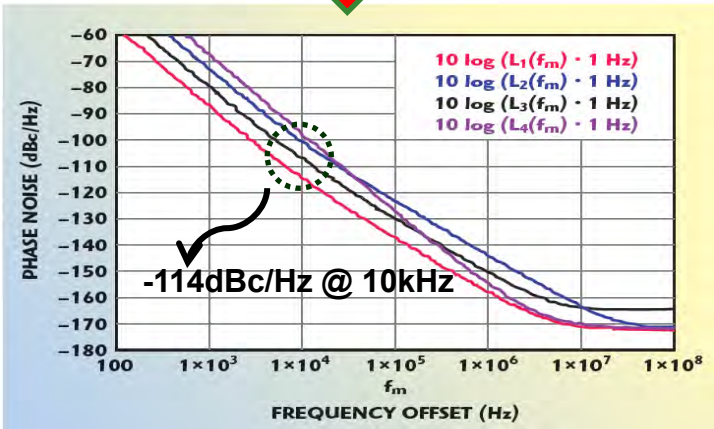

10 GHz Surface Mount DRO

Phase Noise

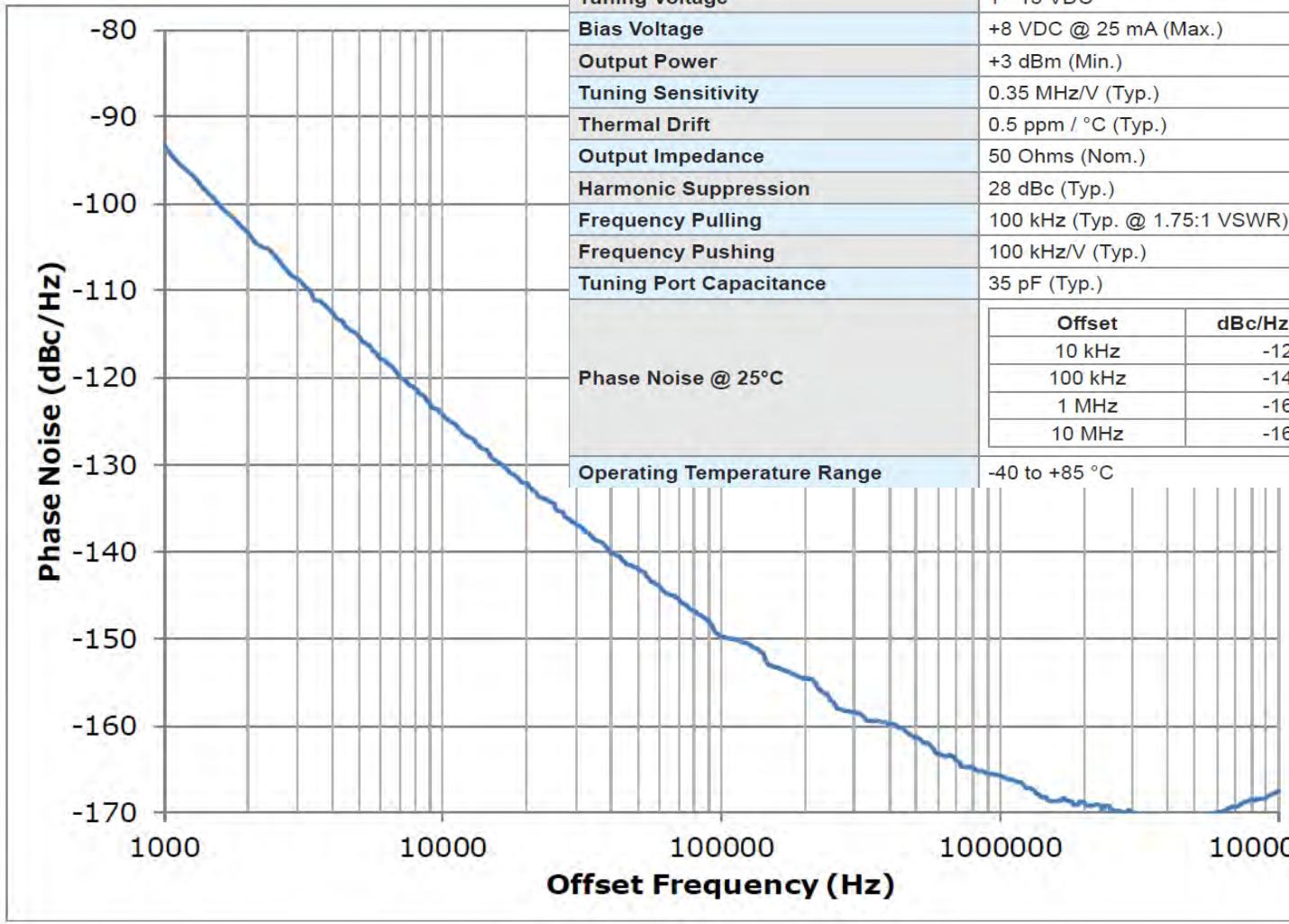

SPECIFICATIONS

Frequency	10 GHz
Tuning Voltage	1 - 15 VDC
Bias Voltage	+8 VDC @ 25 mA (Max.)
Output Power	+3 dBm (Min.)
Tuning Sensitivity	0.35 MHz/V (Typ.)
Thermal Drift	0.5 ppm / °C (Typ.)
Output Impedance	50 Ohms (Nom.)
Harmonic Suppression	28 dBc (Typ.)
Frequency Pulling	100 kHz (Typ. @ 1.75:1 VSWR)
Frequency Pushing	100 kHz/V (Typ.)
Tuning Port Capacitance	35 pF (Typ.)
Phase Noise @ 25°C	
Operating Temperature Range	-40 to +85 °C

Offset	dBc/Hz (Typ.)
10 kHz	-124
100 kHz	-149
1 MHz	-166
10 MHz	-168

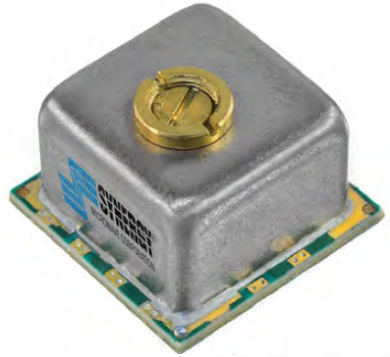

SYNERGY® MICROWAVE CORPORATION

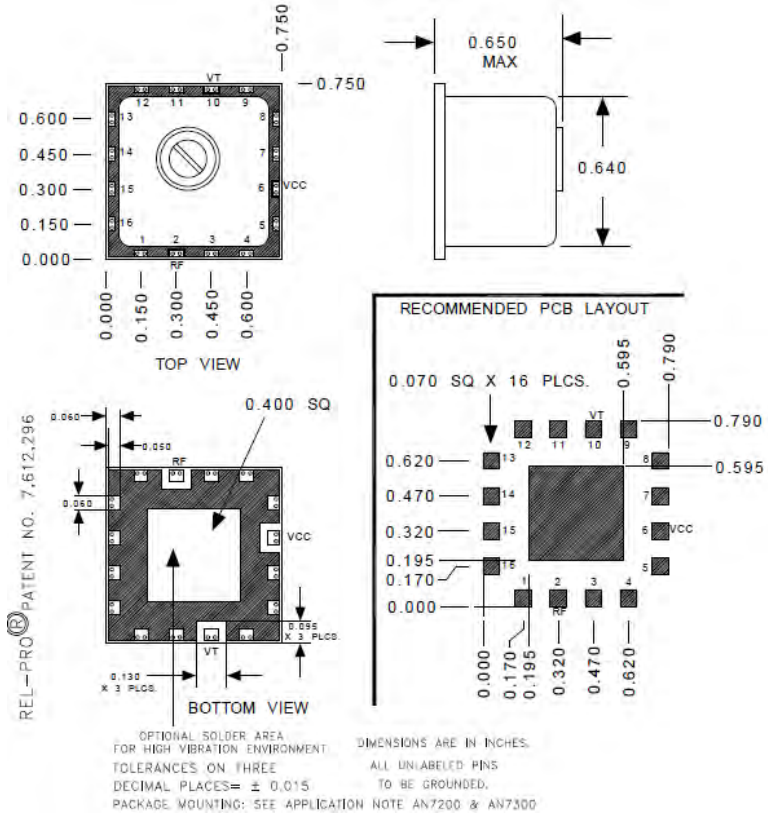

Surface Mount DRO Vibration Test

Fig. 1. Vibration Test Setup-X Axis

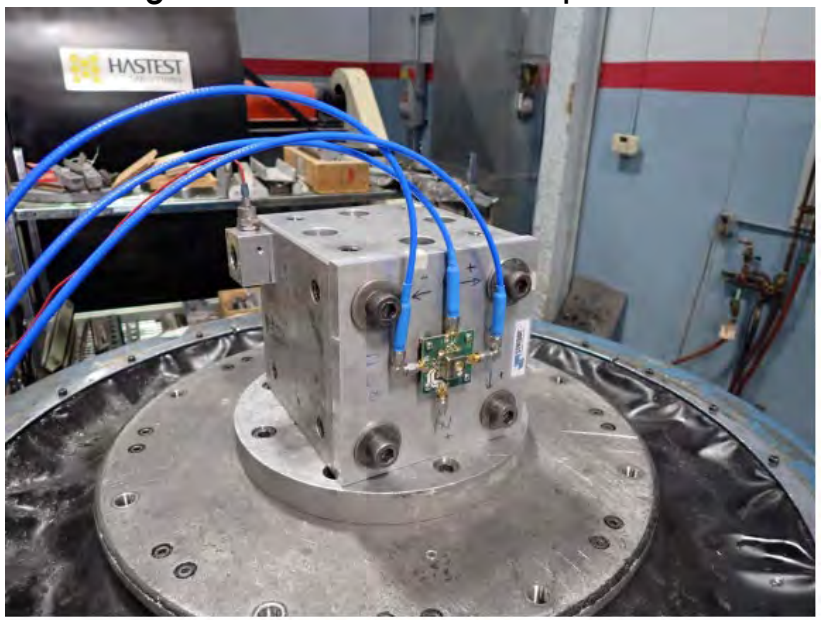

Fig. 2. Vibration Test Setup-Y Axis

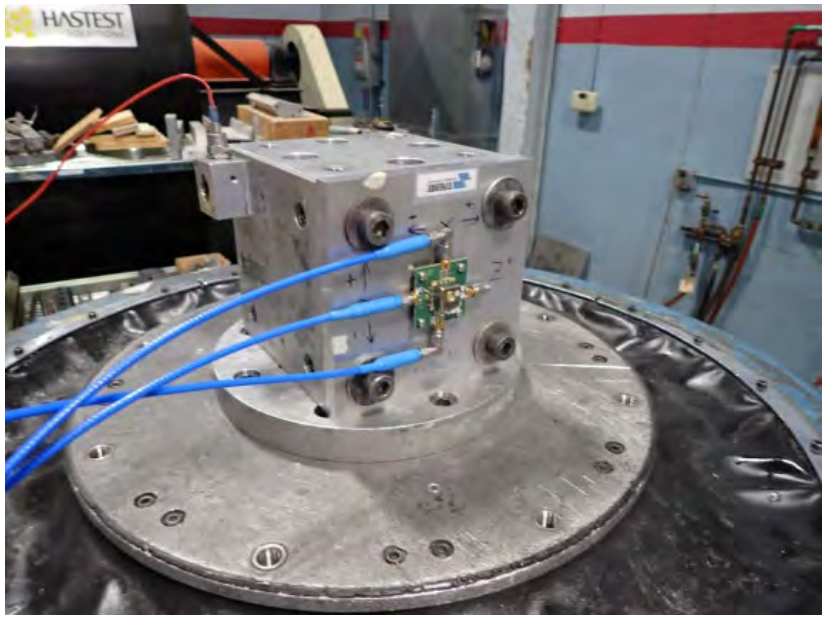

Fig.3. Vibration Test Setup-Z Axis

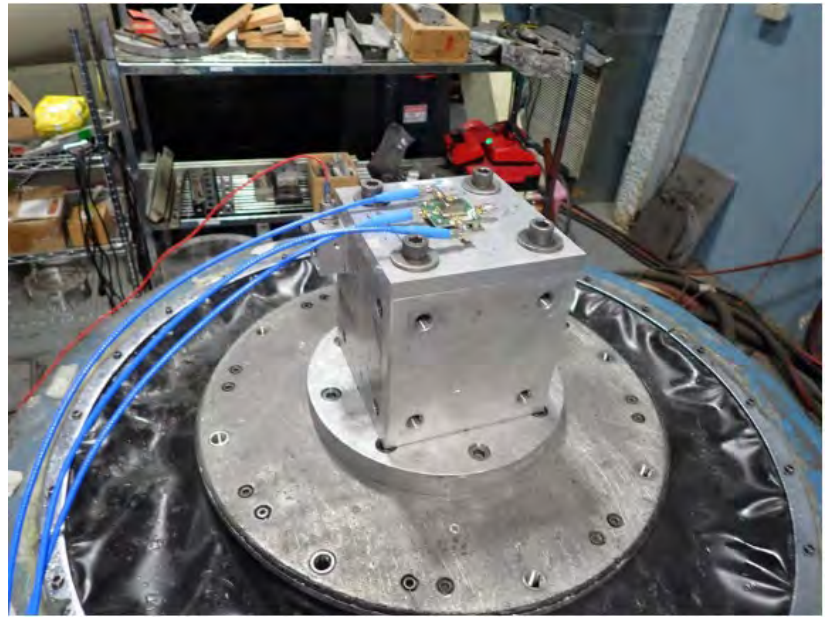

Vibration Test Procedure: The vibration test was performed in accordance with MIL-STD-810E. The unit was attached to a vibration machine as shown in Figures above 1 through 3. The unit was subjected to the input Random and Sine vibration levels listed below in each of the three mutually perpendicular axes:

- **Random Vibration at 10-2000 Hz and 0.02 g2 /Hz**
- **Sine Vibration where the frequencies varied uniformly between the minimum and Maximum limits on a period of 30 seconds.**

Level (g)	Minimum Sine Freq. (Hz)	Maximum Sine Freq. (Hz)
2.0	14.2	20.0
2.5	17.0	24.0
2.5	28.4	40.0
6.0	50.4	71.0
6.0	73.5	103.5

The vibration was applied for a period of 2 hours in each of the three mutually perpendicular axes. The Units survived and fully functions. Phase noise degradations were within 10 dB for closer to carrier (<1kHz offset), and within 2-3 dB at far offset (>10kHz offset)

Technologies for Terahertz Signal sources

Technologies for Terahertz Sources

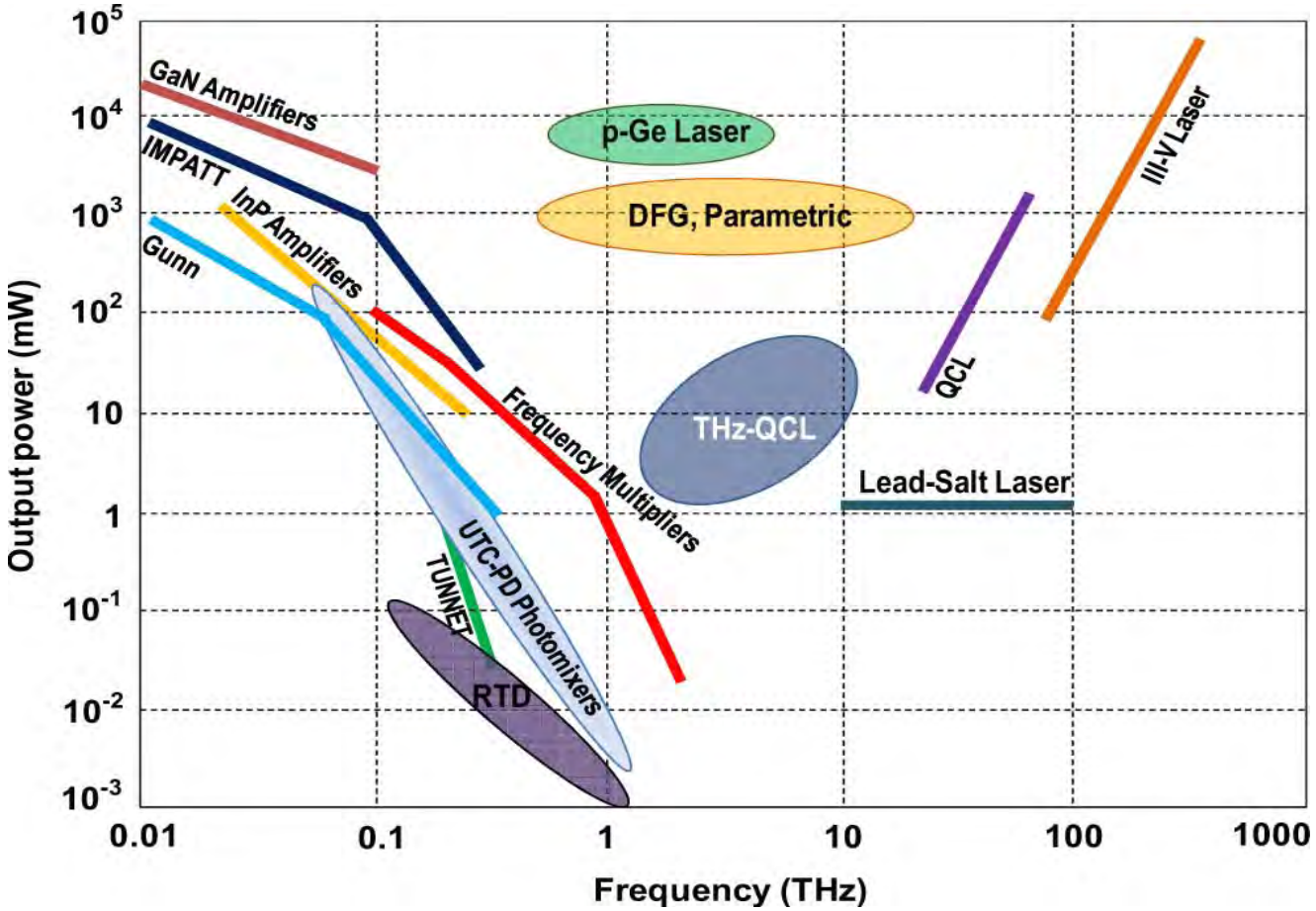

Fig.-Terahertz sources as a function of frequency. Solid lines are for the conventional THz sources [1].

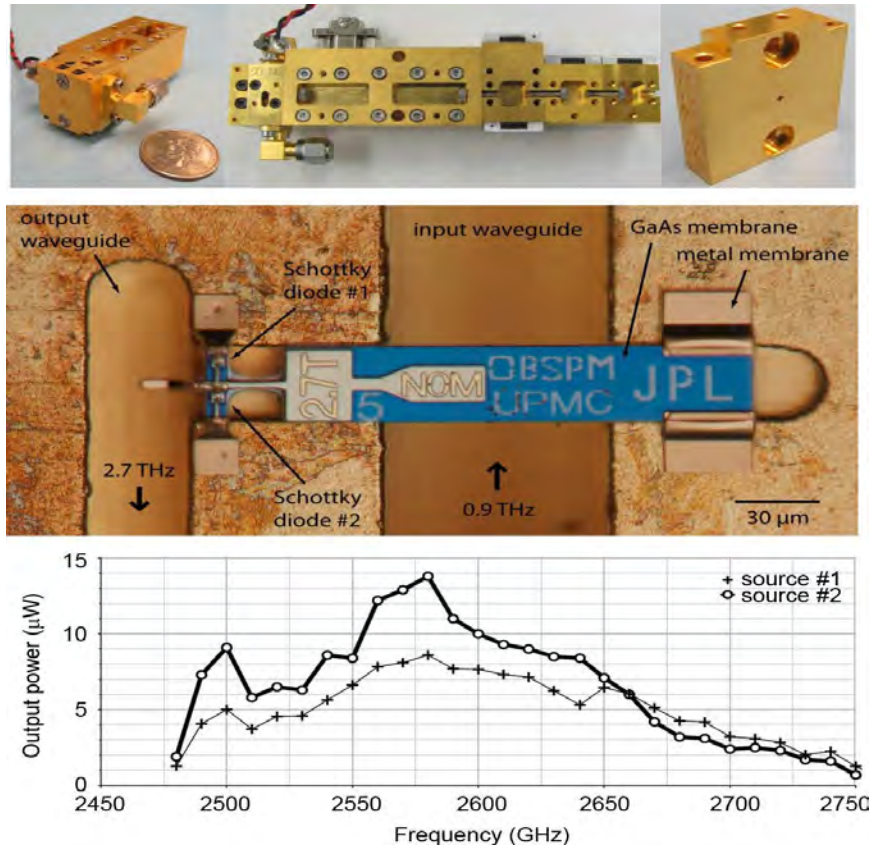

Photo of the 2.7 THz frequency multiplier chain. Top right shows the 2.7 THz Tripler block with integrated diagonal horn. The photo in the middle is the 2.7 THz Tripler chip assembled inside the split-waveguide block. The bottom plot shows the calibrated output power measured over the 2.475–2.750 THz range at room temperature in nitrogen purged environment [1]

Ref. [1] Goutam Chattopadhyay, "Technology, Capabilities, and Performance of Low Power Terahertz Sources", IEEE Transaction on Terahertz Science and Technology, Vol. 1, No. 1, pp. 33-43, Sept. 2011

Conclusion

Low Phase Noise VCO Design Tricks & Techniques: Communication systems rely on low-phase-noise VCO for reliable voice communications and to ensure transmitted data integrity. As data requirements increase beyond 2 Gb/s the phase noise of VCO becomes critical for achieving acceptable bit-error-rate (BER) performance. For low phase noise signal source (VCO) applications, simple tips can cut the design time and will be useful for oscillator design engineers:

- The frequency tuning feature is realized in DR (Dielectric Resonator) and Printed Resonator based tunable Oscillator by varying the capacitance of the tuning diodes (Varactors). Select low loss resistance Varactors and implement back-to-back in tuning circuit for the minimization of tuning network noise. Care must be taken to avoid breakdown, saturation, or overheating effects in the varactor at the cost of reduced loaded-Q.
- Maximize the resonator loaded Q-factor (high group delay); in the series LC-resonant circuits preferably use a large inductor, and in parallel LC-resonant circuits a large capacitor. Care must be taken to suppress the undesired modes in high Q-factor resonator especially quartz crystal, ceramic, dielectric and acoustic resonators by optimizing the drive-level across the resonator for a given dominant modes.
- Use an active device (Bipolar/FET) with low 1/f noise and noise figure at operating frequencies. The trade-off is to use a high frequency transistor having small junction capacitance and operate at moderately high bias voltage to reduce phase modulation due to junction capacitance noise modulation. Care must be taken to prevent modulation of the input and output dynamic capacitances of the transistor, otherwise lead to amplitude-to-phase conversion and therefore introduces noise.

Conclusion

- The 1/f noise depends on the current density in the transistor, therefore transistors with high I_{cmax} used at low currents will exhibit low flicker noise contribution. In BJTs as VCE increases, the flicker corner increases as the white noise increases, but the magnitude of the 1/f noise is constant. As base current increases, the flicker corner frequency increases with the magnitude of the 1/f noise and the increased shot noise current. The effect of flicker noise can be reduced through RF feedback. An un-bypassed emitter resistor of few ohms in a BJT circuit can improve the flicker noise significantly.
- Passive components in the oscillator circuit also exhibit short-term instability. Passive components (resistors, capacitors, inductors, reverse-biased, varactor diodes) exhibit varying levels of flicker-of-impedance instability whose effects can be comparable to or higher than to that of the sustaining stage amplifier 1/f AM and PM noise in the oscillator circuit.
- Maximize the output RF power carefully; otherwise severe Phase Noise degradation can occur due to active device noise elevation at compression. For low phase noise, tap the output signal through the resonator to the output load, thereby using the resonator transmission response selectivity to filter the carrier noise spectrum.
- VCO ground plane must be the same as that of the printed circuit board, including adequate decoupling capacitors between the DC bias and ground.
- The biasing circuit of the active device should be properly regulated and filtered to avoid any unwanted signal modulation ore noise injection.
- For ultra low phase noise, use noise reduction techniques: DC noise-feedback, mode-coupling, injection-locking, degenerative noise filtering, feed-forward and other noise reduction techniques.